

ANALYSIS AND DESIGN OF CONCRETE
FILLED STEEL TUBE STRUCTURE
SUBJECTED TO LATERAL LOADING

By

KETAN P. PATEL

10MCLC10



DEPARTMENT OF CIVIL ENGINEERING

AHMEDABAD-382481

May 2012

ANALYSIS AND DESIGN OF CONCRETE FILLED STEEL TUBE STRUCTURE SUBJECTED TO LATERAL LOADING

Major Project

Submitted in partial fulfillment of the requirements

For the degree of

Master of Technology in Civil Engineering

By

KETAN P. PATEL

10MCLC10



DEPARTMENT OF CIVIL ENGINEERING

AHMEDABAD-382481

May 2012

Declaration

This is to certify that

- i) The thesis comprises my original work towards the degree of Master of Technology in Civil Engineering (Computer Aided Structural Analysis and Design) at Nirma University and has not been submitted elsewhere for a degree.
- ii) Due acknowledgement has been made in the text to all other material used.

Ketan P. Patel

Certificate

This is to certify that the Major Project entitled “Analysis and Design of Concrete Filled Steel Tube Structure Subjected to Lateral Loading” submitted by Mr. Ketan P. Patel (10MCLC10), towards the partial fulfilment of the requirements for the degree of Master of Technology in Civil Engineering (Computer Aided Structural Analysis and Design) of Nirma University of Science and Technology, Ahmedabad is the record of work carried out by him under my supervision and guidance. In my opinion, the submitted work has reached a level required for being accepted for examination. The results embodied in this major project, to the best of my knowledge, haven't been submitted to any other university or institution for award of any degree or diploma.

Prof. S. P. Thakkar
Guide and Asst. Professor,
Department of Civil Engineering,
Institute of Technology,
Nirma University, Ahmedabad

Dr. P. H. Shah
Professor and Head,
Department of Civil Engineering,
Institute of Technology,
Nirma University, Ahmedabad

Dr K Kotecha
Director,
Institute of Technology,
Nirma University,
Ahmedabad.

Examiner

Date of Examination

Abstract

Steel-concrete composite columns are used extensively in modern buildings. Extensive research on composite columns in which structural steel section is encased in concrete have been carried out. In-filled composite columns, however have received limited attention compared to encased columns. In this work, review is carried out on composite columns with emphasis on analytical work. Also it includes review of research work that has been carried out to date, accounting the effects of local buckling, bond strength, lateral loading, confinement of concrete and behavior of steel-concrete composite columns.

Analytical studies of behavior of concrete filled circular steel tubes under lateral loading and study of interactions between steel tube and concrete filled is done. The behavior of the Concrete filled steel tube columns is controlled by both the strength and confinement effect of steel tube and concrete filled in the columns. The confinement provided by a closed steel section allows higher strengths to be attained by the concrete. Circular concrete-filled tubes develop hoop-tension which further increases the overall load-carrying capacity of the concrete.

The objective of the present study is to understand the behavior of the concrete filled tube structural system for high-rise building and to design structural systems including effects of the lateral loading. Also study the confinement effect on concrete due to steel tube is done. Comparative study of concrete filled tube (CFT), R.C.C and steel structure with different storey height of 10, 20 and 30 stories. With all structural systems as frame structure is carried out.

Determination of the design load-carrying capacity and subsequently comparison to several building codes was done. It also shows that the use of concrete filled steel tube columns that now have been consistently applied in the design of tall buildings pro-

vide considerable economy in comparison with conventional steel columns. Their use, allows the adoption of steel or composite floor systems combined with economically constructed columns. The use of these columns also has considerable advantages over reinforced concrete columns as they allow higher percentages of reinforcement to be adopted. Reduction in the column size can provide significant economic benefit since use of high strength steel can be applied in these situations. The use of composite columns becomes much more attractive where the need for high strength within a small "footprint" and good intrinsic fire resistance are considered more important than the basic price of the structural frame. Composite columns are likely to find an increasing role in supporting the very long-span floors which are becoming more usual in commercial constructions and in modern buildings.

When comparative study of CFT, RCC and Steel building is done, CFT building is found to be better in load carrying capacity with small cross section of column and displacement parameter Also number of stories for same structural system is more compared to RCC and Steel building.

Acknowledgements

It gives me great pleasure in expressing my sincere thanks and profound gratitude to my guide Prof. S. P. Thakkar, Asst. Professor, Department of Civil Engineering, Institute of Technology, Nirma University, Ahmedabad. I express my hearty thanks to her, who right from the conceptualization of the problem to the finishing stage of the dissertation work guided me. Her invaluable suggestions and discussions helped me a lot right from start of the project work and also during the work.

My sincere thanks and gratitude to Dr. P. V. Patel, Professor, Department of Civil Engineering, Dr. U. V. Dave, Professor, Civil Engineering Department, Dr. S. P. Purohit, Associate Professor, Department of Civil Engineering, Prof. N. C. Vyas, Professor, Department of Civil Engineering, Shri Himat Solanki, Visiting Faculty, Department of Civil Engineering Institute of Technology, Nirma University, Ahmedabad for their continual kind words of encouragement and motivation during my study.

I further extend my thanks to Dr. P. H. Shah, Head, Department of Civil Engineering, Institute of Technology, Nirma University, Ahmedabad and Dr K. Kotecha, Director, Institute of Technology, Nirma University, Ahmedabad for providing all kind of required resources during my study.

I am very thankful to Mr. Nishant Patel and Mr. Prakash Siyani, P-Cube consultant, Structural engineers, Ahmedabad for helping me to solve the modeling related problem in STRAP software.

And most importantly, I express my deep sense of gratitude to my wife, family members and friends, for their endless love and moral support that constantly encouraged me.

Many others helped me directly and indirectly, I also convey my thanks to them.

Ketan P. Patel

10MCLC10

Abbreviation, Notation and Nomenclature

f_{ck}	compressive strength of concrete at 28 days
f_{sk}	yield strength of reinforcing steel
f_y	yield strength of structural steel
A_a	Cross-sectional area of the structural steel section
A_c	Cross-sectional area of concrete
A_s	Cross-sectional area of reinforcement
W_a	plastic modules of the structural steel
$W_{a,n}$	plastic modules of the structural steel in the height of h_n
W_s	plastic modules of the reinforcement
$W_{s,n}$	plastic modules of the reinforcement in the height of h_n
W_c	plastic modules of the concrete
$W_{c,n}$	plastic modules of the concrete in the height of h_n
h_n	distance between the plastic neutral axis line and the centroid line
γ_c	Partial factor for concrete
γ_s	Partial factor for reinforcing steel
γ_{Ma}	Partial factor for structural steel
λ	Relative slenderness
η_a, η_{ao}	Factors related to the confinement of concrete
η_c, η_{co}	Factors related to the confinement of concrete
e	Eccentricity of loading
d	Overall diameter of circular hollow steel section
b	Width of a composite column section
t	Thickness steel section
b_c	Width of the column section
h_c	Depth of the column section
M_{pl}	Plastic moment
$M_{Max,Rd}$	Maximum design value of the resistance moment of a composite section

M_{Rd}	Design value of the resistance moment of a composite section
$M_{pl,Rd}$	Design value of the plastic resistance moment of the composite section
EI_{eff}	Effective flexural stiffness for calculation of relative slenderness
E_c	Effective modulus of elasticity for concrete
E_{cm}	Secant modulus of elasticity of concrete
E_a	Modulus of elasticity of structural steel
E_s	Design value of modulus of elasticity of reinforcing steel
N_{cr}	Elastic critical normal force
N_{sd}	..	Design value of the plastic resistance of the reinforcing steel to tensile normal force
N_{pl}	Plastic axial resistance of a section
$N_{pl,c}$	Plastic axial resistance of concrete component
$N_{pl,Rd}$		Design value of the plastic resistance of the composite section to compressive normal force
$N_{pl,Rk}$	Characteristic value of the plastic resistance of the composite section to compressive normal force
$N_{pm,Rd}$..	Design value of the resistance of the concrete to compressive normal force
N_{cr}	Elastic critical normal force
I_a	Second moment of area of the structural steel section
I_c	Second moment of area of the un-cracked concrete section
I_s	Second moment of area of the steel reinforcement
σ_r	concrete core internal pressure
σ_t	tensile hoop stress in steel
δ	Factor; steel contribution ratio; central deflection
ϕ_t	Creep coefficient

Contents

Declaration	iii
Certificate	iv
Abstract	v
Acknowledgements	vii
Abbreviation, Notation and Nomenclature	ix
List of Tables	xiv
List of Figures	xvi
1 Introduction	1
1.1 General	1
1.2 Construction Methods	2
1.3 History of Steel-Concrete Composite Structures	3
1.4 Principle Composite Construction Elements	8
1.4.1 Slab	8
1.4.2 Beam	12
1.4.3 Column	13
1.4.4 Joints	15
1.5 Objective of Study	17
1.6 Scope of Work	18
1.7 Organization of the Report	18
2 Literature Survey	20
2.1 General	20
2.2 Research Papers	20
2.2.1 Analytical Work Done on CFT Structure	20
2.2.2 Experimental and Analytical Work Done on CFT Structure	21
2.3 Summary	23

3	Concrete Filled Steel Tube System	24
3.1	General	24
3.2	History of Concrete Filled Steel Tube (CFT) Column	28
3.3	Advantage	28
3.4	Features of Concrete Filled Structural System	30
3.5	Confinement Effect	36
3.5.1	Confinement Parameters	39
3.6	Methodology for Design	39
3.6.1	Local Buckling of Steel Elements	40
3.6.2	Limitation of Simplified Method	41
3.7	Composite Columns Subject to Axial Compression	42
3.7.1	Resistance of the Cross-Section	42
3.7.2	Relative Slenderness of a Composite Column	43
3.8	Resistance to Compression and Bending	44
3.9	Observation of Behavior of CFT Building up to 60m Height by ANUHT [9]	47
4	Analysis and Design of 10 Storey Building	50
4.1	General	50
4.2	CFT Column Capacity Comparison	50
4.3	M-N Interaction Curve[8]	53
4.4	Modeling and Analysis of 10 Storey CFT, RCC and Steel Building	58
4.4.1	General	58
4.4.2	Building Configuration	58
4.4.3	Steps for CFT Structure Modeling in STRAP Software	62
4.4.4	Parametric Study of 10 Storey CFT Building	65
4.4.5	Comparison of 10 Storey CFT, RCC and Steel Building	72
4.4.6	Cost Comparison	76
4.4.7	Detailing of CFT Member	77
4.5	Summary	79
5	Analysis and Design of 20 and 30 Storey Building	80
5.1	General	80
5.2	Parametric Study of 20 Storey CFT Building	80
5.3	Comparison of 20 Storey CFT, RCC and Steel Building	86
5.4	Cost Comparison	90
5.5	Detailing of CFT Member	91
5.6	Parametric Study of 30 Storey CFT Building	93
5.7	Comparison of 30 Storey CFT, RCC and Steel Building	99
5.8	Cost Comparison	103
5.9	Detailing of CFT Member	105
5.10	Summary	107

6	Summary, Conclusion and Future Scope	109
6.1	Summary	109
6.2	Conclusion	110
6.3	Future Scope of Work	112
A	Wind Load Calculation	113
A.1	Manual Wind Load Calculation For 20 Storey	113
A.2	Manual Wind Load Calculation For 30 Storey	116
B	Earthquake Load Calculation	119
B.1	Manual Earthquake Load Calculation For 20 Storey	119
B.2	Manual Earthquake Load Calculation For 30 Storey	120
	References	121

List of Tables

4.1	Axial Load Carrying Capacity	53
4.2	Column Capacity Result	53
4.3	Beam Size	61
4.4	Column Size	61
4.5	Comparison of Base Reaction	66
4.6	Wind Load Parameter	67
4.7	Building Parameter	67
4.8	Wind Load in X-Direction	68
4.9	Wind Load in Y-Direction	68
4.10	Base Shear Due to Wind Load	69
4.11	Base Shear Due to Earthquake Load	69
4.12	1 St and 2 nd Mode Time Period	70
4.13	10Storey Displacement	71
4.14	Load Comparison	72
4.15	Time Period Comparison	73
4.16	Base Shear Comparison	73
4.17	Maximum Load Carrying Capacity	74
4.18	Displacement Comparison	75
4.19	10 Storey Column Rate Analysis	77
5.1	Comparison of Base Reaction	82
5.2	Base Shear Due to Wind Load	82
5.3	Base Shear Due to Earthquake Load	82
5.4	1 St and 2 nd Mode Time Period	83
5.5	Load Comparison	86
5.6	Time Period Comparison	86
5.7	Base Shear Comparison	87
5.8	Maximum Load Carrying Capacity	88
5.9	20 Storey Column Rate Analysis	91
5.10	Base Reaction	94
5.11	Base Shear Due to Wind Load	95
5.12	Base Shear Due to Earthquake Load	95
5.13	1 St and 2 nd Mode Time Period	95

5.14	Load Comparison	99
5.15	Time Period Comparison	99
5.16	Base Shear Comparison	100
5.17	Maximum Load Carrying Capacity	101
5.18	30 Storey Column Rate Analysis	104
5.19	Column Cost Comparison (Rs/m	104
A.1	Wind Load Parameter	113
A.2	Building Parameter	114
A.3	Wind Load in X-Direction	114
A.4	Wind Load in Y-Direction	115
A.5	Wind Load Parameter	116
A.6	Building Parameter	116
A.7	Wind Load in X-Direction	117
A.8	Wind Load in Y-Direction	118

List of Figures

1.1	Mc Graw Building, Column and Floor Section	5
1.2	Mc Graw Building, 39th Street, New York, 1908	5
1.3	Emperger Column	6
1.4	Empire State Building	6
1.5	Bank of China	7
1.6	Pacific First Center	7
1.7	Construction Elements	8
1.8	Types of Concrete Slabs	9
1.9	Prestressed Prefabricated Hollow Core Slab	10
1.10	Frictional Interlock in Composite Slabs	11
1.11	Mechanical Interlock in Composite Slabs	11
1.12	End Anchorages for Composite Slabs	11
1.13	Conventional and Innovative Composite Beams	12
1.14	Types of Shear Connectors	12
1.15	Types of Composite Column	13
1.16	Tubular Column With Nails as Shear Connectors and Reinforcement on Site (Citibank Duisburg, Germany)	14
1.17	HILTI Nail X-DSH32 P10)	15
1.18	Joint Response	16
1.19	Vertical Shear Transfer Between Beams and Composite Columns)	16
3.1	Typical Cross-Sections of Composite Columns	25
3.2	Canton Tower	29
3.3	CFT Column With Footing	32
3.4	Type of Footing	32
3.5	Type of Connection	33
3.6	Shop-fabricated CFT Joint	34
3.7	Effectively Confined Concrete for CFT Columns	37
3.8	Schematic Load-Deformation Relation for CFT Column	38
3.9	Fracture Process in Concrete Core During Phases of Loading	38
3.10	M-N Interaction Curve for Uniaxial Bending	45
3.11	Development of Stress Blocks at Different Points on The Interaction Curve (Concrete Encased Section)	46

4.1	Geometric Characteristics of the Cross-Section	51
4.2	Distribution of Bending Moment in the Column	54
4.3	Geometric Characteristics of the Cross-Section	55
4.4	M-N Interaction Curve	57
4.5	Typical Building Plan	59
4.6	Geometry and Design Tools	62
4.7	Column Property Tool	62
4.8	Beam Property Tool	63
4.9	Seismic Parameter	64
4.10	Load Combination	64
4.11	Mode Shape Vs Time Period Graph	70
4.12	1 st and 2 nd Mode Shape	70
4.13	3 rd Mode Shape	71
4.14	Displacement of 10 Storey CFT Building	72
4.15	Comparison of Time Period	73
4.16	Comparison of Base Shear	74
4.17	Comparison of Design Capacity	74
4.18	Comparison of 10 Storey Displacement	75
4.19	Design Result For 10 Storey CFT Building	78
4.20	10 Storey CFT Building Column and Beam	78
5.1	Mode shape Vs Time period graph	83
5.2	1 st and 2 nd Mode Shape	84
5.3	3 rd Mode Shape	84
5.4	Displacement of 20 Storey CFT Building	85
5.5	Comparison of Time Period	87
5.6	Comparison of Base Shear	87
5.7	Comparison of Design Capacity	88
5.8	Comparison of 20 Storey Displacement	89
5.9	Design Result For 20 Storey CFT Building	92
5.10	20 Storey CFT Building Column and Beam	92
5.11	Mode Shape Vs Time Period Graph	96
5.12	1 st and 2 nd Mode Shape	96
5.13	3 rd Mode Shape	97
5.14	Displacement of 30 Storey CFT Building	98
5.15	Comparison of Time Period	100
5.16	Comparison of Base Shear	100
5.17	Comparison of Design Capacity	101
5.18	Comparison of 30 Storey Displacement	102
5.19	Comparison of Column Cost	105
5.20	30 Storey CFT Building Column and Beam	106
5.21	Design Result For 30 Storey CFT Building	106

Chapter 1

Introduction

1.1 General

Steel and concrete are most widely and inevitably used combination of construction material be it buildings, bridges or modern construction work of today's era. Though these materials may have different properties and characteristic, they both seem to complement each other in many ways. Steel is excellent in resisting tension while concrete is good in compression. Steel components have lesser weight ratio so can be thinner and prone to buckling which can be restrained to some extent by use of concrete. Steel may be used to induce ductility, an important criteria for tall building, while corrosion protection and thermal insulation can be done by concrete. Traditionally in buildings, grid of beams are provided supported by column may have concrete slabs to transfer the loads to the beams. In composite structure to reduce the slip at the steel concrete interface, so that slab and beam section act together as a composite unit, mechanical devices may be provided which may be in form of headed studs or other connectors which can be welded or shot fired to structural steel and enclosed in concrete.

1.2 Construction Methods

Conventionally there are two methods of construction observed, both having their advantages and disadvantages:

- **Concrete construction method:**

This method works very well considering styling, freedom of form and shapes easy to handle on site, thermal resistance, sound insulation and its excellent resistance to chemical attack. But it has poor behavior in terms of the ratio between resistance and dead load, time-consuming shuttering and extension of the construction time due to hardening of concrete. It is also a well known fact that concrete in its own cannot handle tensile stresses and hence have to be provided with reinforcement to take tensile force which again is very time consuming process.

- **Steel construction method:**

This method has high ratio between bearing capacity and weight. As the fabrication can be done in advance independently of the weather the erection is very simple with small tolerances. Fire resistance of bare steel constructions may be problematic which can only be solved by using more of material or by cost-intensive preventive measures. Skilled labor force and good supervision may be disadvantage of the steel construction.

Using both the materials, an economic combination can be developed and advantages of steel and concrete can be utilized while their disadvantages can be compensated forming a rational system. In composite construction, higher bearing capacities can be achieved than in steel and concrete alone. Also stiffness and plastic redistribution can be improved by combining steel with concrete. This allows plastic reserve capacity of the system to be considered, while reducing safety factors due to the inherent ductility at the failure modes. Composite construction is a means of using interaction of two materials within one structural element e.g. a concrete filled tubular steel column.

Building up a composite structure in a very economic way can be divided into the following operations:

- First of all a conventional skeleton structure in steel, braced or unbraced, will be erected. If hollow steel sections are used for the columns the reinforcement cages already can be positioned in the shop.
- Also all brackets, fin plates and vertical shear studs (non-headed bolts or shot-fired nails) for the load transfer between the steel and the concrete encasement have to be prepared in the shop to speed up the erection on site requiring a detailed planning stage. After arranging the columns, the bare steel beams are simply hinged in between.
- Prefabricated concrete elements or profiled steel sheeting are spanned from beam to beam, serving both as shuttering and as a working platform.
- Finally, by concreting the slabs and the columns in one process, the stiffness and resistance of the columns and beams is increased and the joints are transformed from hinged to semi-continuous restrained joints.

1.3 History of Steel-Concrete Composite Structures

Composite construction can be observed in early period of civilization also. The Assyrians were credited with the use of man's first manufactured building material i.e. mud bricks. They made mud bricks that were reinforced with straw and were probably our first composite members.

Composite construction had begun in the middle of the nineteenth century. In 1840, a patent was issued to William Howe for a composite truss of wood and wrought iron. Four years later a patent was issued to Thomas and Caleb Pratt, also for a composite truss of wood and wrought iron. The difference between the Howe and Pratt trusses was in the configuration. The Howe truss used the iron tension rods as vertical members, and the Pratt truss used the diagonals as the iron tension members. It can be

attributed to the soundness of the design that many of old bridges, still in service as covered bridges on rural roads are built using these concepts.

In the mid-nineteenth century, Britain used concrete as fireproofing for iron structural members. These encased beams were the first real composite beams. The use of composite beam began with fireproofing systems for floors. In Canada, the Dominion Bridge Company investigated beams encased in concrete in 1923. The National Physical Laboratory in Britain also was conducting tests on encased beams at the same time. Scott published the results in 1925. In the United States, a patent was issued to J. Kahn in 1926 for a composite beam. Afterwards, R.A.Caughey published the results of his work on composite beam of concrete and structural steel in the Proceedings of the Iowa Engineering Society. In 1929, Caughey and Scott collaborated on a paper that dealt with the design of a steel beam and concrete slab. They pointed out the need for a mechanical shear connector to carry the horizontal shear. Their work also included a discussion of both shored and un-shored construction.

It is always a big boost for any new construction method when a major specification writing body incorporates the new construction method into its latest code revision. For composite construction, this breakthrough came in two steps. In 1944, the American Association of State Highway Officials included composite construction into its specifications. Then in 1952, the American Institute of Steel Construction included provisions for composite construction for buildings into its code.

EARLY EXAMPLES:

In 1912, William H. Burr made tests with steel columns filled with concrete, but gave no design formula, for tests were too few in number. Several years before, in 1908, he had applied such columns successfully in the construction of the Mc Graw Building in New York (Fig.1.1, 1.2), which allowed an increased working load on the inner concrete.

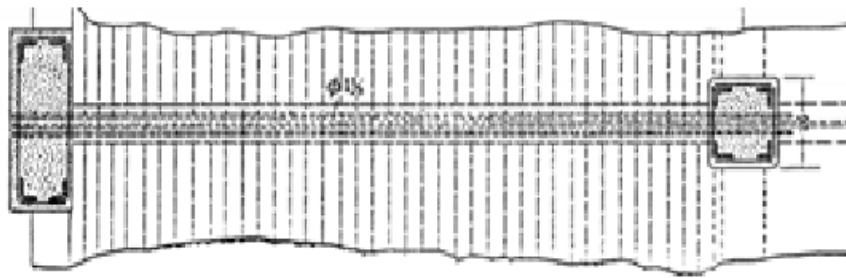


Figure 1.1: Mc Graw Building, Column and Floor Section



Figure 1.2: Mc Graw Building, 39th Street, New York, 1908

In Germany, the first design formula for composite columns was given by Emperger (1913). The column type examined was a concrete column with a core of cast-iron with horizontal reinforcement provided. It was also known as Emperger column (Fig.1.3).

Also, it is found that in Empire State's Building, Bank of China and Pacific First Center building composite construction is used.

1931 - Empire State Building's entire steel frame was encased in concrete, Early 1900 - steel beams encased in concrete for fireproofing(Fig.1.4).

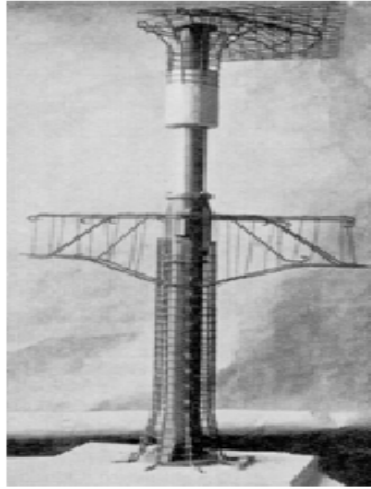


Figure 1.3: Emperger Column



Figure 1.4: Empire State Building

1988 - Bank of China "megatruss" of composite columns(Fig.1.5).

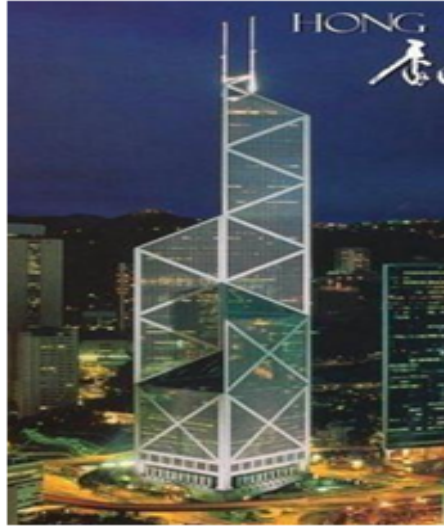


Figure 1.5: Bank of China

Late 1990s - Pacific First Center(Fig.1.6).

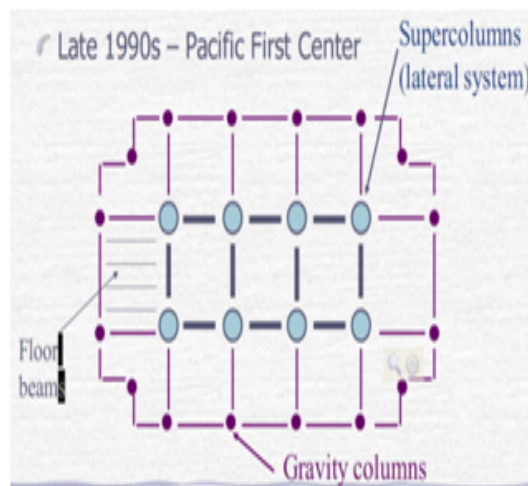


Figure 1.6: Pacific First Center

1.4 Principle Composite Construction Elements

In the composite construction, method generally followed on site is shown in Fig.1.7 , slabs are spanned between the grids of beams which are then supported by columns. The floor itself consists of floor beams and slab, which can form hybrid or mixed building technology system. Slab, beam, column and joints used in composite construction are discussed below.

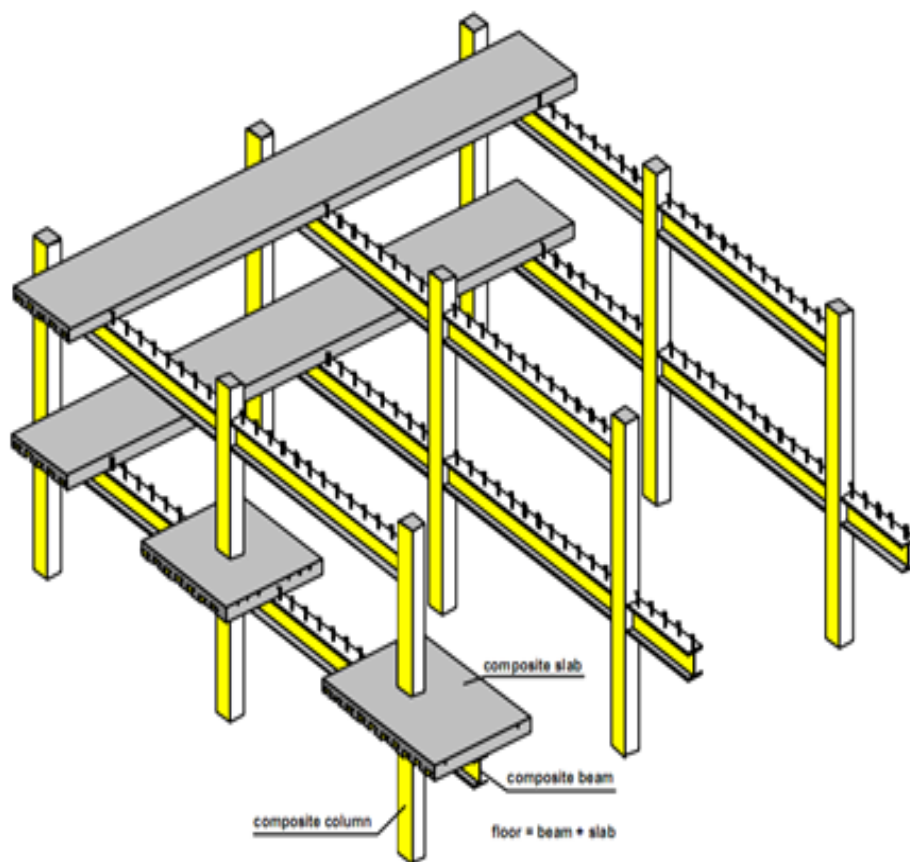


Figure 1.7: Construction Elements

1.4.1 Slab

Slab is one of the main the principal load carrying member can be reinforced concrete slab, Pre-stressed concrete slab or profile steel sheeting.

- **Reinforced concrete slabs:**

Grid pattern, complexity of floor shape, time schedule and capabilities of pre-fabricated shops will be main factors in deciding the method to be adopted for reinforced concrete slabs. They can be manufactured by:

- using shuttering available on site
- using partially prefabricated elements
- using fully prefabricated elements

For all these variations, illustrated in Fig.1.8, normal weight concrete can be used. In the case of fully prefabricated slabs, attention has to be paid to the fact that only a small part of in situ concrete within the clearances can be activated by the beams to act compositely.

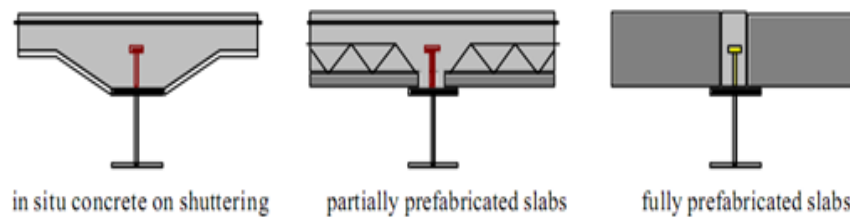


Figure 1.8: Types of Concrete Slabs

- **Pre-stressed concrete slabs:**

Prestressed prefabricated hollow core slabs are very widely used now days. They can be used for large spans between steel beams. Slabs have transverse bending behavior due to flexible support like beam, some modifications like concrete filled in the ends of hollow cores improves its flexible behavior. Bending is still the governing design criteria for usually slender prestressed slabs Fig.1.9.

- **Profiled steel sheeting:**

This type of construction can be done by either using conventional trapezoidal

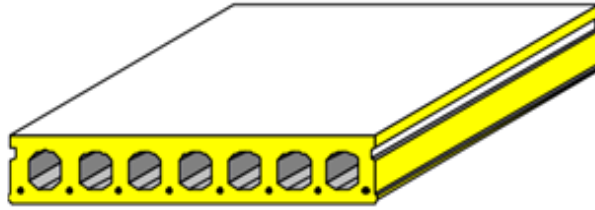


Figure 1.9: Prestressed Prefabricated Hollow Core Slab

metal decking or special sheeting. When there are no proper measures to ensure a composite action, the steel profiles can be used either for full vertical action i.e. by providing deep steel decks (the concrete in between only serves for the load distribution) or they are only used as for so called lost shuttering (neglecting the contribution steel sheet may make in the final state). Both extremes again may lead to an uneconomic use of concrete or steel. In a composite slab there are several possibilities to provide an interlock between steel and concrete. They can be in form of:

- Frictional interlock: which may not able to transfer large shear forces (Fig.1.10).
- Mechanical interlock: Provided by interlocking embossments of the steel decking (Fig.1.11).
- End anchorage: In the form of headed bolts, angle studs or end-deformations of the steel sheeting. This may result into a large concentrated load introduction at the ends and therefore there will be sudden increase in load from the bare steel to the composite section (Fig.1.12).
- Chemical interlock: which is very brittle and unreliable therefore not considered in the design calculations.

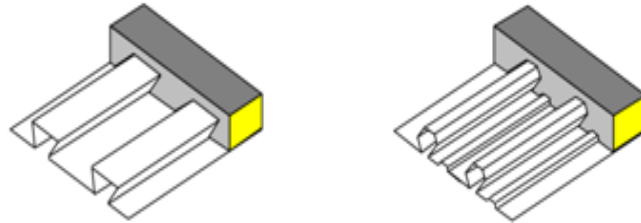


Figure 1.10: Frictional Interlock in Composite Slabs

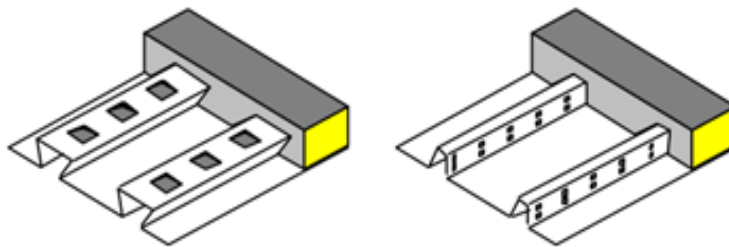


Figure 1.11: Mechanical Interlock in Composite Slabs

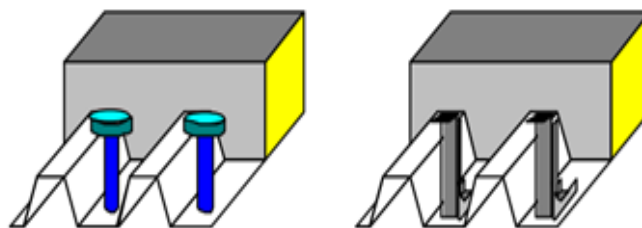


Figure 1.12: End Anchorages for Composite Slabs

1.4.2 Beam

Beams are elements which may be within the floors and are used to carry the loads to columns. Depending upon the grid pattern of the beams, slab may span in one or two direction. In mixed structures, the materials of beams can be of concrete, steel or of steel-concrete composite or even other material and its combination.

In steel concrete composite beam, sagging moment region of the concrete slab is activated in compression by shear connectors. In practical application headed studs are used. This combination provides large relative stiffness and also large deformation capacity. The headed studs may have constant spacing between them. The disadvantage of this is the weld ability at site when galvanized plates or coated steel flanges are used and also regarding water retention between the sheeting and the flange (Fig.1.13 and 1.14).

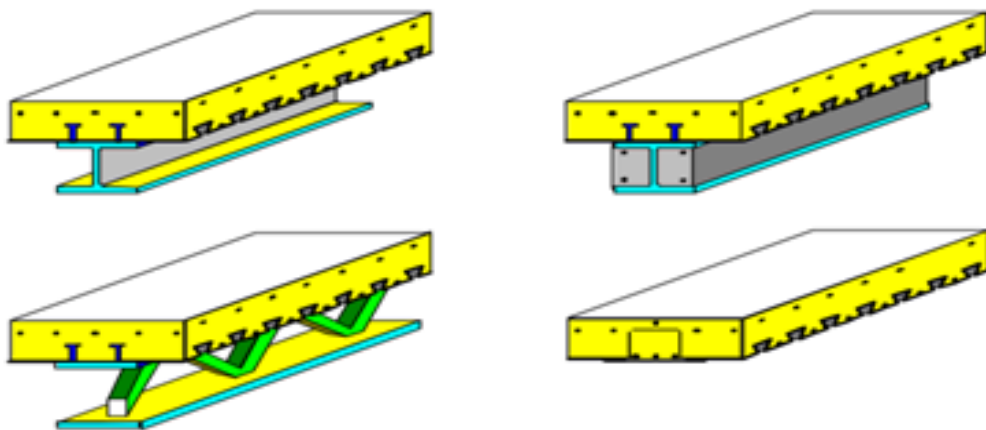


Figure 1.13: Conventional and Innovative Composite Beams

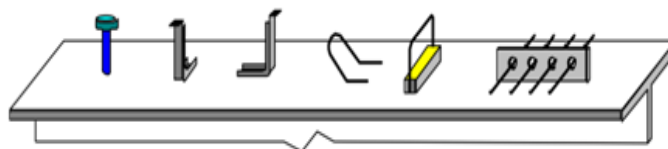


Figure 1.14: Types of Shear Connectors

1.4.3 Column

Two types of composite columns, those with steel section encased in concrete and those with steel section in-filled with concrete are commonly used in buildings. Fig.1.15 represents basic forms of cross-sections of composite columns. Concrete-encased steel composite columns have become the preferred form for many seismic-resistant structures. Under severe flexural overload, concrete encasement cracks resulting in reduction of stiffness but the steel core provides shear capacity and ductile resistance to subsequent cycles of overload. Concrete-filled steel tubular columns have been used for earthquake-resistant structures, bridge piers subject to impact from traffic, columns to support storage tanks, decks of railways, columns in high-rise buildings and as piles [10].

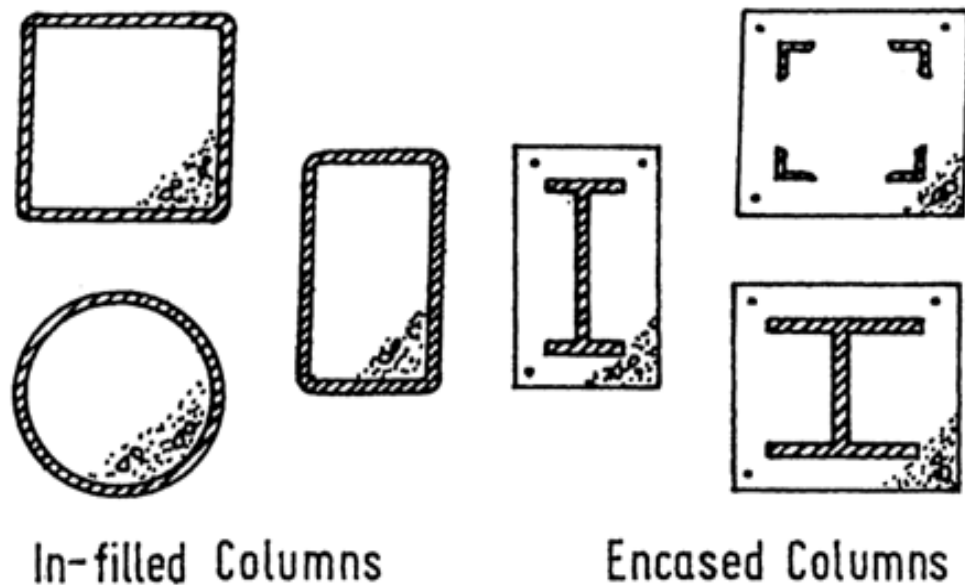


Figure 1.15: Types of Composite Column

In steel section, rolled I- profiles which can be rectangular or tubular hollow sections can be used. I sections can be partially encased (where only chambers are filled with



Figure 1.16: Tubular Column With Nails as Shear Connectors and Reinforcement on Site (Citibank Duisburg, Germany)

concrete) or can be fully encased. In hollow sections further shuttering for concrete is not required and show good behavior under fire and therefore is more preferred by structural engineers. Fig.1.16 shows steel section in-filled with concrete column with reinforcements and nails used as shear connectors.

Shear connectors are placed at a level or just below the floor level so that sufficient composite action between the steel and concrete part takes place in the areas of concentrated load. Headed bolts or angle studs can be used for rolled sections. For hollow sections, non headed bolts inserted in holes and welded at the section surface can be used which will serve the function of bar spacers and also will not hamper the concreting process. But welding becomes relatively time consuming process and therefore economic alternative together with Hilti the nailing technique (Fig.1.17) has been developed for the use as shear connectors in hollow column sections. The placement is easy, very fast and it shows good ductility.

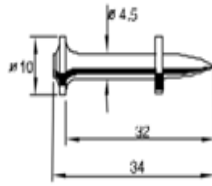


Figure 1.17: HILTI Nail X-DSH32 P10)

1.4.4 Joints

Joints have been regarded traditionally as a part of column but have not been considered in the global calculation. However, since joint essentially consists of parts of column, beams and slab as connecting elements and may also include stiffening elements, their real behavior can only be taken into consideration by defining the joint as a separate element within the structure. This will enable more efficient construction and influence of the joints on the global behavior of structure can be analyzed since the philosophy of perfect hinge or fully continuous restraints does not describe the real behavior of a semi continuous joint (Fig.1.18) . Joints may be assessed with regard to the following three main characteristics:

- **Stiffness:** A joint with vanishing rotational stiffness and which therefore carries no bending moment is called a hinge. A rigid joint is one whose rigidity under flexure is more or less infinite and which thus ensures a perfect continuity of rotations. In between these two extreme boundaries semi -rigid joints are formed.
- **Moment resistance:** In contrast to a hinge, a joint whose ultimate strength is greater than the ultimate resistance of the parts whose linkage it ensures is called a full strength joint. Again a partial strength joint represents a middle course between these extremes.
- **Rotation capacity (ductility):** Brittle behavior is characterized by fracture under slight rotation, usually without plastic deformations. Ductile behavior

is characterized by a clear non-linearity of the moment-rotation curve with a large flat terrain before fracture. It usually indicates the appearance of plastic deformations. The ductility coefficient is the ratio between the ultimate rotation and the elastic rotation limit. Semi-ductility falls in between brittle and ductile behavior.

An example of a connection type is illustrated in Fig.1.19.

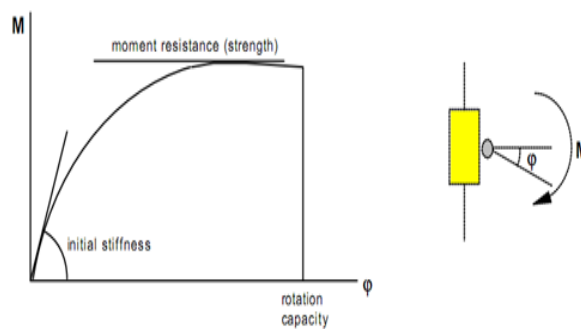


Figure 1.18: Joint Response

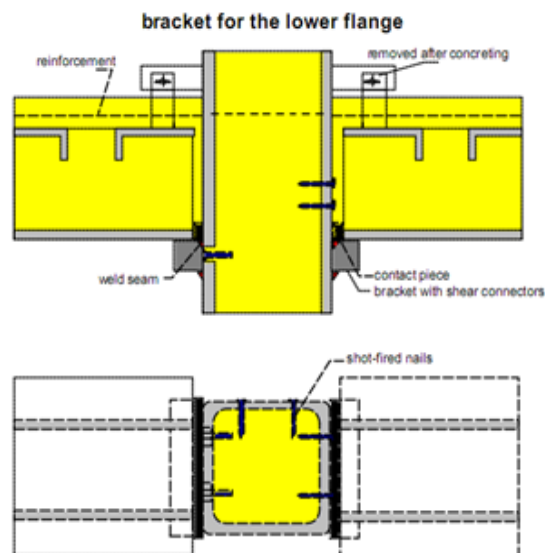


Figure 1.19: Vertical Shear Transfer Between Beams and Composite Columns)

A simple bracket can be welded to the column surface supporting either the beam's upper or lower flange. Bearing on the lower flange requires fire protection to the bracket and in those cases where no suspended ceiling is used the architect might refuse to use a bracket, spoiling architectural appearance. Using a bracket for the upper flange erection difficulty is encountered especially when rigid connection is made.

1.5 Objective of Study

The objective of present work is to understand the behavior of Concrete filled steel tube structure under lateral loading. The main objectives are:

- To study the types of composite columns, which can be used in building structures.
- To understand the behavior of concrete filled tube structural system.
- To understand the principles of the Eurocode 4 "Simplified Method" of design for composite columns.
- To study the confinement effect on concrete due to steel tube.
- To perform parametric study of concrete filled steel tube (CFT) building with different storey heights.
- To do comparative study of CFT, RCC and Steel building.
- To study economy of structure.
- To study its effectiveness in high rise structure.

1.6 Scope of Work

In order to achieve above objectives, scope of major project work is as follows:

- Comparison of capacity of short column in 'STRAP' software with Euro Code 4 and AISC-LRFD provisions.
- Derivation of M-N interaction curve.
- Analysis and design of CFT, RCC and Steel structures with different storey height (10, 20 and 30 storey) using STRAP software (version 12.5).
- Result comparison of CFT, RCC and Steel structure like load intensity, time period, storey displacement, base shear, mode shape, load carrying capacity etc.
- Design the structural members.
- To study the feasibility of CFT structure in terms of number of storey.
- Cost comparisons of CFT, RCC and Steel building.

1.7 Organization of the Report

The report may be viewed as divided into six chapters.

Chapter 1, *Introduction of the concrete filled steel tube structure*. It includes introduction of composite construction methods, history of steel concrete composite building, objective of work and scope of work.

Chapter 2, *Literature review*. It includes literature review for Concrete filled steel tube structure. It provides an overview of the available books, publications, and papers from various journals on this topic. This chapter provides the understanding and behavior of concrete filled steel tube structures.

Chapter 3, *CFT structural system*. It includes general introduction of concrete filled steel tube (CFT) structural system, history of CFT building, confinement effect and construction technology of CFT structure.

chapter 4, *Analysis and design of 10 story building*. It includes column capacity comparison with software and different code (Euro Code EC4 and AISC-LRFD) formula, M-N interaction curve generation and also analysis and design of 10 storey CFT, R.C.C and Steel building and discussion of results.

chapter 5, *Analysis and design of 20 and 30 story building*. It includes Analysis and design of 20 and 30 storey CFT, R.C.C and Steel building and result comparison, cost comparison and detailing of CFT members.

Finally, in **chapter 6** Summary of the study, conclusion and future scope of work.

Chapter 2

Literature Survey

2.1 General

A review of the literature related to the concrete filled steel tube structural systems is presented in this chapter. Different research papers, books, proceedings and guideline, regarding various aspects have been referred to understand the behavior of CFT structural system. The objective of literature review is to develop basic understanding about various parameters like diameter to thickness ratio, concrete confinement effect due to steel, capacity formula based on different codes, analysis methods etc.

2.2 Research Papers

2.2.1 Analytical Work Done on CFT Structure

Choi [6] presented analytical work on lateral interactions between steel tube and filled-in-concrete steel tube under axial compression by preparing a numerical program. He concluded that the behavior of the CFT columns was controlled by both the filled-in-concrete in the columns and strength and confinement effect of steel tube. Various lateral interactions between steel tube and filled-in-concrete in CFT columns were classified into eight different cases by the contact between steel tube and filled-in

concrete at different stress stages.

Shanmugam and Lakshmi [10] presented a review paper on composite columns in which structural steel section was encased in concrete or was infilled in concrete. This paper presented a review of the research carried out on composite columns with data collection of experimental and analytical work done. It also included research work accounting for the effects of local buckling, bond strength, seismic loading, confinement of concrete and secondary stresses on the behavior of steel-concrete composite columns.

Uy [12] discussed investigation of the stability and ductility characteristics of concrete filled columns using high performance steels (HPS) which included both high strength steel and stainless steel having improved strength, corrosion resistance, hardness etc. Both theoretical and experimental analysis proved that use of these steel sections filled with concrete, changed the stability characteristics for both short and slender columns and modified behavior under both local and overall buckling was considered. It also discussed the role of concrete infill in improving the post-peak behavior for both short and slender columns.

2.2.2 Experimental and Analytical Work Done on CFT Structure

Uy [11] presented a comparative study of numerical model prepared based on experiments on concrete filled box type steel tube made of four steel plates of equal length and thickness with fillet weld at edges. A comparison with results of Eurocode 4 was done and this was found to be unconservative in its prediction of axial and combined strength. A mixed analysis technique was therefore presented, which treated the concrete as rigid plastic and the steel as linear elastic. This model calibrated

well with the numerical model presented and both of these models were found to be conservative in predicting the test results.

Luiz et al. [13] discussed an experimental analysis of the confinement effects in steel-concrete composite columns considering parameters like concrete compressive strength and column slenderness. In this paper, sixteen concrete-filled steel tubular columns with circular cross section were tested under axial loading and were filled by concrete with compressive strengths of 30, 60, 80, and 100 MPa, and had length/diameter ratios (L/D) of 3, 5, 7, and 10. The experimental values of the columns ultimate load were compared to Brazilian Code NBR 8800:2008, Eurocode-4 (EN 1994-1-1:2004), AINSI/AISC 360:2005, and CAN/CSA S16-01:2001. The comparison with results showed that the load capacity of the composite columns increased with increasing concrete strength and decreased with increasing length/diameter ratio. Among them, the Brazilian Code was the most conservative, while Eurocode-4 presented the values closest to the experimental results.

Fam, Qie et al. [5] discussed analytical and experimental work on modeling for concrete-filled steel tubes (CFT) subjected to concentric axial compression and combined axial compression and lateral cyclic loading. Evaluation was done for strength and ductility of CFT short columns under different bond and end loading conditions using bonded and unbounded specimens. Application of the axial load was done to the composite steel-concrete section and to the concrete core only. It was observed that axial strengths of the unbounded short columns were slightly increased, compared to those of the bonded ones, while the stiffness of the unbounded specimens was slightly reduced.

Zhijing et al. [14] discussed an experimental and analytical investigation of concrete-filled steel tubular (CFT) laced columns. In this paper, the load deflection curve was obtained by considering four concrete-filled steel tubes that were laced together.

These curves were subsequently used to quantify the structural behavior for each element of the hybrid column. Experimental results indicated that the compression force in the longitudinal members dominated the failure mechanism in the CFT columns while in-plane bending occurred when member segments reached the compression failure load. The forces in the lacing members (diagonal and horizontal bracing) were found to be small and remained in the elastic range through failure. The analytical study showed that increasing slenderness ratios and eccentricities reduced the ultimate load capacity. Additionally, finite-element analysis of CFT columns based on four in situ structures were performed to determine the ultimate load-carrying capacity and were subsequently compared to several building codes. On the basis of the analytical results, a new methodology for calculating the ultimate load-carrying capacity was proposed.

2.3 Summary

In this chapter, brief review of relevant literature was presented. The literature reviews was base on gave the idea of the structural systems, behavior of structure, limitation of length to diameter ratio and diameter to thickness ratio and also the comparative advantage of CFT system.

Chapter 3

Concrete Filled Steel Tube System

3.1 General

In this work, focus was on studying the behavior of composite columns hence they are discussed in details. Composite columns may be classified into two principal types:

- Partially or fully encased section
- Concrete-filled hollow steel sections

Fig.3.1 show different types of composite columns.

Partially or fully encased columns: (Fig.3.1 b and 3.1 c) are in form of steel I- or H-sections, with the void between the flanges filled with concrete. In fully encased columns (Fig. 3.1a) the whole of the steel section is embedded providing a minimum cover of concrete.

Concrete-filled hollow steel sections: (Fig.3.1 d to 3.1 f) can be circular or rectangular in section. Concrete fills the section and its compressive strength is enhanced by its confinement. This is an additional advantage for the compression resistance of the column.

Compared to steel columns, composite column have distinct advantage. For same dimensions, the slender composite column may carry higher axial load while if cross

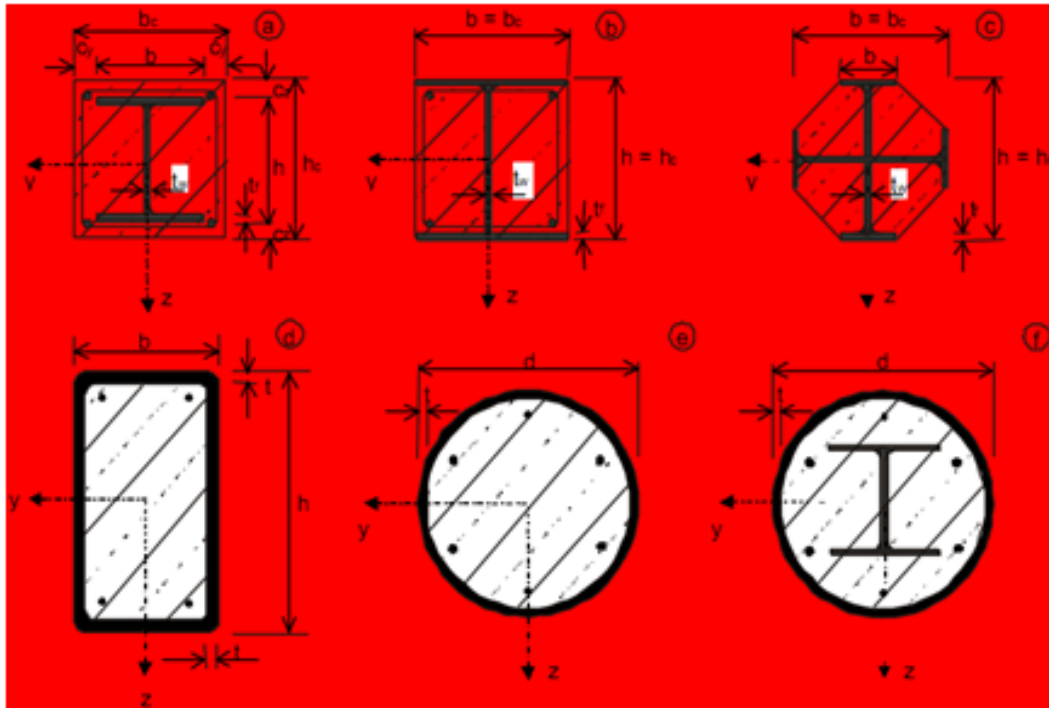


Figure 3.1: Typical Cross-Sections of Composite Columns

sections are different and exterior dimensions are same, variation of loads is possible depending upon the thickness of steel section, strength of concrete and area of reinforcement used. Also dimensions of column can be kept same for several storey's of a building which provides both functional and architectural advantages.

In the case of concrete-filled hollow sections, the steel provides a permanent formwork to the concrete core which allows erection of the steel frame and the hollow column sections subsequently to be filled with pumped concrete. This leads to appreciable savings in the time and cost of erection. In addition, the confinement provided by the closed steel section allows higher strength to be attained by the concrete.

Confinement of concrete is provided by concrete filled tubes particularly of circular sections, which develop hoop tension and increase overall load carrying capacity, though they can be ignored in design but will add to reserve strength. Creep and shrinkage of concrete can also be neglected in concrete filled steel tube design. Com-

plete encasement will also lead to fire protection and will satisfy the most stringent requirements without use of other protection systems. For partially encased sections and for concrete-filled hollow sections, codes of practice on fire resistance require additional reinforcement. In order to ensure adequate force transfer between the steel and concrete it is sometimes necessary to use stud connectors or reinforcement connected directly or indirectly to the metal profile.

Concrete-filled steel tubular (CFT) columns have been increasingly used all over the world due to their inherent advantages, and in particular because of their favorable behavior under seismic loads. The steel tube effectively confines the concrete core, providing a highly ductile response under compression and a high energy absorption capacity. This type of composite column has been used primarily in bridges, reservoirs and tall buildings. However, in structures under fire conditions, these composite columns may require additional protection.

In addition to the mechanical advantages previously mentioned, the use of CFT columns also permits formwork economy, since the steel tube can resist loads during the construction phase when the concrete filling is unable to contribute. Also, in comparison with reinforced concrete columns (RCC), the cross section of CFT columns are smaller.

CFT columns have been studied by researchers like Kloppel and Goder, who established lower and upper limits to predict the strength of concentrically loaded CFT columns. The lower limit was expressed as the buckling load of the transformed area of the composite section and the upper limit was determined by calculating the buckling load considering an equivalent stiffness as the sum of steel and concrete stiffness. Gardner and Jacobson revealed that as the steel tube restrains the concrete core at failure, an internal pressure (σ_r) develops between the steel tube and concrete, creating a tensile hoop stress (σ_t) in the steel tube. Due to this confining effect, the

compressive strength of the concrete would be augmented [13].

Concrete-filled steel tubes (CFT) used in many structural applications including columns supporting platforms of offshore structures, roofs of storage tanks and columns in seismic zones can lead to 60% total saving of steel in comparison to a structural steel system (Zhong, 1988). Steel tubes were also used as permanent formwork and provided well-distributed reinforcement located at the most efficient position (Furlong 1967). Test results (Fam 2000) have shown that the concrete core delays the local buckling and forces steel tube to buckle outwards rather than inwards, resulting in higher flexural strength. Therefore, tubes with thinner walls could reach the yielding strength before local buckling occurs (Lu and Kennedy 1992). Under axial compression, the steel tube confines the concrete, therefore, improves both the axial load resistance and ductility of the CFT members. Fam and Rizkalla (2002) reported a 50% increase in the flexural strength by filling a hollow steel tube with concrete. This can be achieved without significant increase in cost or increase in size. Due to the large shear capacity of concrete-filled steel tubular members, they predominantly fail in flexure in a ductile manner (Tomii and Sakino 1979). Furlong (1967) reported that using expansive cement enhances the bond and provides chemically prestressed elements.

Furlong (1967) reported that when steel tube is axially loaded, the confinement effect gets delayed, until the expansion of concrete is overcomes. Different researchers concluded that confinement effectiveness can be reduced by use of rectangular or square tubes, high strength concrete and increase in slenderness of columns or by pure flexural members. Several mathematical models have been developed to predict the strength of CFST columns, including Furlong(1968), Xiao (1989), and Zhong (1985). Design specifications including CAN/CSA (1994) and AISC LRFD (1998), are very conservative due to the lack of consideration of the confinement effect in CFT [5].

3.2 History of Concrete Filled Steel Tube (CFT) Column

Since 1970, extensive investigations have verified that framing systems consisting of concrete-filled steel tube (CFT) columns have more benefits than ordinary reinforced concrete and steel systems. As a result, this system has very frequently been utilized in the construction of middle- and high-rise buildings in Japan. In 1961, Naka, Kato, et al., wrote the first technical paper on CFT in Japan which discussed a circular CFT compression member used in a power transmission tower. Building Research Institute (BRI) of the Ministry of Construction along with industrial collaboration started a five-year experimental research project called New Urban Housing Project (NUHP), which accelerated the research and use of this system. Another five-year research project on composite and hybrid structures started in 1993 as the fifth phase of the U.S.-Japan Cooperative Earthquake Research Program and the investigation of the CFT column system was included in the program [9].

Recent example of concrete filled steel tube structure use in, World's tallest TV tower also known as Canton tower. China (completed in May 2009). This tower use concrete filled steel tube concept in column, beam and bracing of outer most structure system and height of structure is 600m shown in Fig.3.2 .

3.3 Advantage

The CFT column system has many advantages compared with ordinary steel or reinforced concrete systems.

- Interaction between steel tube and concrete
 - Local buckling of the steel tube is delayed, due to the restraining effect of the concrete. On the other hand, the strength of the concrete is increased due to the confining effect provided by the steel tube.



Figure 3.2: Canton Tower

- Concrete spalling is prevented by the tube.
- Drying shrinkage and creep of the concrete are much smaller than in ordinary reinforced concrete.
- Cross-sectional properties
 - The steel ratio in the CFT cross section is much larger than in reinforced concrete and concrete-encased steel cross sections.
 - The steel of the CFT section is well under bending because it is located most outside the section.
- Construction efficiency
 - Labor for forms and reinforcing bars is omitted, and concrete casting is done by Tremie tube or the pump-up method. This efficiency leads to a

cleaner construction site and a reduction in manpower, construction cost, and project length.

- Shuttering material is not used so ultimate reduction in material cost.
- Fire resistance
 - Concrete improves fire resistance so CFT column is fireproof compared to steel structure.
- Cost performance
 - Because of the merits listed above, better cost performance is obtained by replacing a steel structure with a CFT structure.
- CFT column reduce large amount of steel required to support a given design load.
- Dimensions of CFT column are smaller than reinforced concrete column, so increasing available floor space.
- Ecology
 - The environmental burden can be reduced by omitting the formwork and by reusing steel tubes and using high-quality concrete with recycled aggregates.

3.4 Features of Concrete Filled Structural System

The Concrete filled steel tube structural system consists of compression member, beam-columns, connection between them, frames. Salient features of each are discussed below [9]:

- **Compression members:**

In centrally loaded circular short column, the difference between ultimate strength and nominal crushing load is obtained by the confining effect and estimated as a linear function of the steel tube yield strength. For a square short column, increase in strength due to the confining effect is much less compared to a circular short column as local buckling significantly affects the strength of a square short column. The buckling strength of a CFT long column can be evaluated as the sum of the tangent modulus strengths calculated for a steel tube long column and a concrete long column, separately. Confining effect on the buckling strength was not observed regardless of the cross-sectional shape. Elastic axial stiffness can be evaluated by the sum of the stiffness of the steel tube and the concrete. However, factors affecting stiffness like the effects of stresses generated in the steel tube at the construction site, the mechanism which transfers beam loads to a CFT column through the steel tube skin, creep and drying shrinkage of the concrete must be considered. Constitutive laws for concrete and steel in a CFT column have been established that take into account the increase in concrete strength due to confinement, the scale effect on concrete strength, the strain softening in concrete, the increase in tensile strength and decrease in compressive strength of the steel tube due to ring tension stress, the local buckling of the steel tube, the effect of concrete restraining the progress of local buckling deformation, and the strain hardening of steel.

- **Construction of CFT column with footing:**

The connection of CFT column with footing can be constructed by placing the concrete in two lifts as illustrated in Fig.3.3. First the lower lift is cast, and the tube is then temporarily attached to the lower lift by anchor bolts. Then the remainder of the footing and concrete fill of the tube are cast in a second lift. Fig.3.4 shows different type of column to footing connection.

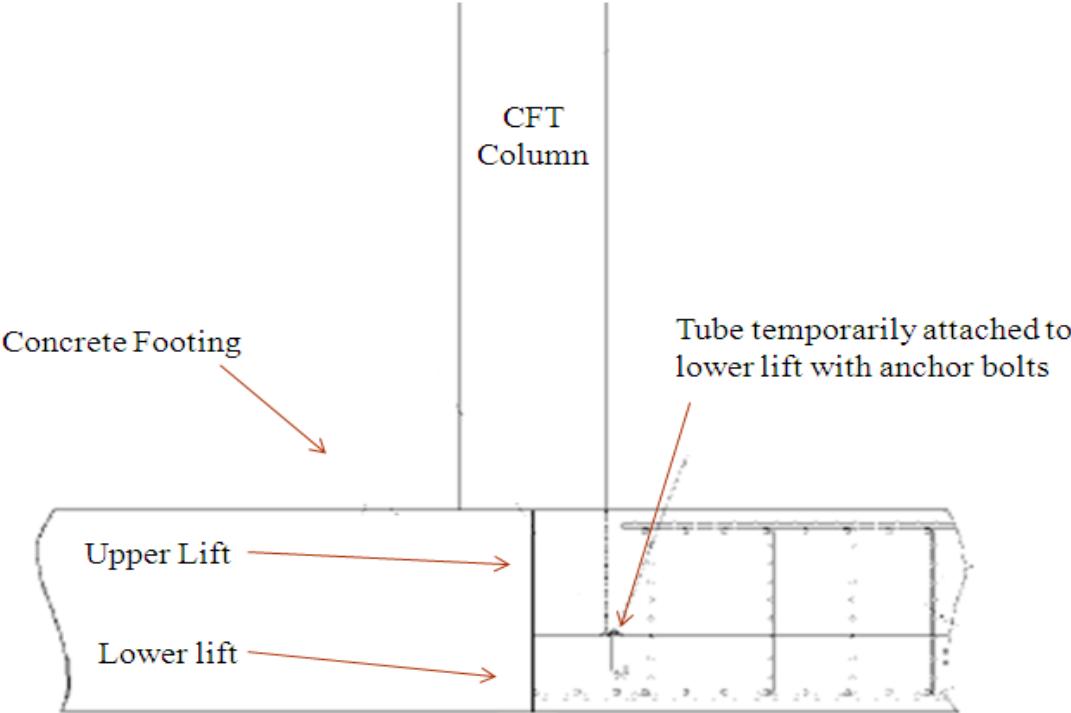


Figure 3.3: CFT Column With Footing

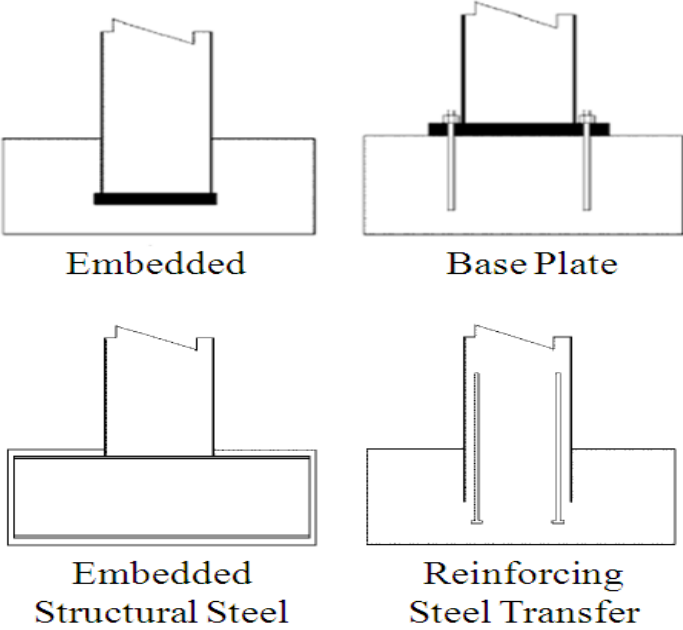


Figure 3.4: Type of Footing

- **Beam-to-column connections:**

Design formulas have been established for outer and through diaphragms and the ring stiffener. Yield line theory have been used to propose formulae for strength evaluation for inner diaphragms. To find the load-deformation behavior of a CFT column sub-assembly, consisting of a diagonal concrete strut and a surrounding steel frame formed by tube walls and diaphragms stress mechanism is used. Several new types of connections like connections using vertical stiffeners, long tension bolts, and a thicker tube at the shear panel without a diaphragm are used. Generally use bolted connection or welded connection shown in Fig.3.5.

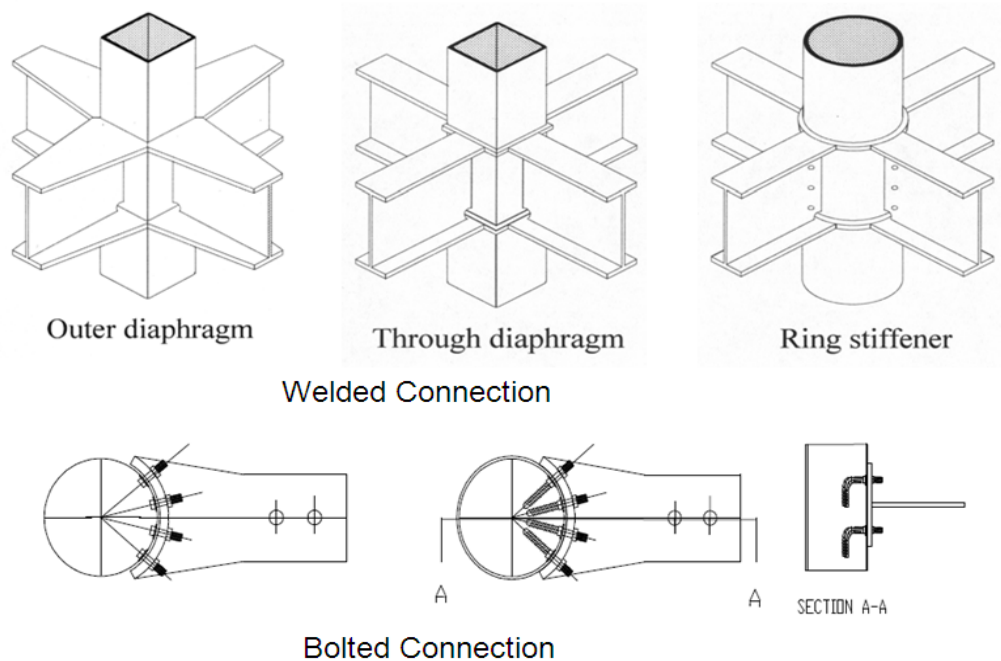


Figure 3.5: Type of Connection

- **Beam-columns:**

Bending strength in beam column of circular cross section exceed the superimposed strength (sum of strength of concrete and steel tube) due to confining effect compared to square cross sectional area CFT beam column. Also effect of

local buckling was more significant in square CFT beam-column, while ductility was smaller. It was also researched that though use of high strength concrete gave reduction in ductility in general, in case of circular cross section its non-ductile behavior can be improved by confining concrete in high strength steel tubes. Empirical formulas to estimate the rotation angle limit of a CFT beam-column have been proposed. Based on constitutive laws flexural behavior and ultimate strength of an eccentrically loaded CFT column was also established. Neglecting the effect of local buckling of steel tube, mathematical model has been established considering combined compression, bending, and shear. A hysteretic restoring force characteristic model for a CFT beam-column has been proposed, which accurately predicts the behavior when the rotation angle is less than 1.0%. Some of site photo shows in Fig.3.6.



Figure 3.6: Shop-fabricated CFT Joint

- **Frames:**

Tests of sub-assemblages showed ductile behavior in case where shear panels were designed to be weaker than beams and columns. Practically this can be achieved when steel tube thinner than the CFT column is used for the shear panel. The energy dissipation capacity of a column- failing CFT frame is equivalent to that of a steel frame.

- **Design characteristics:**

The lateral storey stiffness of the CFT column system was larger compared to the steel system, but the storey weight increased. This leads to no major differences in the vibration characteristics of either system. No significant difference in elasto plastic behavior or energy dissipation capacity was observed between the CFT and steel systems as long as the overall frame mechanism was designed so plastic hinges mainly form in the beams. Total steel weight of the CFT column system is about 10% less than that of the steel system.

- **Quality of concrete and casting:**

The bleeding of concrete underneath the diaphragm may produce a gap between the concrete and steel and therefore concrete with a small water-to-cement ratio should be used. Use of super plasticizer is effective to keep good workability. The pumping-up method is recommended to cast compact concrete without a void area underneath the diaphragm. Lateral pressure on the steel pipe caused by pumping usually increases the liquid pressure of concrete (the unit weight of fresh concrete times the casting height) up to 1.3 times, which causes ring tension stress in the steel tube. The pressure and stress may distort the square shape of the tube if the wall thickness of the tube is too thin. When the casting height is not too high, the tremie tube method is effective with the use of a vibrator to obtain compact concrete. If the vibrator is not used, it is necessary to cast the concrete with high flow ability and resistance against segregation.

- **Fire resistance:**

CFT columns elongate at an early stage of heat loading, and then shorten until failure. CFT columns can sustain axial load from filled concrete after the capacity of the steel tube is lost by heating thus fireproof material use can be reduced or omitted. Rigidity at the beam-to-column connection reduces because of the heat loading, which leads to the reduction of bending moments transferred from beams to columns. Thus, the column carries only axial load at the final stage of heat loading. Fire tests of CFT beam-columns which were forced to sway by the thermal elongation of adjacent beams have shown that square and circular CFT beam-columns could sustain the axial load for two hours and one hour, respectively, under an axial load ratio of 0.45 and a sway angle of 1/100, but CFT beam-columns could not resist bending caused by the forced sway after 30 minutes of heating.

3.5 Confinement Effect

The confinement introduced by the steel tube in the concrete core is an important aspect of the structural behavior of CFT columns. The confinement effect in the first stages of loading can be neglected, since the Poisson coefficient of the concrete is smaller than the steel's coefficient. Therefore, the steel tube expands faster than the concrete core in the radial direction and the steel tube does not restrain the concrete core. At this point, the steel tube is subjected to compressive stresses, with no separation between the tube and the concrete core. However, when the applied load reaches the level of the uniaxial strength of the concrete, the micro cracking of concrete is increased. In this situation, the lateral expansion of the concrete reaches its maximum, mobilizing the steel tube and efficiently confining the concrete core. In this way, the ultimate capacity of the CFT columns is higher than the sum of the resistance of their components, which are the steel tube ($A_a \cdot f_y$) and the concrete core ($A_c \cdot f_{ck}$) [13].

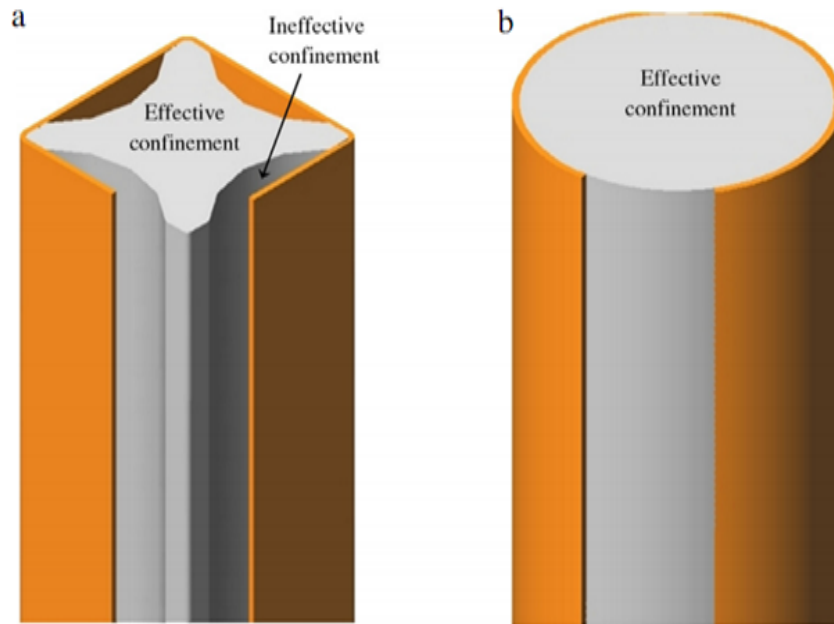


Figure 3.7: Effectively Confined Concrete for CFT Columns

The lateral stress introduced by the steel tube is responsible for the additional resistance of the concentrically loaded CFT columns. In this situation, the concrete core is subjected to a triaxial stress state, while the steel tube is in a biaxial stress state. Only the circular CFT columns present this gain of load capacity due to confinement effect, as shown in Fig.3.7(b). The square and rectangular cross sections do not show this behavior, as shown in Fig.3.7(a) (the separation of steel and concrete is little exaggerated in the caption). The plane portions of the steel tube of the square sections are not rigid enough to resist the internal pressures due to the expansion of the concrete core; therefore, only the concrete in the center and in the corners of the cross section are effectively confined.

Fig.3.8 shows the three states of response observed in the load vs. displacement curve: linear elastic, inelastic to the maximum load and inelastic softening.

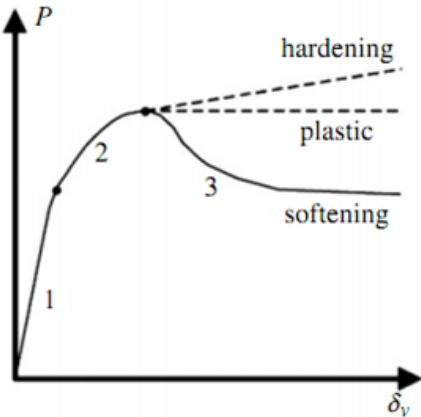


Figure 3.8: Schematic Load-Deformation Relation for CFT Column

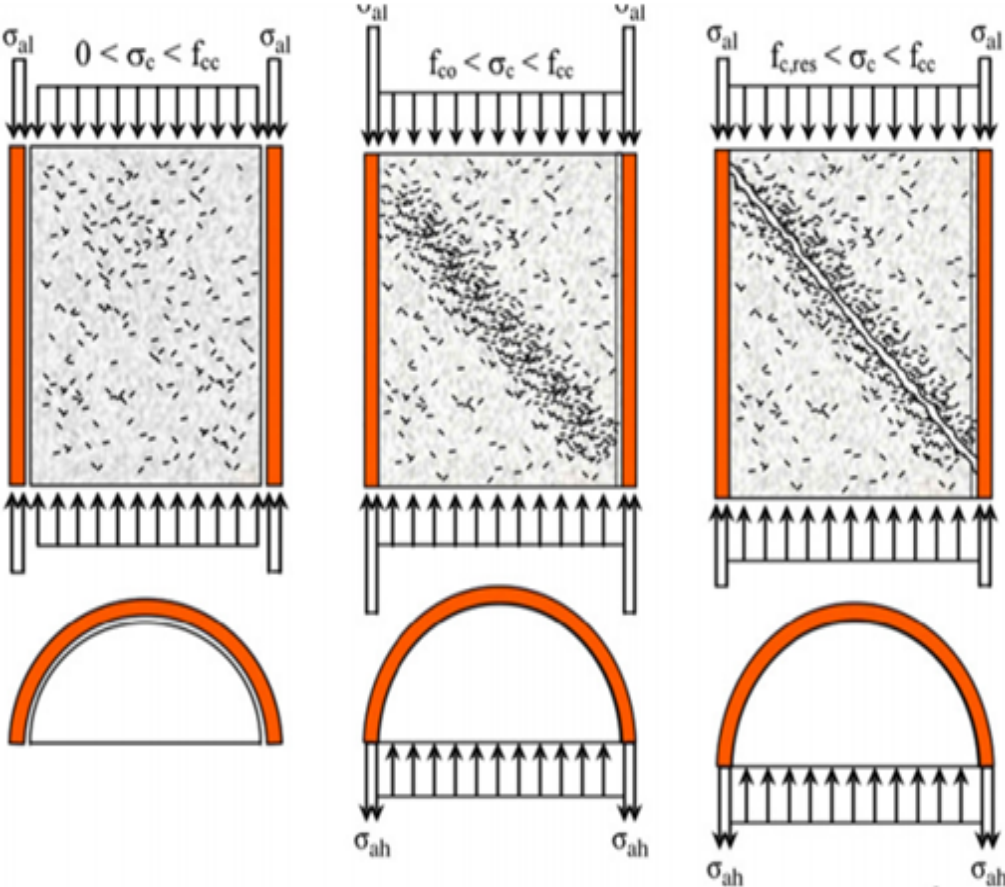


Figure 3.9: Fracture Process in Concrete Core During Phases of Loading

Under axial compression (Fig.3.9(a)), the failure mode of the unconfined concrete is due to a combination of shear and splitting failures, frequently causing a sudden drop in the load vs. displacement curve (softening). Under confinement, the concrete splitting failure is avoided, even for the lower confinement level, and the shear failure is dominant (Fig.3.9(b)). In this way, the shear damage starts near the maximum stress and occurs in a restricted zone of the CFT column. The behavior of the confined concrete in the descending branch depends on the cracking level at this zone. With increasing cracking, the concrete core is divided into two volumes laterally restrained by the confinement stresses (Fig.3.9(c)). Therefore, the residual resistant capacity is a result of the equilibrium between the already damaged concrete and the confinement stresses.

3.5.1 Confinement Parameters

The concrete confinement provided by the steel tube depends on such parameters, like

- Diameter-to-thickness ratio (d/t)
- Length-to-diameter ratio (L/d)
- Eccentricity of the load (e/d)
- Strength and deformability of the materials
- Cross section shape

3.6 Methodology for Design

Eurocode 4 provides two methods for calculation of the resistance of composite columns. The first is a **General Method** which takes explicit account of both second-order effects and imperfections. This method can in particular be applied to

columns of asymmetric cross-section as well as to columns whose section varies with height. It requires the use of numerical computational tools, and can be considered only if suitable software is available. The second is a **Simplified Method** which makes use of the European buckling curves for steel columns, which implicitly take account of imperfections. This method is limited in application to composite columns of bisymmetric cross-section which does not vary with height. Assumptions used in these two methods are :

- There is full interaction between the steel and concrete sections until failure occurs.
- Geometric imperfections and residual stresses are taken into account in the calculation, although this is usually done by using an equivalent initial out-of-straightness or member imperfection.
- Plane sections remain plane whilst the column deforms.

Only the Simplified Method will be applicable to the majority of practical cases and hence elaborated.

3.6.1 Local Buckling of Steel Elements

The presence of concrete firmly held in place prevents local buckling of the walls of completely encased steel sections, provided that concrete cover thickness was adequate. This thickness should not be less than the larger of the two following values:

- 40 mm.
- One sixth of the width 'b' of the flange of the steel section.

This cover, provided primarily to prevent premature separation of the concrete must be laterally reinforced, to protect the encasement against damage from accidental impact and to provide adequate restraint against buckling of the flanges. For partially

encased sections and concrete-filled closed sections, the slenderness of the elements of the steel section must satisfy the following conditions:

- $d/t \leq 90\varepsilon^2$ (concrete-filled circular hollow sections of diameter d and wall thickness t).
- $d/t \leq 52\varepsilon$ (concrete-filled rectangular hollow sections of wall depth d and thickness t).
- $d/t_f \leq 52\varepsilon$ (partially encased H-sections of flange width b and thickness t_f).

In which $\varepsilon = \sqrt{\frac{235}{f_y}}$, where f_y is the characteristic yield strength of the steel section. Since Eurocode-3 uses buckling curve of simplified method effect of local buckling of steel elements is taken into account.

3.6.2 Limitation of Simplified Method

- The column cross-section must be prismatic and symmetric about both axes over its whole height, with its ratio of cross-sectional dimensions in the range $5.0 > \frac{h_c}{b_c} > 0.2$.
- The relative contribution of the steel section to the design resistance of the composite section, given by $\delta = \frac{(A_a * f_y \div \gamma_a)}{N_{pl,rd}}$ must be between 0.2 and 0.9.
- The relative slenderness λ of the composite column must be less than 2.0.
- For concrete-encased sections, the area of longitudinal reinforcement must be at least 0.3% of the concrete cross-section area, and the concrete cover must satisfy the following limits:
 - In the Y-direction: $40mm \leq c_y \leq 0.4b_c$
 - In the Z-direction: $40mm \leq c_z \leq 0.4h_c$

3.7 Composite Columns Subject to Axial Compression

3.7.1 Resistance of the Cross-Section

The cross-sectional resistance of a composite column to axial compression is the aggregate of the plastic compression resistances of each of its constituent elements as follows:

For fully or partially concrete-encased steel sections:

$$N_{pl.Rd} = A_a \frac{f_y}{\gamma_{Ma}} + A_C \cdot 0,85 \frac{f_{ck}}{\gamma_c} + A_s \frac{f_{sk}}{\gamma_s} \quad (3.1)$$

For concrete-filled hollow sections:

$$N_{pl.Rd} = A_a \frac{f_y}{\gamma_{Ma}} + A_C \frac{f_{ck}}{\gamma_c} + A_s \frac{f_{sk}}{\gamma_s} \quad (3.2)$$

In which A_a , A_c and A_s are respectively the cross-sectional areas of the steel profile, the concrete and the reinforcement. The increase of concrete resistance from $0.85f_{ck}$ to f_{ck} for concrete-filled hollow sections is due to the effect of confinement.

For a concrete-filled circular hollow section, a further increase in concrete compressive resistance is caused by hoop stress in the steel section. This happens only if the hollow steel profile is sufficiently rigid to prevent most of the lateral expansion of the concrete under axial compression. This enhanced concrete strength may be used in design when the relative slenderness λ of a composite column composed of a concrete-filled circular tube does not exceed 0.5 and the greatest bending moment $M_{max.Sd}$ (calculated using first-order theory) does not exceed $0.1N_{Sd}d$, where d is the external diameter of the column and N_{Sd} the applied design compressive force. The plastic compression resistance of a concrete-filled circular section can then be calculated as:

$$N_{pl.Rd} = A_a \eta_a \frac{f_y}{\gamma_{Ma}} + A_C \frac{f_{ck}}{\gamma_c} \left[1 + \eta_c \frac{t}{d} \frac{f_y}{f_{ck}} \right] + A_s \frac{f_{sk}}{\gamma_s} \quad (3.3)$$

In which t represents the wall thickness of the steel tube. The coefficients η_a and η_c are defined as follows for $0 < e \leq d/10$, where $e = M_{max.Sd}/N_{Sd}$ is the effective eccentricity of the axial compressive force:

$$\eta_a = \eta_{ao} + (1 - \eta_{ao})\left(10\frac{e}{d}\right) \quad (3.4)$$

$$\eta_c = \eta_{co} + \left(1 - 10\frac{e}{d}\right) \quad (3.5)$$

When $e > d/10$ it is necessary to use $\eta_a = 1.0$ and $\eta_c = 0.0$. In equations 3.4 and 3.5 above the terms η_{ao} and η_{co} are the values of η_a and η_c for zero eccentricity e . They are expressed as functions of the relative slenderness λ as follows:

$$\eta_{ao} = 0.25(3 + 2\lambda) \leq 1 \quad (3.6)$$

$$\eta_{co} = 4.9 - 18.5\lambda + 17\lambda^2 \geq 0 \quad (3.7)$$

Bending moment M_{Sd} reduces the average compressive stress in column at failure stage, thereby reducing the favorable effect of hoop compression on its resistance. The effects of eccentricity and slenderness respectively on load carrying capacity can be taken into consideration by factors η_a and η_c , and on η_{ao} and η_{co} .

3.7.2 Relative Slenderness of a Composite Column

The elastic critical load N_{cr} of a composite column is calculated using the usual Euler buckling equation.

$$N_{cr} = \frac{\pi^2(EI)_{eff.k}}{L_{fl}^2} \quad (3.8)$$

in which $(EI)_{eff.k}$ is the bending stiffness of the composite section about the buckling axis considered, and L_{fl} is the buckling length of the column. If the column forms part of a rigid frame this buckling length can conservatively be taken equal to the system length L . For short term loading the effective elastic bending stiffness $(EI)_{eff.k}$

of the composite section is given by:

$$(EI)_{eff,k} = E_a I_a + K_e E_{cm} I_c + E_s I_s \quad (3.9)$$

For long-term loading the bending stiffness of the concrete is determined by replacing the elastic modulus E_{cd} with a lower value E_c which allows for the effect of creep and is calculated as follows:

$$E_c = E_{cm} \frac{1}{1 + \frac{N_{G,sd}}{N_{sd}} \varphi t} \quad (3.10)$$

where $N_{G,sd}$ is the permanent part of the axial design loading N_{sd} . The term φt is a creep coefficient defined in Eurocode-2, which depends on the age of the concrete at loading and at the time considered; for a practical building column it should normally be sufficient to consider the column at infinite time.

The relative slenderness 'l' of a composite column in the plane of bending considered is given by

$$\lambda = \sqrt{\frac{N_{pl,RK}}{N_{cr}}} \quad (3.11)$$

3.8 Resistance to Compression and Bending

- Cross-section resistance under moment and axial force

Requirements of resistance in each of principal planes is satisfied taking slenderness, bending moment diagram and bending resistance in plane under consideration. M-N interaction curve shown in Fig.3.10 represents the cross sectional resistance of a composite column under axial compression and uniaxial bending.

The point D on this interaction curve corresponds to the maximum moment resistance $M_{max,Rd}$ that can be achieved by the section. This is greater than $M_{pl,Rd}$ because the compressive axial force inhibits tensile cracking of the concrete, thus enhancing its flexural resistance.

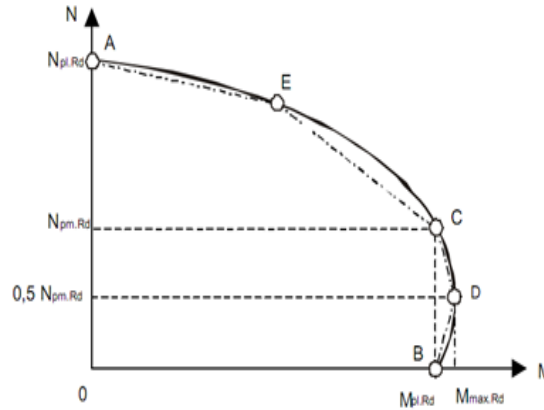


Figure 3.10: M-N Interaction Curve for Uniaxial Bending

The above interaction curve can be determined point by point, by considering different plastic neutral axis positions in the principal plane under consideration. The concurrent values of moment and axial resistance are then found from the stress blocks, together with the two equilibrium equations for moments and axial forces. Fig.3.11 illustrates this process for the example of a concrete-encased section, for four particular positions of the plastic neutral axis corresponding respectively to the points A, B, C, D marked on Fig.3.10.

- Point A : Axial compression resistance alone:

$$N_A = N_{pl.Rd}$$

$$M_A = 0$$

- Point B : Uniaxial bending resistance alone:

$$N_B = 0$$

$$M_B = M_{pl.Rd}$$

- Point C : Uniaxial bending resistance identical to that at point B, but with non-zero resultant axial compression force:

$$N_C = N_{pm.Rd} = A_c * 0.85 * f_{ck} / \gamma_c \text{ (for Concrete encased section)}$$

$$N_C = N_{pm.Rd} = A_c * f_{ck} / \gamma_c \text{ (for Concrete filled section)}$$

$$M_C = M_{pl.Rd}$$

Note: f_{ck} may be factored by $[1 + \eta_c * \frac{t \cdot f_y}{d \cdot f_{ck}}]$ for a circular concrete-filled hollow section.

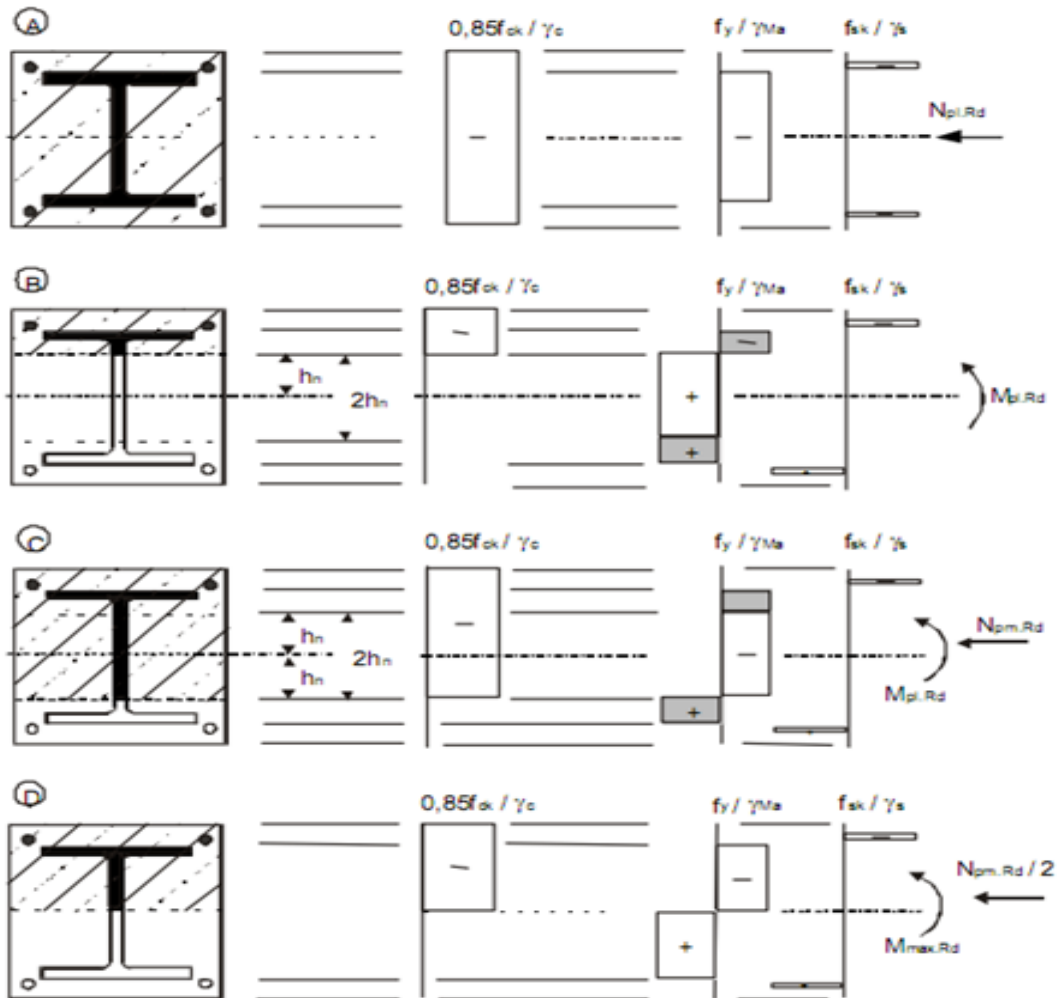


Figure 3.11: Development of Stress Blocks at Different Points on The Interaction Curve (Concrete Encased Section)

- Point D : Maximum moment resistance:

$$N_D = 0.5 * N_{pm,Rd} = 0.5 * A_c * 0.85 * f_{ck} / \gamma_c \text{ (for Concrete encased section)}$$

$$N_D = 0.5 * N_{pm,Rd} = 0.5 * A_c * f_{ck} / \gamma_c \text{ (for Concrete filled section)}$$

Again f_{ck} may be factored by $[1 + \eta_c * \frac{t \cdot f_y}{d \cdot f_{ck}}]$ for a circular concrete-filled hollow section.

$$M_D = W_{pa} \cdot \frac{f_y}{\gamma_a} + W_{ps} \cdot \frac{f_s}{\gamma_s} + 0.5 * W_{pc} \cdot \frac{f_{ck}}{\gamma_c}$$

in which W_{pa} , W_{ps} , and W_{pc} are the plastic modular respectively of the steel section, the reinforcement and the concrete.

- Point E : Situated midway between A and C:

The enhancement of the resistance at point E is little more than that given by direct linear interpolation between A and C, and the calculation can therefore be omitted. It is usual to substitute the linearized version AECDB (or the simpler ACDB) shown in Fig.3.10 for the more exact interaction curve, after doing the calculation to determine these points.

3.9 Observation of Behavior of CFT Building up to 60m Height by ANUHT [9]

In Japan, Association of New Urban Housing Technology (ANUHT) was established in 1996 for inspecting the structural and fire resistance designs of newly planned CFT buildings shorter than 60m and authorizing the construction of those structures. In addition to these inspection works, the Association provided CFT system design and construction technology, education to the member companies, and promoted research on the CFT system. In the construction data, collected by the Association, structural designs of 175 CFT buildings were inspected by the Association from April 1998 to March 2002. For buildings taller than 60m, inspection was done by the Building Center of Japan.

Observations made from the data for the CFT buildings shorter than 60m were as follows:

- From 175 buildings it was found that about 65% were shops and offices, and their total floor area constituted about 60% of the total floor space. Application of CFT to those buildings indicated the building designers' recognition of the

effectiveness of the CFT system for long spans in buildings with large open spaces.

- The CFT system was not very often applied to brace frame buildings. It was observed that use of braces was not necessary since the tube section has identical strength and stiffness in both x- and y-directions. Also use of structural walls with the CFT system was not common.
- The floor area supported by one column was much larger than in ordinary reinforced concrete or pure steel buildings. The floor area per column exceeds $90m^2$ in about 40% of all residential and office buildings emphasizing again the application of the CFT system to buildings with large open spaces.
- A wide variety of aspect ratios (ratio of the longer distance between two columns to the shorter one in x- and y-directions of a floor plan) of span grids indicated the CFT system's potential for free planning about the span grid. In the case of office buildings, 40% had rectangular span grid of $8m * 18m$ used and the aspect ratio exceeds 2.2 , while the span grid of shop buildings was nearly square in about 50% of cases.
- Both square and circular sections are used together in a number of buildings. The size of the tube section often used was between 500 and 700mm in the case of square CFT columns. Circular tubes (diameter: 400 to 1117mm; diameter-thickness ratio: 16 to 90) are mainly used for buildings with irregular plan grids, and square and rectangular tubes (width: 300 to 950mm; width-thickness ratio: 10 to 54) were used for the case of regular plans. Most tubes were cold-formed, since they were inexpensive and widely available. Box sections built-up by welding were used when the plate becomes thick and or large ductility was required. Cast-steel tubes were used to simplify the beam-to-column connection.
- Inner or through diaphragms were used in most beam-to-column connections (about 80% of cases). The type of diaphragm used seems to be determined

by the plate thicknesses of the column and the beam: the through diaphragm was often employed when the beam flange was thicker than the column skin plate; otherwise, the inner diaphragm was employed. The through diaphragm is usually used for cold- formed tubes and the inner diaphragm for built-up tubes. Inner and through diaphragms have openings with diameters of 200 to 300mm for concrete casting, and several small holes for air passage. The outer diaphragm was used as an easy solution, which ensures compaction of the concrete.

- Embedded column bases are the most widely used, as they are the most structurally reliable. This trend also indicated that the CFT system was often applied to large-scale buildings. If the building had basement stories, encased column bases were often employed, in which column tube sections were changed to cross-H sections, and CFT columns become concrete encased steel columns in the basement.
- The ratio of the column effective length to the column depth was much larger than that in ordinary reinforced concrete or pure steel buildings. This difference indicates the relatively large axial load-carrying capacity of the CFT column.
- The design standard strength of steel most often used was 325MPa and that of concrete was 36 and 42MPa.

Chapter 4

Analysis and Design of 10 Storey Building

4.1 General

In this chapter capacity comparison of short column with software and different code formula results like Euro Code EC-4 and AISC-LRFD is included. M-N interaction curve and its graphical representation is done by taking a small column element and applying axial force and moment on it. Analysis and design of 10 storey CFT, RCC and Steel building and result discussion also modeling step and cost comparison is included.

4.2 CFT Column Capacity Comparison

Circular concrete filled steel tube column is used in this project, hence its capacity comparison is done with software (STRAP) and different other code provisions (EC-4 & AISC-LRFD).

CFT column under concentric load with compressive strength of 32.7 MPa and $\frac{L}{d}$ ratio of 3 is used to determine load carrying capacity of CFT column. The main geometric characteristics of the tested specimens are $d = 114.3$ mm and thickness of

steel tube $t = 3.35$ mm.

Design Data :

Column diameter $d = 114.3$ mm

Thickness $t = 3.35$ mm

$L/d = 3$

$f_y = 287.33$ N/mm²

$f_{ck} = 32.7$ N/mm²

$E_s = 206:000$ N/mm²

$A_c = 9088.54$ mm²

$A_a = 1167.1$ mm²

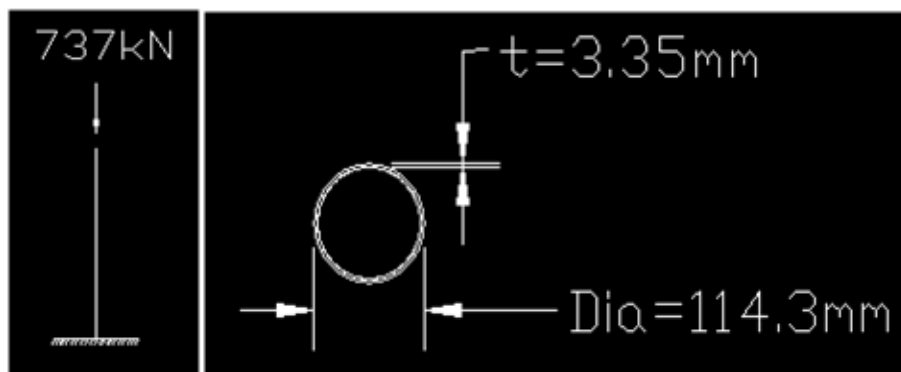


Figure 4.1: Geometric Characteristics of the Cross-Section

- **According to Provisions of Eurocode-4:** The “design” plastic axial resistance of the section N_{pl} is evaluated by dividing the “characteristic” strength of material f_y , f_{sk} , and f_{ck} by means of the partial safety factors as follows [7]:

– **Circular hollow steel section:**

$$\frac{d}{t} \leq 90 \cdot \sqrt{\frac{235}{f_y}} \quad (4.1)$$

$$\frac{d}{t} = \frac{114.3}{3.35} < 90 \sqrt{\frac{235}{287.33}}$$

$$\frac{d}{t} = 34.12 < 81.39$$

Hence OK

– **Concrete filled sections:**

$$N_{pl} = \frac{f_y \cdot A_a}{1.18} + \frac{f_{sk} \cdot A_s}{1.18} + \frac{f_{ck} \cdot A_c}{1.38} \quad (4.2)$$

$$N_{pl} = \frac{287.33 \cdot 1167.1}{1.18} + 0 + \frac{32.7 \cdot 9088.54}{1.38}$$

$$N_{pl} = 499.5 \text{ kN}$$

- **According to Provisions of AISC:** The resistance of the section is computed as the product of the “nominal strength” of the materials f_y , f_{sk} , and f_{ck} .

– **Circular hollow steel section:**

$$\frac{d}{t} \leq 85 \cdot \sqrt{\frac{235}{f_y}} \quad (4.3)$$

$$\frac{d}{t} = \frac{114.3}{3.35} < 85 \sqrt{\frac{235}{287.33}}$$

$$\frac{d}{t} = 34.12 < 76.87$$

Hence OK

– **Concrete filled sections:**

$$N_{pl} = 0.85 \cdot (f_y \cdot A_a + f_{sk} \cdot A_s + f_{ck} \cdot A_c) \quad (4.4)$$

$$N_{pl} = 0.85 * (287.33 * 1167.1 + 0 + 0.85 * 32.7 * 9088.54)$$

$$N_{pl} = 499.76 \text{ kN}$$

- According to STRAP Software Result:

Table 4.1: Axial Load Carrying Capacity

DESIGN	EQUATION	FACTORS	VALUES	CAPACITY RATIO
Axial Force	$\frac{N_{sd}}{N_{b.rd}} < 1.0$	$(k_L/r)_x = 10$ $(k_L/r)_y = 10$ $X_{fy} = 471$	$N_{sd} = 737.00$ $A_g = 11.68$ $N_{b.rd} = \mathbf{500.76}$	1.47

- Software Result Comparison With EC-4 and AISC Codal Provisions

Table 4.2: Column Capacity Result

Result compare	STRAP	EC-4	AISC
Column capacity (kN)	500.76	499.5	499.76

4.3 M-N Interaction Curve[8]

Eurocode-4 procedure is used to develop M-N interaction curve with reference to bending moment pattern and axial load, in a circular concrete-filled cross-section, It is analyzed as follows. The column is characterized by the following conditions:

- Length $L = 4000$ mm
- Restraints: fixed at the lower end and simply supported at the top end in both vertical planes
- Axial load: $N = 850$ kN
- Bending moment: linear pattern as illustrated in Fig.4.2 characterized by $M = 140$ kN.m at the top end and $M = -70$ kN.m at the bottom end.

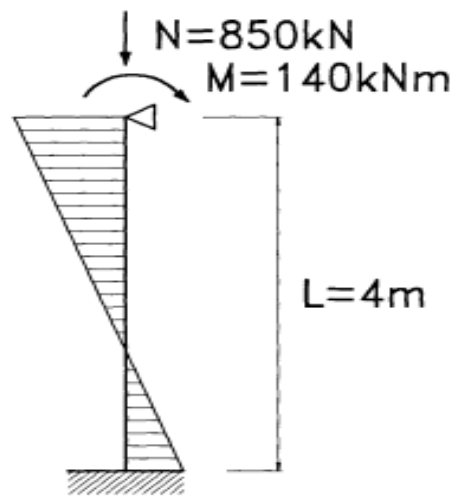


Figure 4.2: Distribution of Bending Moment in the Column

Materials are characterized by the following characteristic strength, design strength, and elasticity modulus:

- Structural steel: $f_y = 355$ N/mm², $E_a = 210000$ N/mm²
- Concrete: $f_{ck} = 30$ N/mm², $E_c = 27386$ N/mm²

Circular steel section filled of concrete is characterized by the dimension column diameter $d = 250\text{mm}$, and thickness of steel tube $t = 5\text{mm}$ as shown in Fig.4.3

$$A_a = 3846.5 \text{ mm}^2 \text{ and } A_c = 45216 \text{ mm}^2$$

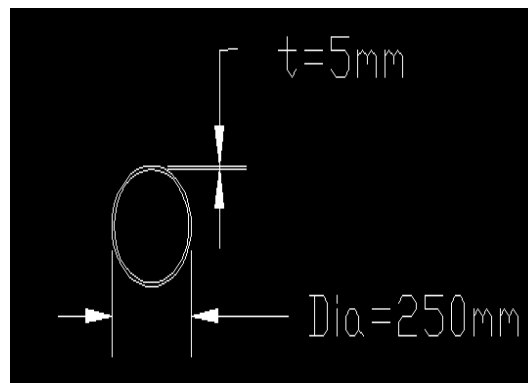


Figure 4.3: Geometric Characteristics of the Cross-Section

1 Application of the Simplified Rules and Shear Interaction

The plastic axial resistance of the cross section

Concrete filled sections:

$$N_{pl} = (f_y * A_a / 1.18) + (f_{sk} * A_s / 1.18) + (f_{ck} * A_c / 1.38)$$

$$N_{pl} = \mathbf{2140.2kN}$$

The local slenderness is:

$$d/t \leq 90 * \sqrt{(235/f_y)}$$

$$d/t = 250/5 < 90 * \sqrt{(235/355)}$$

$$= 50 < 73.2$$

Hence OK

Thus, the simplified method of Eurocode-4 can be applied. However, it should be observed that: the design value of shear is

$$v = (140+70)/4$$

$$v = 52.5 \text{ kN}$$

2 Determination of the M-N Interaction Curve

The evaluation of interaction M-N curve requires the definition of a number of couple (M-N) by using the two equations of equilibrium and the Bernoulli assumption. The full interaction curve of the cross-section defined in this example can be evaluated point by point by means of a numerical procedure, as illustrated in Fig.4.4 In this case, the linear curve by means of the points A, B, C, and D defined as follows:

Point A: ($N = N_{pl}$; $M = 0$)

Point B: ($N = 0$; $M = M_{pl}$)

Point C: ($N = N_{pl.c}$; $M = M_{pl}$)

Point D: ($N = N_{pl.c}$; $M = M_{max}$)

The resistance of the concrete area $N_{pl.c}$

$$N_{pl.c} = f_{ck} * A_c / 1.5$$

$$N_{pl.c} = 30 * 45216 / 1.5$$

$$N_{pl.c} = \mathbf{904 \text{ kN}}$$

$$M_{max} = W_a f_y + W_s f_{sk} + \frac{W_c}{2} . 85 . f_{ck} \quad (4.5)$$

$$M_{pl} = (W_a - W_{a.n}) . f_y + (W_s - W_{s.n}) . f_{sk} + \frac{1}{2} . (W_c - W_{c.n}) . 0.85 . f_{ck} \quad (4.6)$$

Where,

$$W_a = 2[b.t.(\frac{b-t}{2}) + (\frac{b-t}{2})^2.t] \quad (4.7)$$

$$W_a = 450250 \text{ mm}^3$$

$$W_c = \frac{(b-2.t)^3}{4} \quad (4.8)$$

$$W_c = 3456000 \text{ mm}^3$$

$$W_{c.n} = (b-2.t).45^2 \quad (4.9)$$

$$W_{c.n} = 138200 \text{ mm}^3$$

$$W_{a.n} = b.45^2 - W_{c.n} \quad (4.10)$$

$$W_{a.n} = 5800 \text{ mm}^3$$

Put value in above equation 4.5 and 4.6,

$$M_{max} = \mathbf{203.9 \text{ kN.m}}$$

$$M_{pl} = \mathbf{200.1 \text{ kN.m}}$$

Point A: (N = 2140; M = 0)

Point B: (N = 0; M = 200.1)

Point C: (N = 904; M = 200.1)

Point D: (N = 452; M = 203.9)

As per above mention point A, B, C and D draw M-N interaction curve show in Fig.4.4

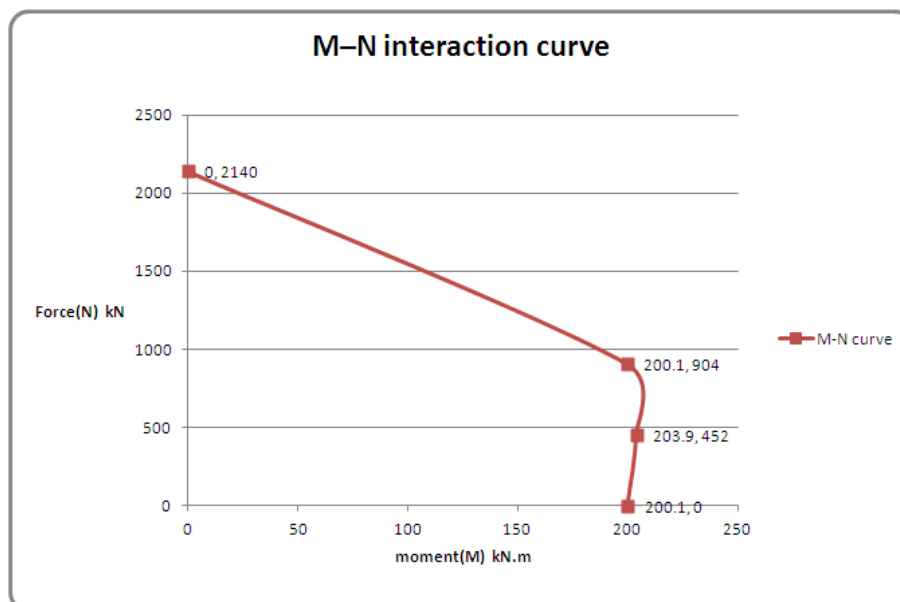


Figure 4.4: M-N Interaction Curve

4.4 Modeling and Analysis of 10 Storey CFT, RCC and Steel Building

4.4.1 General

Comparison of Analysis results for Concrete Filled Steel Tube, Reinforce Concrete and Steel building is done in this section. STRAP software is used for modeling, analysis and design of CFT, RCC and Steel building. In order to validate results of STRAP software, manual comparison is also done. Reference codes used for CFT building is Eurocode-4[7] while for RCC and Steel buildings Indian Standard code i.e IS 456(2000)[2] and IS 800 (2007)[3] respectively are used. The analysis is carried out for wind load as per IS 875(III)-1987[4] and earthquake load as per IS 1893 (2002)[1] considering 26 load combinations.

4.4.2 Building Configuration

Plan of CFT, RCC and Steel building was 38.4m * 32m as shown in Fig 4.5. Columns were placed 6.4 m center to center both ways. Typical storey height was taken as 3m while beam size and column size are taken as given in Table.4.3 and Table.4.4 respectively.

Design Data

- o Plan area - 38.4 m x 32.0m
- o No. of bays in X dir - 6
- o No. of bays in Y dir - 5
- o Ht. of Storey - 3m
- o No. of storey - 10 (G + 9th Floor)
- o Column c/c distance in X dir - 6.4m
- o Column c/c distance in Y dir - 6.4m

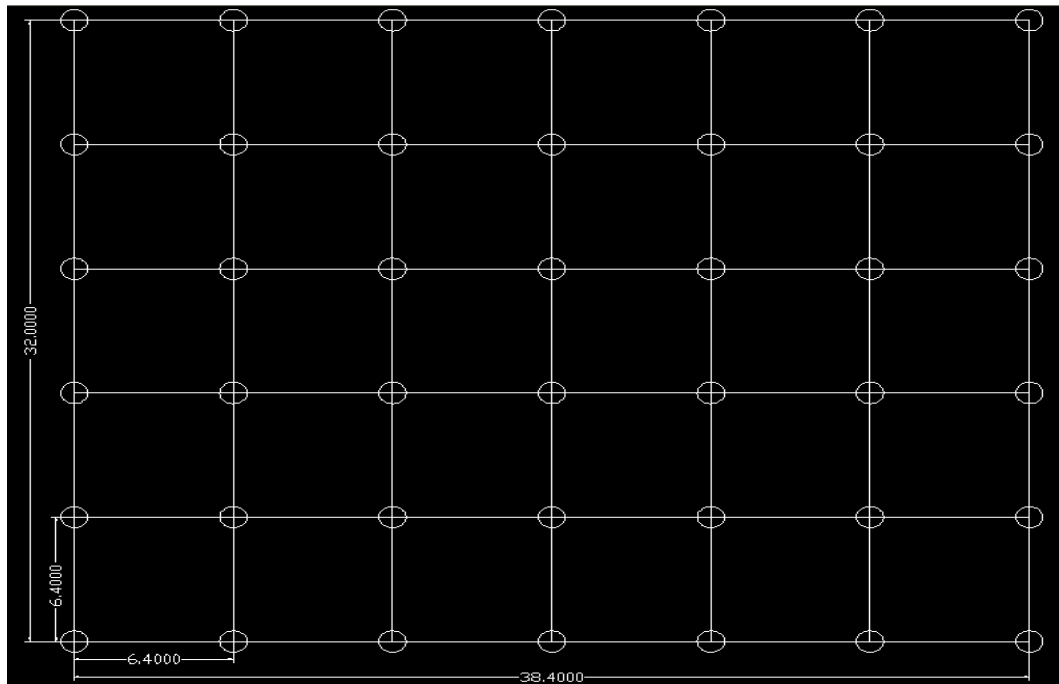


Figure 4.5: Typical Building Plan

- o Concrete grade $f_{ck} - 30N/mm^2$
- o Reinforce Steel $f_{sk} - 415N/mm^2$
- o Structural Steel $f_y - 340N/mm^2$
- o Slab thickness - 150mm

Loading:

- *On all story:*
 - o *LiveLoad* = $2kN/m^2$
 - o *FloorFinish* = $1kN/m^2$
- *Earthquake Force:*
 - o Location: Zone - III (for Ahmedabad)
 - o Zone Factor : 0.16

- o Response Reduction Factor - 5.0 (SMRF)
- o Medium Soil Strata

- *Wind Force:*
 - o Basic wind Speed $V_b = 39\text{m/s}$
 - o Probability factor $K_1 = 1$
 - o Topography factor $K_3 = 1$

Load Combination:

DL + LL

1.5(DL + LL)

1.2(DL + LL + EQX)

1.2(DL + LL - EQX)

1.2(DL + LL + EQY)

1.2(DL + LL - EQY)

1.5(DL + EQX)

1.5(DL - EQX)

1.5(DL + EQY)

1.5(DL - EQY)

 $0.9 * DL + 1.5 * EQX$ $0.9 * DL - 1.5 * EQX$ $0.9 * DL + 1.5 * EQY$ $0.9 * DL - 1.5 * EQY$

1.2(DL + LL + WLX)

1.2(DL + LL - WLX)

1.2(DL + LL + WLY)

1.2(DL + LL - WLY)

1.5(DL + WLX)

1.5(DL - WLX)

1.5(DL + WLY)

1.5(DL - WLY)

$0.9 * DL + 1.5 * WLX$

$0.9 * DL - 1.5 * WLX$

$0.9 * DL + 1.5 * WLY$

$0.9 * DL - 1.5 * WLY$

- Beam Size

Table 4.3: Beam Size

BEAM SIZE			
Number of Storey	10 Storey	20 Storey	30 Storey
RCC Building (mm)	230X400	250X550	250X550
CFT Building	ISMB550	ISWB600	Up to 15 floor ISWB600 16 to 30 floor ISWB550
Steel Building	ISMB550	ISWB550	ISWB550

- Column Size

Table 4.4: Column Size

COLUMN SIZE			
Number of Storey	10 Storey	20 Storey	30 Storey
RCC Building (mm)	Diameter (D)=550mm	Up to 10 floor D= 900mm 11 to 20 floor D=700mm	Up to 10 floor D= 1100mm 11 to 20 floor D=900mm 21 to 30 floor D= 700mm
CFT Building	D=550mm and t= 6mm	D=800mm and t= 9mm	D=1000mm and t=11mm
Steel Building	2ISWB450 Flange dis=20mm	2ISWB600A Flange dis=40mm	D=1000mm and t=20mm

4.4.3 Steps for CFT Structure Modeling in STRAP Software

Step-1 Geometry:

Strap follows nodal point method as base for geometry creation. Therefore, geometry is created by mentioning the base of column as node point as per plan and the same can be extended up to number of storey shows in Fig.4.6.



Figure 4.6: Geometry and Design Tools

Column Property:

This can be done in following steps as shows in Fig.4.7

Select the beam → Define column dimension → For CFT column, select filled section

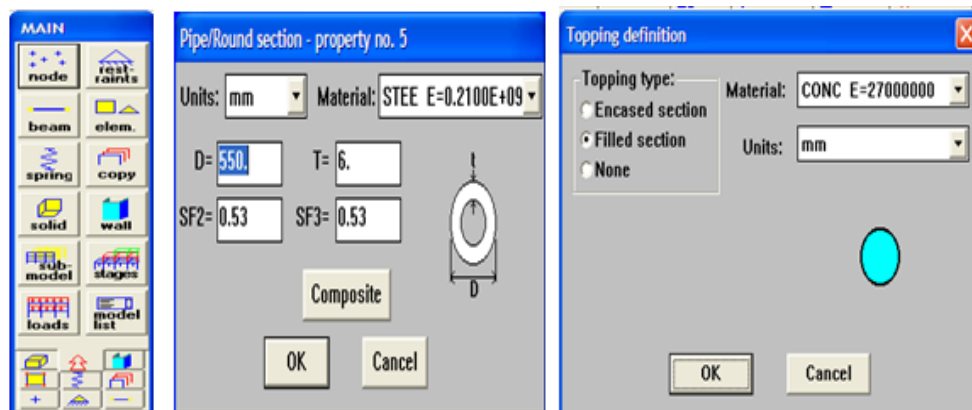


Figure 4.7: Column Property Tool

Beam Property:

This can be done in following steps shows in Fig.4.8

Select the beam → Define property → Beam dimension

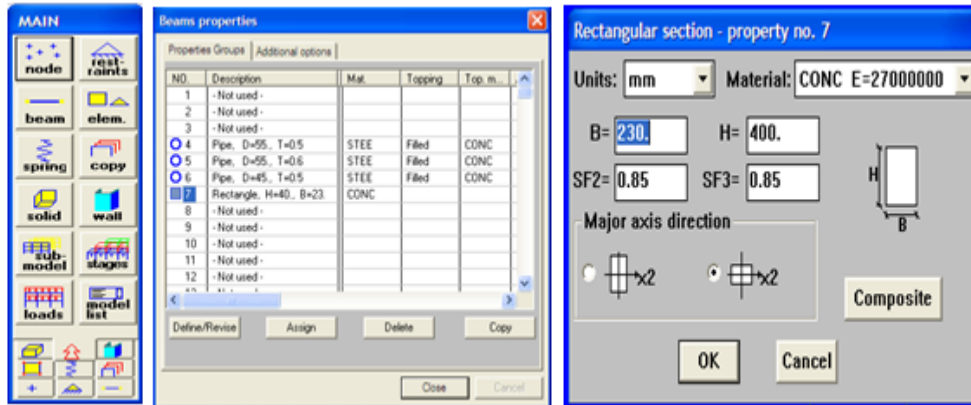


Figure 4.8: Beam Property Tool

Step-2 Load:

Select Load option (Ref Fig.4.6)

Select new load and define all load case.

1. For point load application select joint load → select node and apply load
2. For line load application select beam load → select beam and apply load
3. For area load application select global load → select area and apply load

After application of the load on the model 'SOLVE' to find necessary values like Base Reaction, Deflections, and Base Shear etc.

Step-3 Weight:

Select weight option (Ref Fig.4.6) for seismic weight calculation.

Define static load factor (Reduction factor for Live Load) and mode shapes.

After application of weight on the model 'SOLVE' for seismic weight.

Step-4 Seismic Analysis (Dynamics):

Select dynamics option (Ref Fig.4.6)

Select Seismic analysis → click method for combining node → select CQC or SRSS method

Then define seismic parameter in X and Y direction shown in Fig.4.9

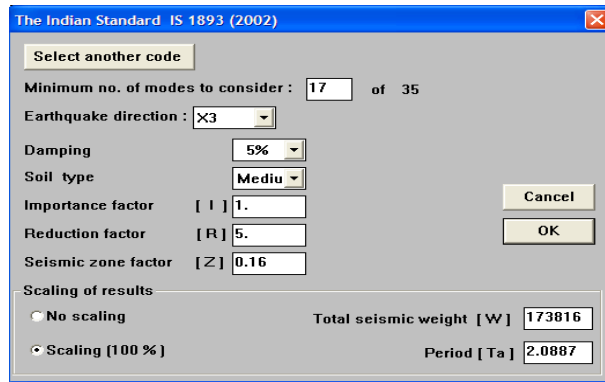


Figure 4.9: Seismic Parameter

Step-5 Results:

Select result option (Ref Fig.4.6)

Select combination → click define combination

All load combination define shown in Fig.4.10

Combinations definition								
No.	Title	1:FF+SLAB	2:LL	3:SW	4:Wind X1	5:Wind X3	6:CQC OV...	7:CQC OVER...
1	DL+LL	1.	1.	1.				
2	1.5DL+1.5LL	1.5	1.5	1.5				
3	1.5DL+1.5WLX1	1.5		1.5	1.5			
4	1.5DL+1.5WLX3	1.5		1.5		1.5		
5	1.5DL-1.5WLX1	1.5		1.5	-1.5			
6	1.5DL-1.5WLX3	1.5		1.5		-1.5		
7	1.2DL+1.2LL+1.2WLX1	1.2	1.2	1.2	1.2			
8	1.2DL+1.2LL+1.2WLX3	1.2	1.2	1.2		1.2		
9	1.2DL+1.2LL-1.2WLX1	1.2	1.2	1.2	-1.2			
10	1.2DL+1.2LL-1.2WLX3	1.2	1.2	1.2		-1.2		
11	0.9DL+1.5WLX1	0.9		0.9	1.5			
12	0.9DL+1.5WLX3	0.9		0.9		1.5		
13	0.9DL-1.5WLX1	0.9		0.9	-1.5			
14	0.9DL-1.5WLX3	0.9		0.9		-1.5		
15	1.5DL+1.5EQX1	1.5		1.5			1.5	
16	1.5DL+1.5EQX3	1.5		1.5				1.5
17	1.5DL-1.5EQX1	1.5		1.5			-1.5	
18	1.5DL-1.5EQX3	1.5		1.5				-1.5
19	1.2DL+1.2LL+1.2EQX1	1.2	1.2	1.2			1.2	
20	1.2DL+1.2LL+1.2EQX3	1.2	1.2	1.2				1.2
21	1.2DL+1.2LL-1.2EQX1	1.2	1.2	1.2			-1.2	
22	1.2DL+1.2LL-1.2EQX3	1.2	1.2	1.2				-1.2
23	0.9DL+1.5EQX1	0.9		0.9			1.5	
24	0.9DL+1.5EQX3	0.9		0.9				1.5
25	0.9DL-1.5EQX1	0.9		0.9			-1.5	
26	0.9DL-1.5EQX3	0.9		0.9				-1.5
27								
28								
29								
30								

Figure 4.10: Load Combination

Step-6 Design:

For concrete member design select concrete (Ref Fig.4.6)

Define concrete and steel grade, deflection limit, design code, reinforcement cover etc.

For composite and steel member design select steel Ref Fig.4.6

Define concrete and steel grade, deflection limit, design code, steel and composite member etc.

Design results along with detail analysis can be viewed.

4.4.4 Parametric Study of 10 Storey CFT Building

- **Base Reaction:**

Table 4.5 shows the base reaction due to gravity load, both manually and by ‘STRAP’ software.

Building Configuration

No. of storey	= 10
Width of building (a)	= 32 m
Length of building (b)	= 38.4 m
Typical height of storey	= 3 m
Beam ISMB550 Unit Wt	= 1.04kN/m
Slab Thickness t	= 150mm
Column diameter D	= 550mm t=6mm
Column c/c distance	= 6.4m

CFT Building Load Calculation

Wt. of slab	= 4608 kN
Wt. of Beam	= 472.576 kN
Column Weight:	
Wt. of concrete	= 715.722 kN
Wt of Steel	= 101.372 kN
Total DL on each floor	= 5897.671 kN
Total DL on Building	= 58976 kN
LL	= 2kN/m ²
Total LL on Building	= 24576 kN
FF	= 1kN/m ²
Total FF on Building	= 12288 kN
Total Wt on Building	= 95840 kN
Load Intensity	= 7.7995 kN/m²
Seismic Weight	= 77408.711 kN

Table 4.5: Comparison of Base Reaction

Load Type	STRAP	Manual
Dead load (kN)	58681	58976
Live load (kN)	24576	24576
Floor finish (kN)	12288	12288
Total load (kN)	95545	95840
Load intensity (kN/m ²)	7.775	7.799
Seismic weight W (kN)	77113	77408

- **Wind Force:**

The base shear for wind load along X-direction and along Y-direction, as per IS: 875(III)-1987 [4] is shown and compared with STRAP results in Table.4.10.

Following are the steps of wind load calculation by using IS 875(III)-1987 [4].

Manual Wind Load Calculation

Basic Wind speed V_b = 39 m/s

Terrain category = II

Class = B

k_1 (Probability factor) = 1

k_3 (Topography factor) = 1

Design wind speed $V_z = V_b \times k_1 \times k_2 \times k_3$

Table 4.6: Wind Load Parameter

HEIGHT(m)	K1	K2	K3	Vb	Vz	Pz
10	1	0.88	1	39	34.32	706.72
15	1	0.94	1	39	36.66	806.37
20	1	0.98	1	39	38.22	876.46
30	1	1.03	1	39	40.17	968.18
50	1	1.09	1	39	42.51	1084.26
100	1	1.17	1	39	45.63	1249.26

Table 4.7: Building Parameter

DIMENSION	WIND AT 0	WIND AT 90
a/b	1.20	0.83
h/b	0.94	0.78
Cf	1.39	1.22

Table 4.8: Wind Load in X-Direction

Wind at 0 Degree					
STOREY	CF	Ae		PZ	FORCE(kN)
		Width(m)	Length(m)	N/mm ²	
1	1.39	32	3	706.7	94.30
2	1.39	32	3	706.7	94.30
3	1.39	32	2.5	706.7	78.59
	1.39	32	0.5	806.4	17.93
4	1.39	32	3	806.4	107.60
5	1.39	32	1.5	806.4	53.80
	1.39	32	1.5	876.5	58.48
6	1.39	32	3	876.5	116.95
7	1.39	32	0.5	876.5	19.49
	1.39	32	2.5	968.2	107.66
8	1.39	32	3	968.2	129.19
9	1.39	32	3	968.2	129.19
10	1.39	32	1.5	968.2	64.60
	1.39	32	1.5	1084.3	72.34
Total base shear due to wind load					1144.45

Table 4.9: Wind Load in Y-Direction

Wind at 90 Degree					
STOREY	CF	Ae		PZ	FORCE(kN)
		Width(m)	Length(m)	N/mm ²	
1	1.22	38.4	3	876.5	123.18
2	1.22	38.4	3	876.5	123.18
3	1.22	38.4	2.5	876.5	102.65
	1.22	38.4	0.5	949.5	22.24
4	1.22	38.4	3	949.5	133.44
5	1.22	38.4	1.5	949.5	66.72
	1.22	38.4	1.5	1006.1	70.70
6	1.22	38.4	3	1006.1	141.41
7	1.22	38.4	0.5	1006.1	23.57
	1.22	38.4	2.5	1104.2	129.33
8	1.22	38.4	3	1104.2	155.20
9	1.22	38.4	3	1104.2	155.20
10	1.22	38.4	1.5	1104.2	77.60
	1.22	38.4	1.5	1206.9	84.81
Total base shear due to wind load					1409.23

Table 4.10: Base Shear Due to Wind Load

Load Type	STRAP	Manual
Wind X-dir(kN)	1282.9	1144.45
Wind Y-dir(kN)	1539.5	1409.23

- **Earthquake Force:**

The base shear force for earthquake load acting along X-direction and along Y-direction as per IS: 1893-2002 [1] is shown and compared with STRAP results in Table.4.11.

Manual Earthquake Load Calculation

Time period as per “STRAP”:

$$T_y = 1.332 \text{ sec}$$

$$T_x = 1.316 \text{ sec}$$

$$\text{Zone factor} = 0.16$$

$$\text{Importance factor} = 1$$

$$\text{Response reduction factor} = 5$$

$$\text{Soil Strata} = \text{Medium}$$

$$A_{hy} = (Z/2) * (I/R) * (S_a/g) = 0.01633$$

$$A_{hx} = (Z/2) * (I/R) * (S_a/g) = 0.01653$$

Base Shear

$$Vb_y = A_h * W = 1264.574 \text{ kN}$$

$$Vb_x = A_h * W = 1279.949 \text{ kN}$$

Table 4.11: Base Shear Due to Earthquake Load

Load Type	STRAP	Manual
Base shear X-dir(kN)	1317	1280
Base shear Y-dir(kN)	1325	1265

• **Time Period and Mode Shape:**

Fig.4.11 shows the Mode Shape v/s Time Period graph of 10 story CFT building. The first three mode shape are in Y-direction, X-direction Fig.4.12 and XY-direction(torsion) Fig.4.13 respectively.

Table 4.12: 1st and 2nd Mode Time Period

Direction	CFT
Time period Y-dir (sec)	1.332
Time period X-dir (sec)	1.316

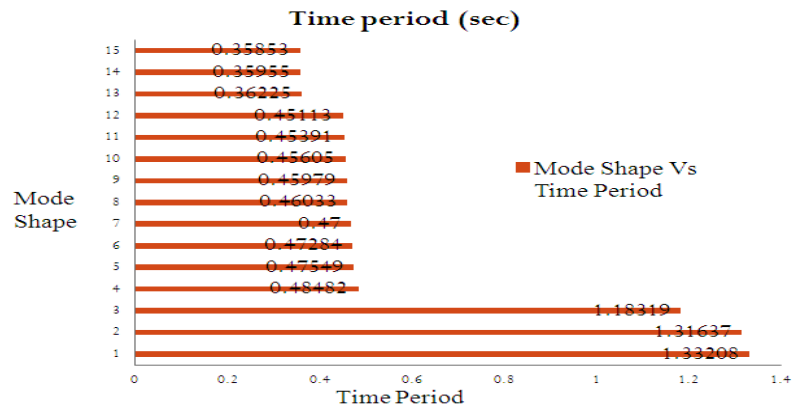


Figure 4.11: Mode Shape Vs Time Period Graph

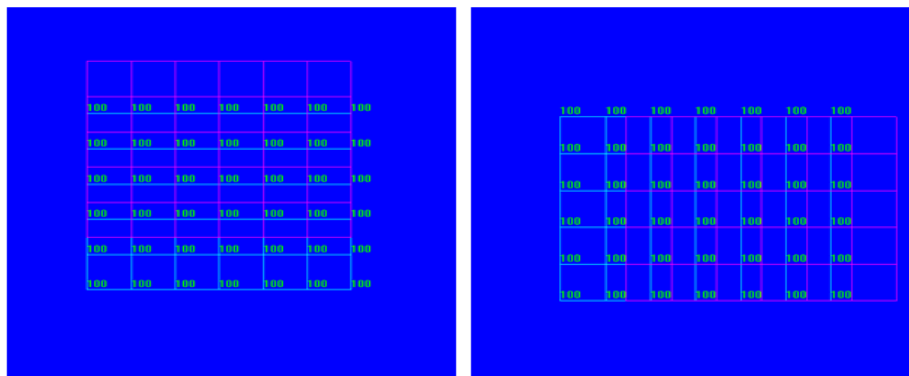
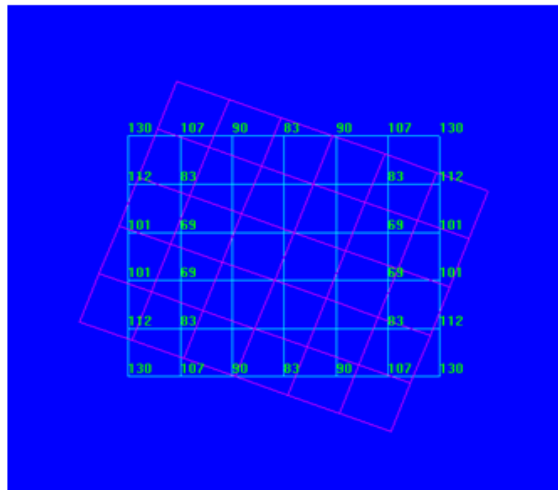


Figure 4.12: 1st and 2nd Mode Shape

Figure 4.13: 3rd Mode Shape

- **Displacement:**

Ten storey Concrete Filled Steel tube buildings, storey displacement values due to earthquake and wind load are as shown in Table.4.13 . Maximum displacement occurs due to Earthquake in Y direction, thus becoming a governing case. Graph of displacement v/s storey is shown in Fig.4.14 .

Table 4.13: 10Storey Displacement

Storey	EQ X	EQ Y	WL X	WL Y
10	10.9	11.2	8.6	10.6
9	10.6	10.9	8.5	10.4
8	10.0	10.3	8.1	10.0
7	9.3	9.5	7.6	9.4
6	8.3	8.6	7.1	8.6
5	7.2	7.4	6.2	7.5
4	5.8	5.9	5.1	6.2
3	4.3	4.4	3.9	4.7
2	2.6	2.7	2.4	2.9
1	1.0	1.1	1.0	1.1
0	0.0	0.0	0.0	0.0

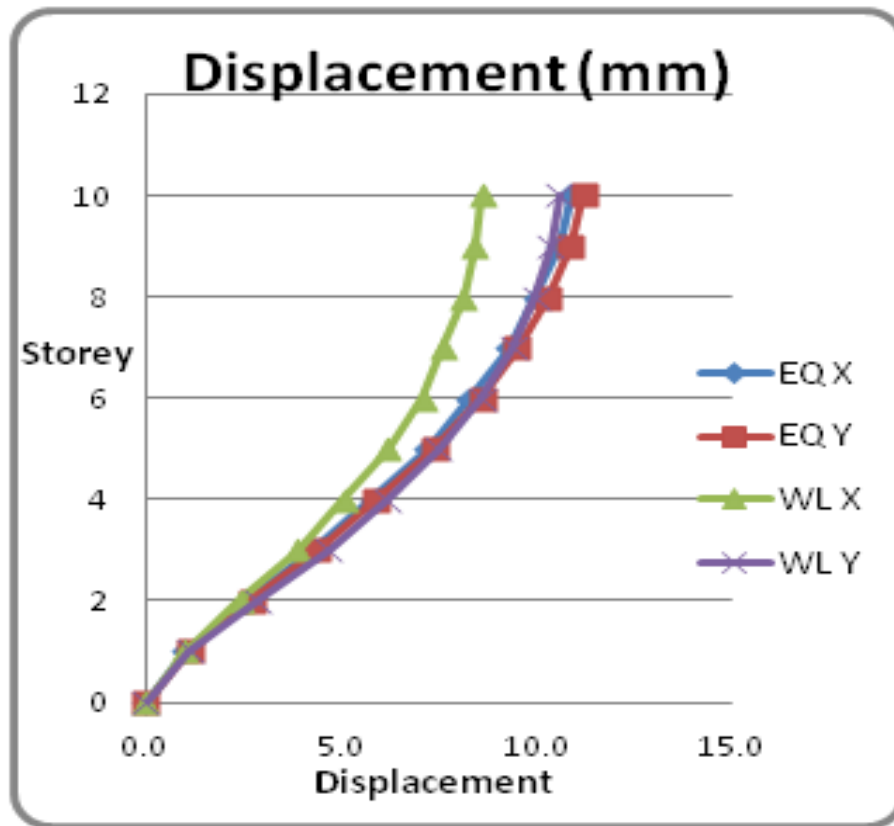


Figure 4.14: Displacement of 10 Storey CFT Building

4.4.5 Comparison of 10 Storey CFT, RCC and Steel Building

For Comparison of various parameters and behavior of CFT, RCC and Steel building, load intensity in all three types of buildings was kept nearly same (Refer to Table.4.14). The comparison is done for Time period, base shear, maximum load carrying capacity, displacement and cost.

Table 4.14: Load Comparison

Structure	CFT	RCC	STEEL
Dead load (kN)	58681	63297.6	52794
Live load (kN)	24576	24576	24576
Floor finish (kN)	12288	12288	12288
Total load (kN)	95545	100161.6	89658
Load intensity (kN/m^2)	7.78	8.15	7.29

- **Time Period Comparison:**

As seen in Table.4.15 , maximum time period is in first mode for CFT, RCC and Steel buildings. Graphical representation of Time period shown in Fig.4.15 indicates that CFT building has lesser time period compared to both RCC and Steel building. Percentage reduction in time period of CFT building is 44.1% and 17.4% with compared to RCC and Steel building respectively.

Table 4.15: Time Period Comparison

Load Type	CFT	RCC	STEEL
Time period(sec) for 1st mode	1.33	2.38	1.61



Figure 4.15: Comparison of Time Period

- **Base Shear Comparison:**

Base shear variation in X and Y direction due to earthquake load is presented in Fig.4.16, It is observed that for RCC structure base shear is less while for CFT it is lesser than steel but more than RCC.

Table 4.16: Base Shear Comparison

Load Type	CFT	RCC	STEEL
Base shear X-dir(kN)	1317	788.9	1434
Base shear Y-dir(kN)	1325	758.7	1390

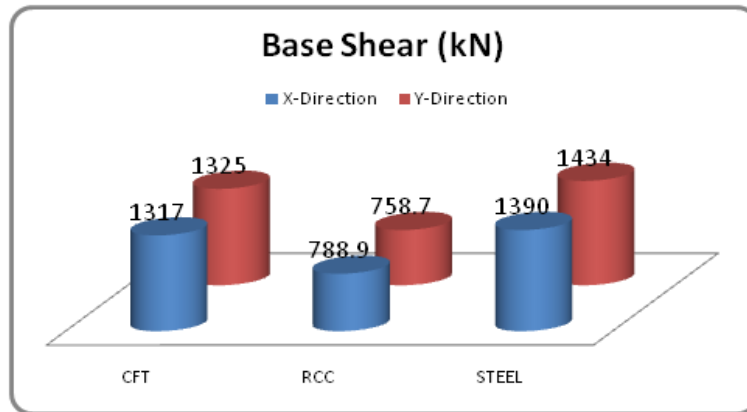


Figure 4.16: Comparison of Base Shear

- **Maximum Load Carrying Capacity:**

Load carrying capacity of CFT building is found to be higher than RCC by 15.2%, while for steel by 6.8% as shown in Table.4.17 and Graphical representation of Design capacity shown in Fig.4.17 .

Table 4.17: Maximum Load Carrying Capacity

Structure Type	CFT	RCC	STEEL
Design capacity (kN)	5809	4924	5414

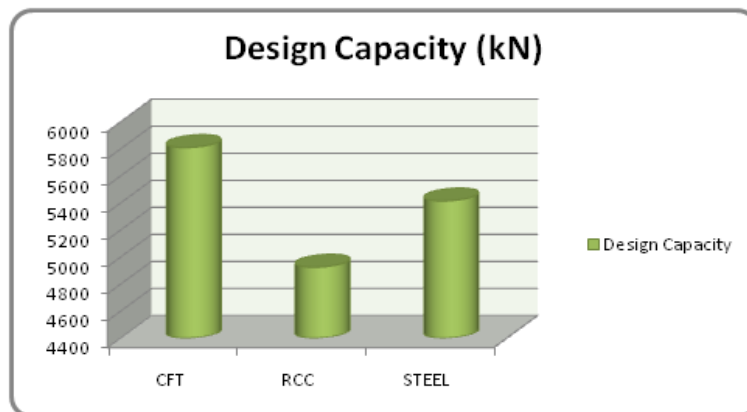


Figure 4.17: Comparison of Design Capacity

- **Displacement Comparison:**

Storey displacement variation along the height of building is presented in Fig.4.18. Percentage reduction in top storey displacement of CFT building is 65.1% and 39.1% with compared to RCC and Steel building respectively, indicating its rigid behavior.

Table 4.18: Displacement Comparison

10 Storey Displacement (mm)			
Storey	CFT	RCC	STEEL
Load Case	1.5(DL ± EQY)	1.5(DL ± WLY)	1.5(DL ± EQX)
10	16.8	48.1	27.6
9	16.4	47.7	26.9
8	15.5	45.7	25.5
7	14.3	42.8	23.7
6	12.9	38.8	21.5
5	11.1	33.6	18.6
4	8.9	27.3	15.3
3	6.6	19.9	11.6
2	4.1	11.9	7.5
1	1.7	4.4	3.3
0	0.0	0.0	0.0

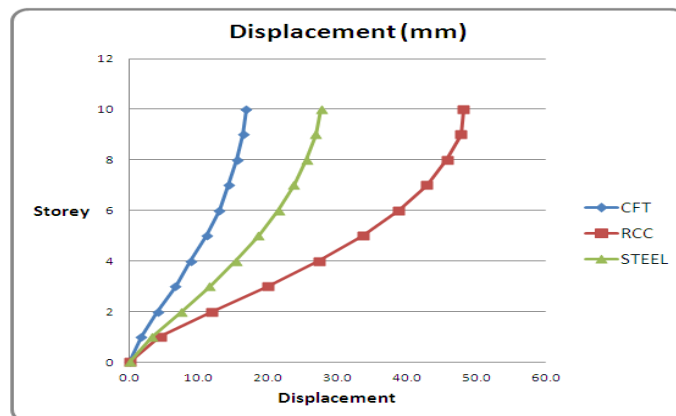


Figure 4.18: Comparison of 10 Storey Displacement

4.4.6 Cost Comparison

The total quantity of material required for 10 storey CFT, RCC and Steel building calculation is below and cost wise analysis is presented in Table.4.19.

CFT Building Quantity

Column dia D = 550mm and t = 6mm

$$\text{Concrete Qty} = \pi \div 4 * (0.538)^2 * 30 * 42 = 286.3m^3$$

$$\text{Structural Steel Qty} = \pi \div 4 * [(0.550)^2 - (0.538)^2] * 30 * 42 * 7850 \div 1000 = 101.37 \text{ tonnes}$$

RCC Building Quantity

Column dia D = 550 mm

$$\text{Concrete Qty} = \pi \div 4 * (0.550)^2 * 30 * 42 = 299.2m^3$$

Average Pt = 2.55% as per STRAP results

$$\text{Reinforce Steel Qty} = 2.55 \div 100 * \pi \div 4 * [(0.550)^2] * 30 * 42 * 7850 \div 1000 = 59.89 \text{ tonnes}$$

$$\text{Shuttering Qty} = [\pi * 0.550] * 30 * 42 = 2172.2m^2$$

Steel Building Quantity

Column 2ISWB450 Flange dis =20mm Unit Wt = 79.4 kg/m

$$\text{Structural Steel Qty} = 2 * 79.4 * 30 * 42 \div 1000 = 200.09 \text{ tonnes}$$

- **10 Storey Building Rate Analysis:**

Table 4.19: 10 Storey Column Rate Analysis

Sr No	Description	Quantity	units	Rate	Amount (Rs)
CFT Building					
1	Str. Steel	101.37	tonnes	60140	6096392
2	Concrete (M30)	286.3	cu.m	7669	2195635
Total					8292027
Column cost per meter					6581
RCC Building					
1	Rein. Steel	59.89	tonnes	57375	3436189
2	Concrete (M30)	299.2	cu.m	7669	2294565
3	Shuttering	2172.2	sq.m	808	1755138
Total					7485892
Column cost per meter					5941
Steel Building					
1	Str. Steel	200.09	tonnes	60140	12033413
Total					12033413
Column cost per meter					9550

Cost analysis data shows that 10 storey CFT building is 9.7% costly compared to RCC building and 31.1% cheaper compared to Steel building

4.4.7 Detailing of CFT Member

Fig.4.19 shows the design result and all design parameter like moment, Deflection, Combine stress and axial force criteria is within permissible limit. Also Fig.4.20 shown cross section view of beam and column member.

DESIGN	EQUATION	FACTORS	VALUES	RESULT
M3 Moment [8.2] Notes:	$\frac{M}{M_d} < 1.00$ LOW Shear Load Used for Moment Design	$Z_{eff} = 1379.52$ $Z_{el} = 1379.52$	$M = 9.70$ $M_d = 426.40$	0.02
V3 Shear [8.4]	$V/V_d < 1.00$	$A_v = 65.28$	$V = 66.11$ $V_d = 1164.88$	0.06
M2 Moment [8.2] Notes:	$\frac{M}{M_d} < 1.00$ LOW Shear Load Used for Moment Design	$Z_{eff} = 1379.52$ $Z_{el} = 1379.52$	$M = 138.53$ $M_d = 426.40$	0.32
Deflection	$\frac{defl.}{L / 325} < 1.00$		$defl = 0.00042$	0.05
Combined Stresses (Local) [9.3]	$\frac{N}{N_d} + \frac{M_x}{M_{dx}} + \frac{M_y}{M_{dy}} < 1.00$	$M_{dx} = 426.40$ $M_{dy} = 426.40$ $M_x = 9.70$ $M_y = 138.53$	$N = 3377.17$ $A_g = 86.15$	0.93
Axial Force [7.1] Note:	$\frac{P}{P_d} < 1.00$ buckling curve used is : a	$(kL/r)_x = 19$ $(kL/r)_y = 19$ $\chi_{fy} = 741$	$P = 3377.17$ $A_g = 102.54$ $P_d = 5809.36$ $A_{eff} = 86.15$	0.58

Figure 4.19: Design Result For 10 Storey CFT Building

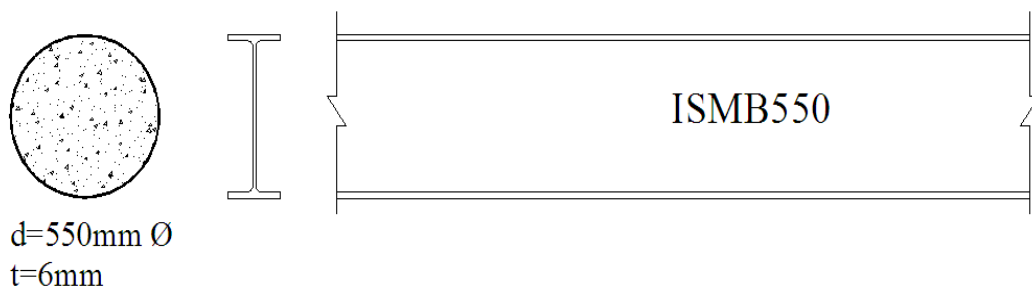


Figure 4.20: 10 Storey CFT Building Column and Beam

4.5 Summary

This chapter discussed concrete filled tube column capacity with different options and comparison was done with various codal provisions. Comparison of load intensity, Time Period, Base shear, maximum load carrying capacity and displacement of top storey was done, which indicated that CFT column system was found to be much better than RCC and Steel building system. When result of CFT and RCC were compared, it shows that the CFT building is effective performance wise in terms of 10 storey building, due to reduction in the time period by 44.1%, reduction in top storey displacement by 65.1%, increase load carrying capacity 15.2%. But cost wise CFT building is 9.7% costly. While when comparison was done with steel building, it was found effective both performance and cost wise. The reduction in time period was observed as 17.4%, while top storey displacement was reduced by 39.1% and increase load carrying capacity 6.8% for CFT building compared to Steel. Also cost wise CFT building is 31.1% cheaper than steel.

Chapter 5

Analysis and Design of 20 and 30 Storey Building

5.1 General

This chapter includes analysis and design of 20 and 30 storey of CFT, RCC and Steel buildings. Design data (CL.4.4.2), plan view (Fig.4.5), Beam size (Table.4.3) and Column size (Table.4.4) were same as mentioned in Chapter-4 (CL.4.4.2). Manual load calculations, wind load calculation was shown in Appendix-A and earthquake load calculations was shown in Appendix-B. Also In order to validate results of STRAP software, manual comparison is also done. The comparison is done for Time period, base shear, maximum load carrying capacity, displacement and cost for CFT, RCC and Steel building.

5.2 Parametric Study of 20 Storey CFT Building

- **Base Reaction:**

Table.5.1 shows the base reaction due to gravity load, both manually and by 'STRAP' software.

Manual Load Calculation:

Building Configuration

No. of storey	=	20
Width of building (a)	=	32 m
Length of building (b)	=	38.4 m
Typical height of storey	=	3 m
Beam ISWB600	=	1.337kN/m
Slab Thk. t	=	150mm
Column dis D	=	800mm t=9mm
Column c/c distance	=	6.4m

CFT Building Load Calculation

Wt. of slab	=	4608 kN
Wt. of Beam	=	607.533 kN
Column Weight:		
Wt. of concrete	=	1512.146 kN
Wt of Steel	=	221.10 kN
Total DL on each floor	=	6948.78 kN
Total DL on Building	=	138976 kN
LL	=	2kN/m ²
Total LL on Building	=	49152 kN
FF	=	1kN/m ²
Total FF on Building	=	24576 kN
Total Wt on Building	=	212704 kN
Load Intensity	=	8.65 kN/m ²
Seismic Weight	=	175840 kN

Table 5.1: Comparison of Base Reaction

Load Type	STRAP	Manual
Dead load (kN)	137789	138976
Live load (kN)	49152	49152
Floor finish (kN)	24576	24576
Total load (kN)	211517	212704
Load intensity (kN/m ²)	8.61	8.65
Seismic weight W (kN)	174653	175840

- **Wind Force:**

The base shear for wind load along X-direction and along Y-direction, as per IS: 875(III)-1987 [21] is shown and compared with STRAP results in Table.5.2. Manual wind load calculation is shown in Appendix-A.1.

Table 5.2: Base Shear Due to Wind Load

Load Type	STRAP	Manual
Wind X-dir (kN)	2603	2634
Wind Y-dir (kN)	3124	3290

- **Earthquake Force:**

The base shear force for earthquake load acting along X-direction and along Y-direction as per IS: 1893-2002 ([1]) is shown and comparison with STRAP results is done in Table.5.3. Manual wind load calculation is shown in Appendix-B.1.

Table 5.3: Base Shear Due to Earthquake Load

Load Type	STRAP	Manual
Base shear X-dir (kN)	1949	1861
Base shear Y-dir (kN)	1881	1832

• **Time Period and Mode Shape:**

Fig.5.1 shows the Mode Shape v/s Time Period graph of 20 story CFT building. The first three mode shape are shown Fig.5.2, and 5.3 for Y-direction, X-direction and XY-direction (torsion).

Table 5.4: 1St and 2nd Mode Time Period

Direction	CFT
Time period Y-dir (sec)	2.089
Time period X-dir (sec)	2.056

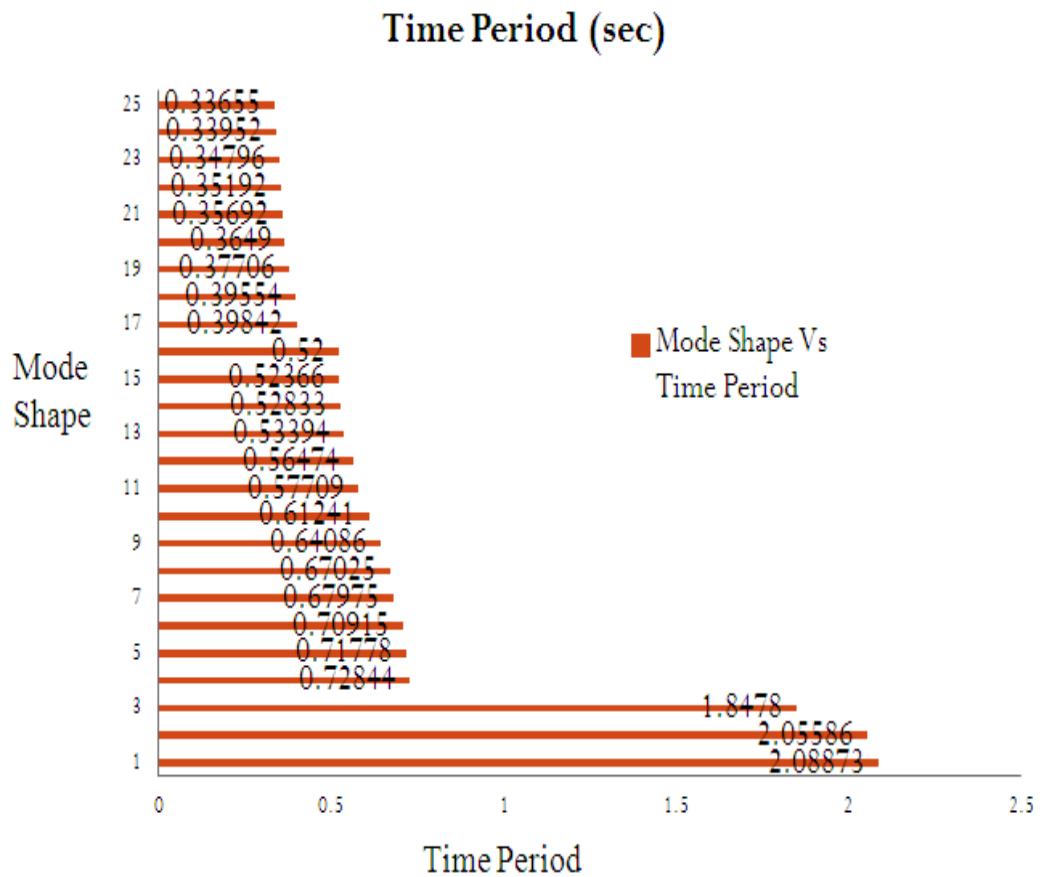


Figure 5.1: Mode shape Vs Time period graph

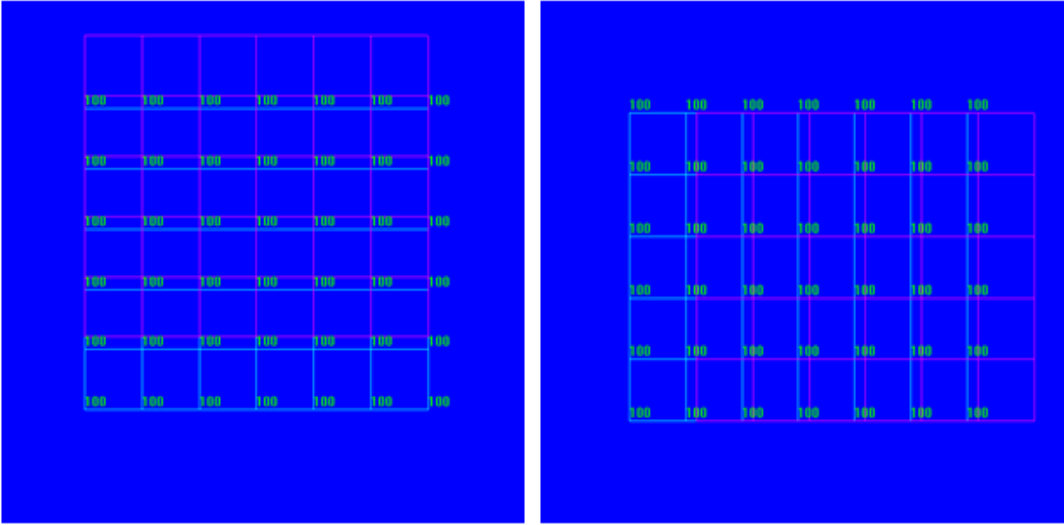


Figure 5.2: 1st and 2nd Mode Shape

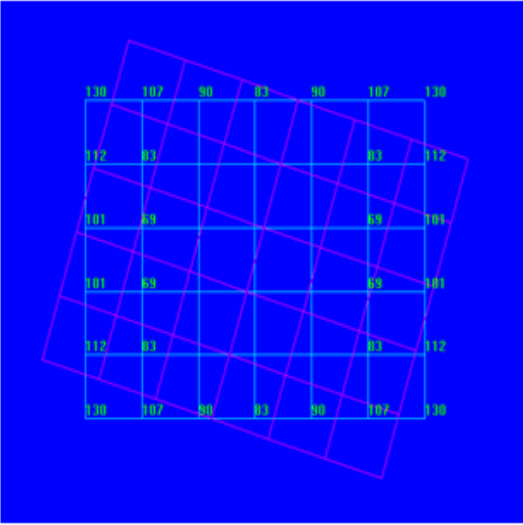


Figure 5.3: 3rd Mode Shape

• **Displacement:**

20 storey Concrete Filled Steel tube buildings, storey displacement due to earthquake and wind load are as shown in Fig.5.4. Maximum displacement occurs due to wind load in Y direction, thus becoming a governing case.

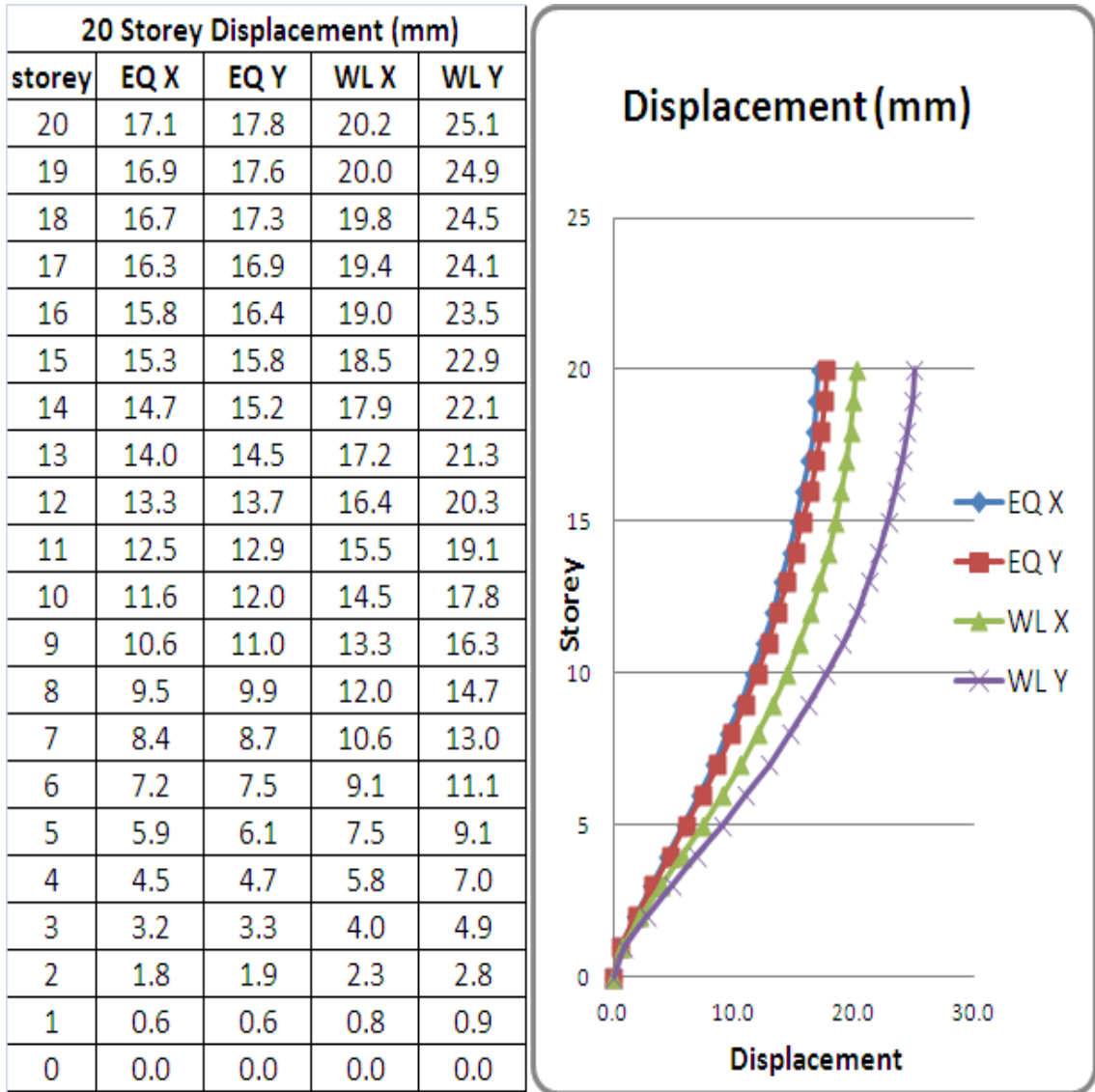


Figure 5.4: Displacement of 20 Storey CFT Building

5.3 Comparison of 20 Storey CFT, RCC and Steel Building

- **Load Comparison:**

CFT, RCC and Steel building load intensity like Live load, Floor finish was kept same, while Dead load varied due to member size effect. Refer to Table.5.5 for load intensity application and total load on the structure.

Table 5.5: Load Comparison

Structure	CFT	RCC	STEEL
Dead load (kN)	137789	159024	109699
Live load (kN)	49152	49152	49152
Floor finish (kN)	24576	24576	24576
Total load (kN)	211517	232752	183427
Load intensity (kN/m ²)	8.61	9.47	7.46

- **Time Period Comparison:**

Table.5.6 shows the CFT, RCC and Steel building maximum time period due to 1st mode of building and graphical representation of Time period is shown in Fig.5.5. Percentage reduction in time period of CFT building is 25.5% and 17.8% with compared to RCC and Steel building respectively.

Table 5.6: Time Period Comparison

Load Type	CFT	RCC	STEEL
Time period(sec) for 1st mode	2.089	2.805	2.54

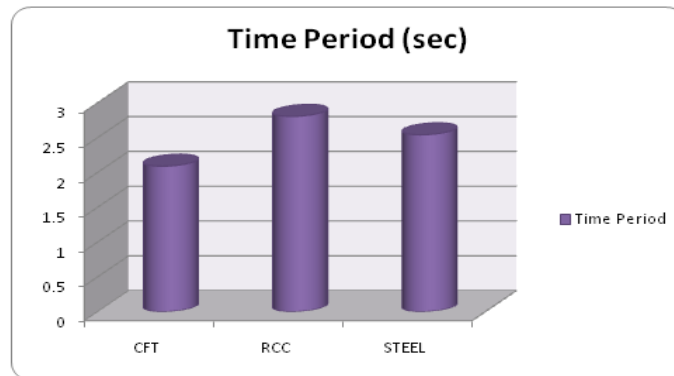


Figure 5.5: Comparison of Time Period

• **Base Shear Comparison:**

Base shear variation in X and Y direction due to earthquake load is presented in Table.5.7. and Graphical representation of base shear shown in Fig.5.6.

Table 5.7: Base Shear Comparison

Load Type	CFT	RCC	STEEL
Base shear X-dir (kN)	1949	1695	1918
Base shear Y-dir (kN)	1881	1529	1969

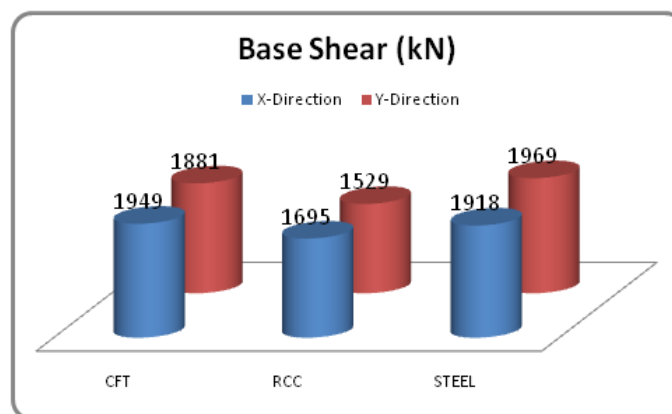


Figure 5.6: Comparison of Base Shear

- Maximum Load Carrying Capacity:** Load carrying capacity of CFT building is found to be higher than RCC by 19.1% and Steel by 27.3% shown in Table.5.8.and Graphical representation of maximum load carrying capacity shown in Fig.5.7.

Table 5.8: Maximum Load Carrying Capacity

Structure Type	CFT	RCC	STEEL
Design capacity (kN)	14093.6	11402.2	10250.1

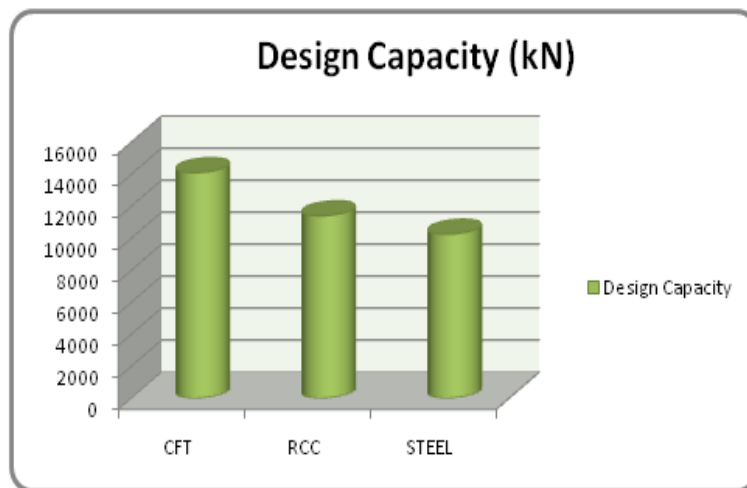


Figure 5.7: Comparison of Design Capacity

- Displacement Comparison:**

Storey displacement variation along the height of building is presented in Fig.5.8. Percentage reduction in top storey displacement of CFT building is 39.5% and 33.5% with compared to RCC and Steel building respectively.

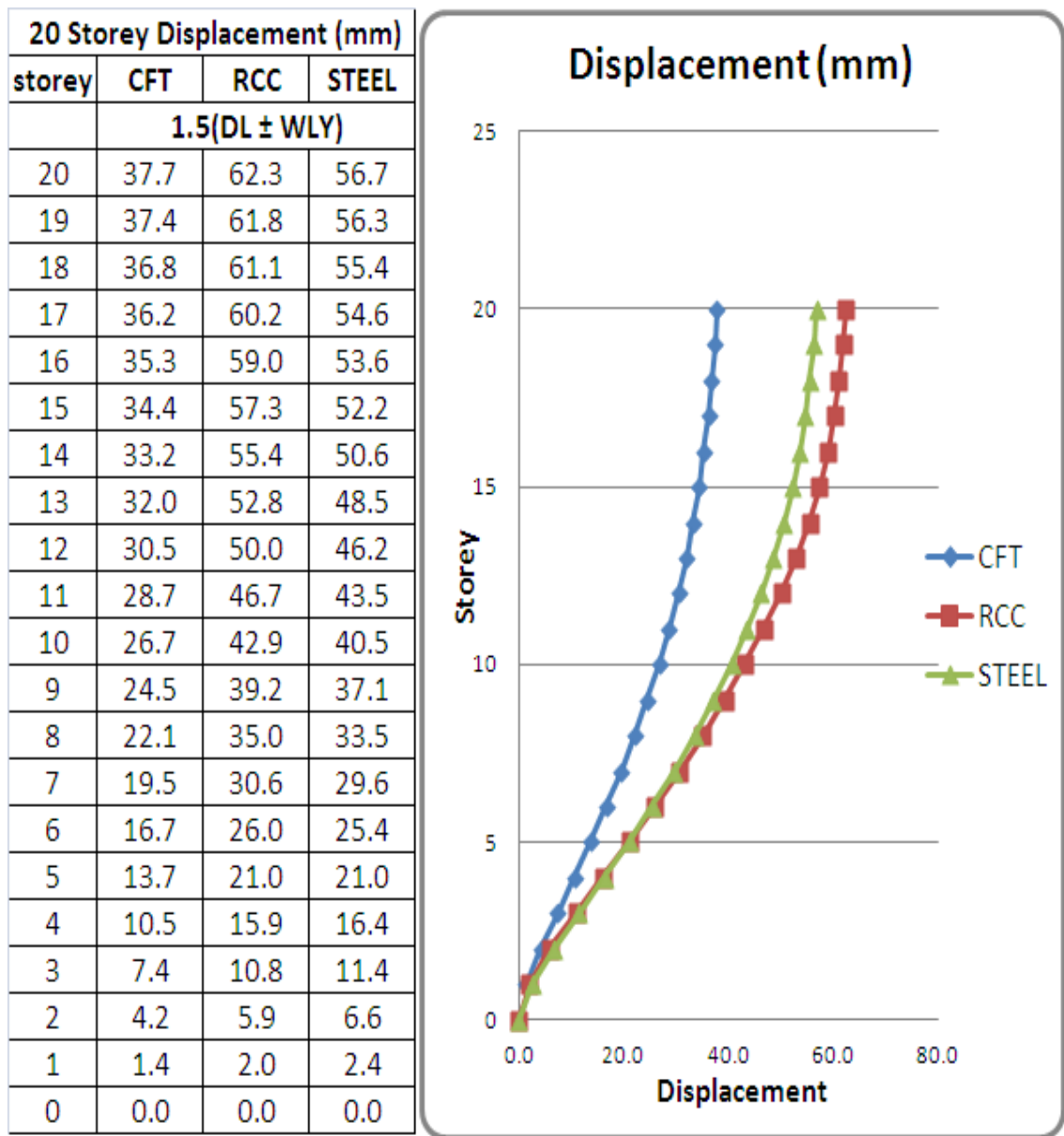


Figure 5.8: Comparison of 20 Storey Displacement

5.4 Cost Comparison

The total quantity of material required for 20 storey CFT, RCC and Steel building calculation is below and cost wise analysis is presented in Table.5.9.

CFT Building Quantity

Column dia D = 800mm and t = 9mm

$$\text{Concrete Qty} = \pi \div 4 * (0.782)^2 * 60 * 42 = 1209.72m^3$$

$$\text{Structural Qty} = \pi \div 4 * [(0.800)^2 - (0.782)^2] * 60 * 42 * 7850 \div 1000 = 442.2 \text{ tonnes}$$

RCC Building Quantity

Column dia D (Gf to 10 floor) = 900mm

Column dia D (11 floor to 20 floor) = 700mm

$$\text{Concrete Qty} = \pi \div 4 * [(0.900)^2 + (0.700)^2] * 30 * 42 = 1285.83m^3$$

Average Pt = 2.46% as per STRAP results

$$\text{Reinforce Steel Qty} = 2.46 \div 100 * \pi \div 4 * [(0.900)^2 + (0.700)^2] * 30 * 42 * 7850 \div 1000 = 248.31 \text{ tonnes}$$

$$\text{Shuttering Qty} = [\pi * 0.900 + \pi * 0.700] * 30 * 42 = 6330.24m^2$$

Steel Building Quantity

Column 2ISWB600A Flange dis=40mm Unit Wt = 145.1 kg/m

$$\text{Structural Steel Qty} = 2 * 145.1 * 60 * 42 \div 1000 = 731.304 \text{ tonnes}$$

- **20 Storey Building Rate Analysis:**

Table 5.9: 20 Storey Column Rate Analysis

Sr No	Description	Quantity	units	Rate	Amount (Rs)
CFT Building					
1	Str. Steel	442.2	tonnes	60140	26593908
2	Concrete (M30)	1209.72	cu.m	7669	9277343
Total					35871251
Column cost per meter					14235
RCC Building					
1	Rein. Steel	248.31	tonnes	57375	14246786
2	Concrete (M30)	1285.83	cu.m	7669	9861030
3	Shuttering	6330.24	sq.m	808	514834
Total					29222650
Column cost per meter					11596
Steel Building					
1	Str. Steel	731.3	tonnes	60140	43980623
Total					43980623
Column cost per meter					17453

Cost analysis data shows that 20 storey CFT building is 18.5% costly compared to RCC building and 18.4% cheaper compared to Steel building.

5.5 Detailing of CFT Member

Fig.5.9 shows the design result and all design parameter like moment, Deflection, Combine stress and axial force criteria is within permissible limit. Also Fig.5.10 shown cross section view of beam and column member.

DESIGN	EQUATION	FACTORS	VALUES	RESULT
M3 Moment [8.2] Notes:	$\frac{M}{M_d} < 1.00$ LOW Shear Load Used for Moment Design	$Z_{eff} = 4373.49$ $Z_{el} = 4373.49$	$M = 11.88$ $M_d = 1351.81$	0.01
V3 Shear [8.4]	$V/V_d < 1.00$	$A_v = 142.38$	$V = 127.97$ $V_d = 2540.68$	0.05
M2 Moment [8.2] Notes:	$\frac{M}{M_d} < 1.00$ LOW Shear Load Used for Moment Design	$Z_{eff} = 4373.49$ $Z_{el} = 4373.49$	$M = 385.02$ $M_d = 1351.81$	0.28
Deflection	$\frac{defl.}{L / 325} < 1.00$		$defl = 0.00040$	0.04
Combined Stresses [Local] [9.3]	$\frac{N}{N_d} + \frac{M_x}{M_{dx}} + \frac{M_y}{M_{dy}} < 1.00$	$M_{dx} = 1351.81$ $M_{dy} = 1351.81$ $M_x = 11.88$ $M_y = 385.02$	$N = 7493.68$ $A_g = 190.82$	0.83
Axial Force [7.1] Note:	$\frac{P}{P_d} < 1.00$ buckling curve used is : a	$(kL/r)_x = 13$ $(kL/r)_y = 13$ $\chi_{fy} = 812$	$P = 7493.68$ $A_g = 223.65$ $P_d = 14093.6$ $A_{eff} = 190.82$	0.53

Figure 5.9: Design Result For 20 Storey CFT Building

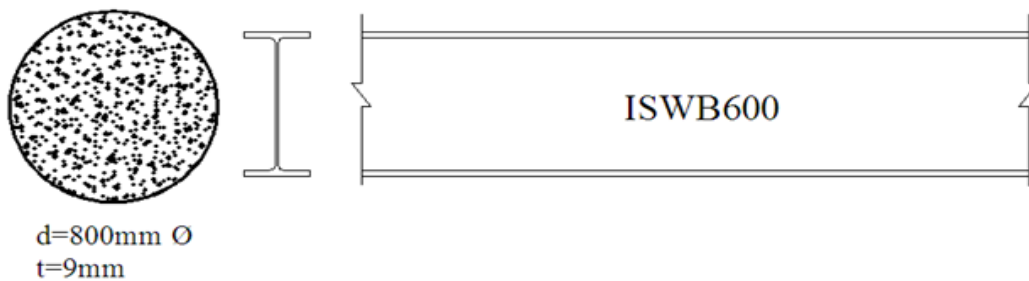


Figure 5.10: 20 Storey CFT Building Column and Beam

5.6 Parametric Study of 30 Storey CFT Building

- **Base Reaction:**

Table.5.10 shows the base reaction due to gravity load, both manually and by STRAP software.

Manual Load Calculation:

Building Configuration

No. of storey	= 30
Width of building (a)	= 32 m
Length of building (b)	= 38.4 m
Typical height of storey	= 3 m
Beam ISWB600 lower 15th floor	= 1.337kN/m
Beam ISWB550 upper 15th floor	= 1.125kN/m
Slab Thickness. t	= 150mm
Column diameter D	= 1000mm t=11mm
Column c/c distance	= 6.4m

CFT Building Load Calculation

Wt. of slab	= 4608 kN
Wt. of Beam ISWB600	= 607.533 kN
Wt. of Beam ISWB550	= 511.2 kN
Column Weight:	
Wt. of concrete	= 2365.15 kN
Wt of Steel	= 337.88 kN
Total DL on each floor	= 7870.39 kN
Total DL on Building	= 236112 kN
LL	= 2kN/m ²
Total LL on Building	= 73728 kN
FF	= 1kN/m ²
Total FF on Building	= 36864 kN
Total Wt on Building	= 346704 kN
Load Intensity	= 9.40 kN/m ²
Seismic Weight	= 291408 kN

Table 5.10: Base Reaction

Load Type	STRAP	Manual
Dead load (kN)	233317	236112
Live load (kN)	73728	73728
Floor finish (kN)	36864	36864
Total load (kN)	343909	346704
Load intensity (kN/m ²)	9.33	9.40
Seismic weight W (kN)	288613	291408

- **Wind Force:**

The base shear for wind load along X-direction and along Y-direction, as per IS: 875(III)-1987 [4] is shown and compared with STRAP results in Table.5.11. Manual wind load calculation is shown in Appendix-A.2.

Table 5.11: Base Shear Due to Wind Load

Load Type	STRAP	Manual
Wind X-dir (kN)	4227	4446
Wind Y-dir (kN)	5073	5639

- **Earthquake Force:**

The base shear force for earthquake load acting along X-direction and along Y-direction as per IS: 1893-2002 ([1]) is shown and compared with STRAP results in Table.5.12. Manual wind load calculation is shown in Appendix-B.2.

Table 5.12: Base Shear Due to Earthquake Load

Load Type	STRAP	Manual
Base shear X-dir (kN)	2175	1958
Base shear Y-dir (kN)	1927	1923

- **Time Period and Mode Shape:**

Fig.5.11 shows the Mode Shape Vs Time Period graph of 30 story CFT building. The first three mode shape as shown Fig.5.12 and 5.13 in Y-direction, X-direction and XY-direction (torsion).

Table 5.13: 1St and 2nd Mode Time Period

Direction	CFT
Time period Y-dir (sec)	3.297
Time period X-dir (sec)	3.238

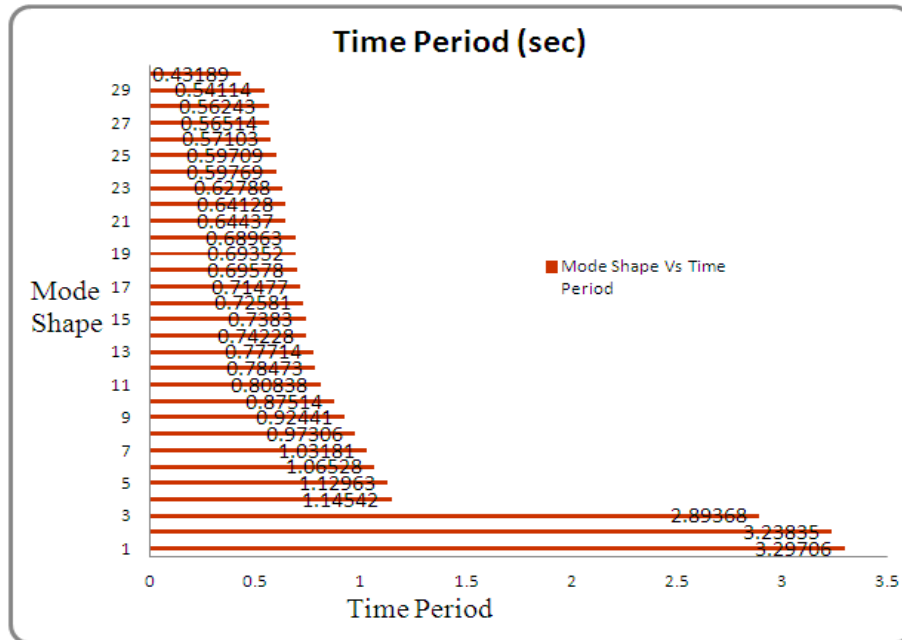


Figure 5.11: Mode Shape Vs Time Period Graph

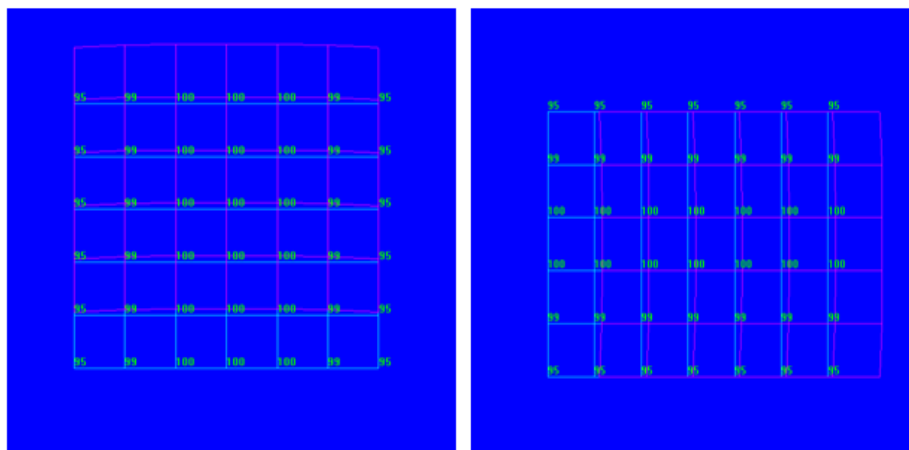


Figure 5.12: 1st and 2nd Mode Shape

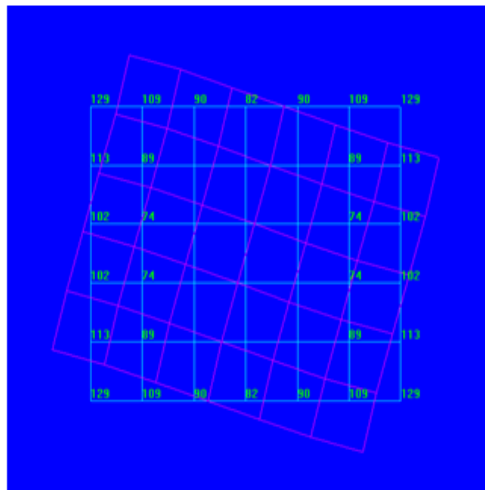


Figure 5.13: 3rd Mode Shape

- **Displacement:**

30 storey Concrete Filled Steel tube buildings, storey displacement due to earthquake and wind load are as shown in Fig.5.14. Maximum displacement occurs due to wind load in Y direction, thus becoming a governing case.

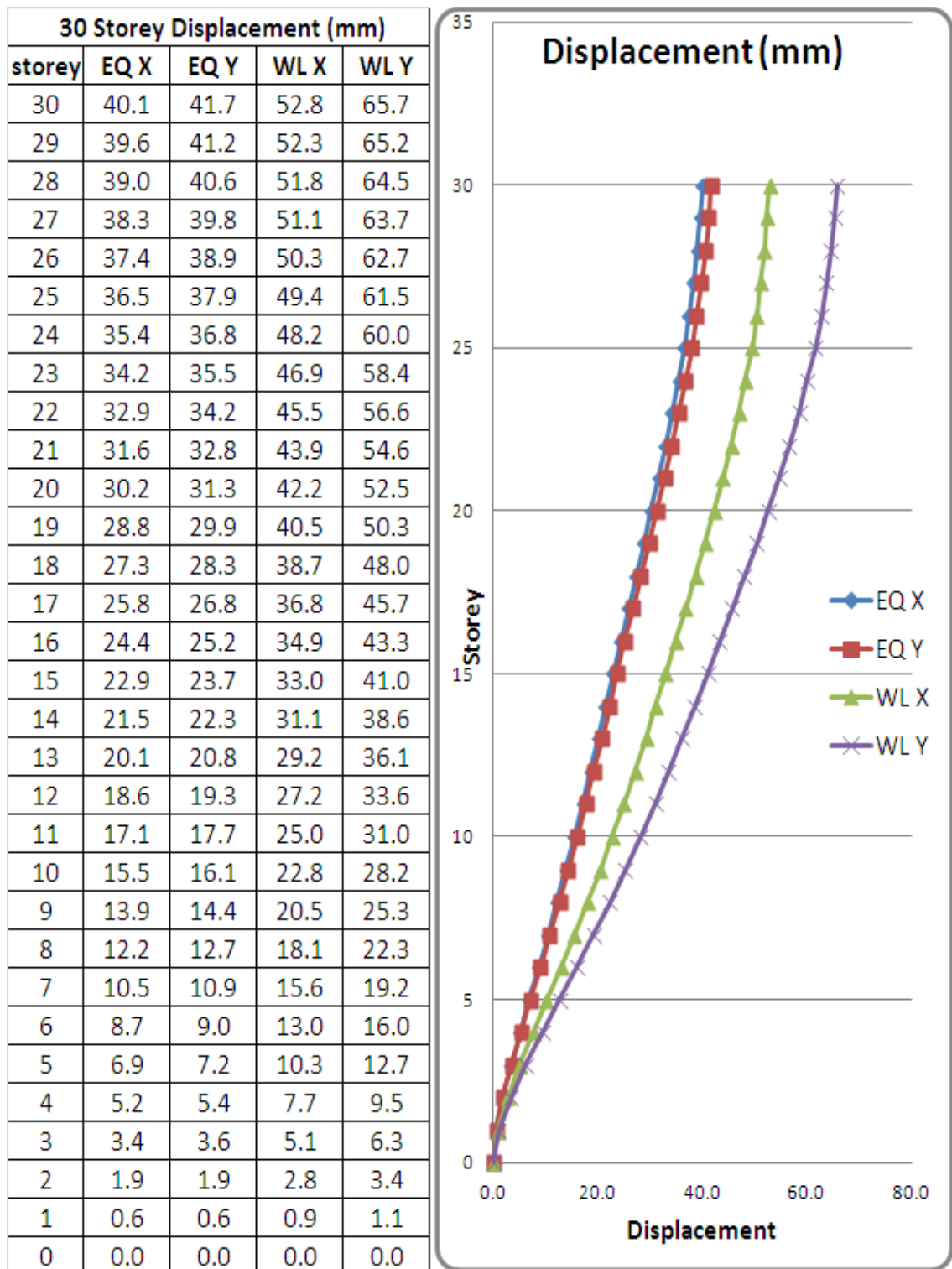


Figure 5.14: Displacement of 30 Storey CFT Building

5.7 Comparison of 30 Storey CFT, RCC and Steel Building

- **Load Comparison:**

CFT, RCC and Steel building load intensity like Live load, Floor finish was kept same, while Dead Load varied due to member size effect. Refer to Table.5.14 for load intensity application and total load on the structure.

Table 5.14: Load Comparison

Structure	CFT	RCC	STEEL
Dead load (kN)	233317	242794	171846
Live load (kN)	73728	73728	73728
Floor finish (kN)	36864	36864	36864
Total load (kN)	343909	353386	282438
Load intensity (kN/m ²)	9.329	9.586	7.662

- **Time Period Comparison:**

Table.5.15 shown the CFT, RCC and Steel building maximum time period due to 1st mode of building and graphical representation of Time period is shown in Fig.5.15. Percentage reduction in time period of CFT building is 26.2% and 3.5% with compared to RCC and Steel building respectively.

Table 5.15: Time Period Comparison

Load Type	CFT	RCC	STEEL
Time period(sec) for 1st mode	3.3	4.47	3.42

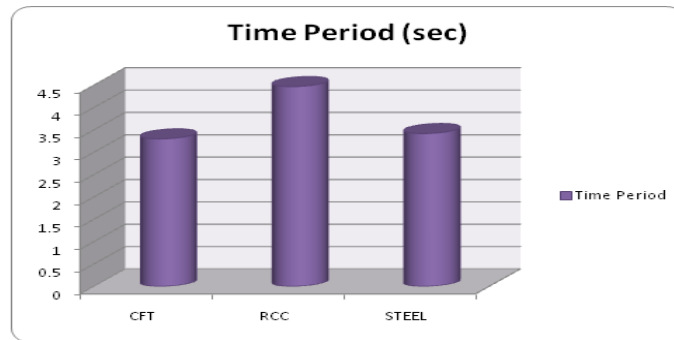


Figure 5.15: Comparison of Time Period

• **Base Shear Comparison:**

Base shear variation in X and Y direction due to earthquake load is presented in Table.5.16. and Graphical representation of base shear shown in Fig.5.16. It shows that for CFT structure base shear is 15.26% higher than RCC while 2.44% higher than steel.

Table 5.16: Base Shear Comparison

Load Type	CFT	RCC	STEEL
Base shear X-dir (kN)	2175	1946	2256
Base shear Y-dir (kN)	1927	1633	1880

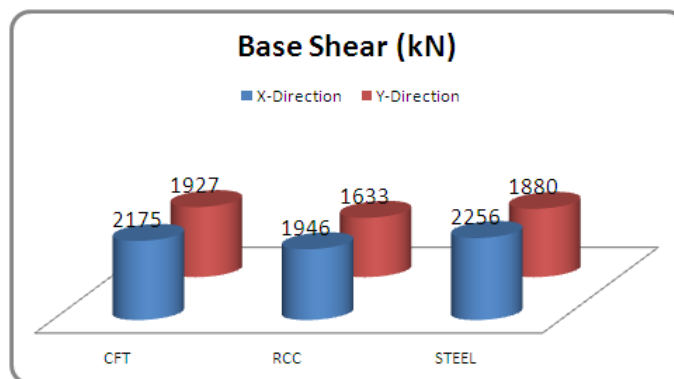


Figure 5.16: Comparison of Base Shear

- **Maximum Load Carrying Capacity:**

Load carrying capacity of CFT building is found to be higher than RCC by 22.8% and Steel by 11.8% shown in Table.5.17.and Graphical representation of maximum load carrying capacity shown in Fig.5.17.

Table 5.17: Maximum Load Carrying Capacity

Structure Type	CFT	RCC	STEEL
Design capacity (kN)	21588	16675	19032

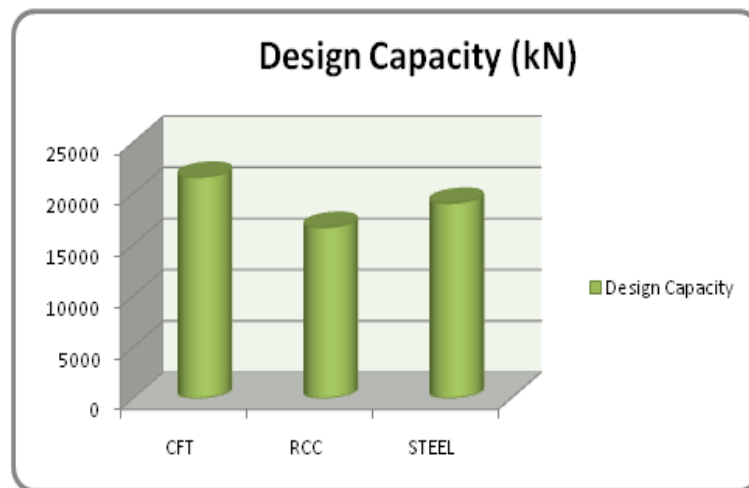


Figure 5.17: Comparison of Design Capacity

- **Displacement Comparison:**

Storey displacement variation along the height of building is presented in Fig.5.18. Percentage reduction in top storey displacement of CFT building is 45.1% and 24.6% with compared to RCC and Steel building respectively

30 Storey Displacement (mm)			
storey	CFT	RCC	STEEL
Load	1.5(DL ± WLY)		
30	98.6	179.6	130.8
29	97.8	177.9	129.5
28	96.8	176.7	128.3
27	95.6	175.2	126.6
26	94.1	173.4	124.8
25	92.3	171.5	122.6
24	90.0	167.3	120.2
23	87.6	163.8	117.3
22	84.9	159.5	114.2
21	81.9	153.5	110.9
20	78.8	148.2	107.4
19	75.5	143.3	103.7
18	72.0	138.5	99.8
17	68.6	132.5	95.6
16	65.0	125.6	91.2
15	61.5	119.0	86.7
14	57.9	112.1	81.8
13	54.2	104.7	76.7
12	50.4	96.9	71.3
11	46.5	88.5	65.7
10	42.3	79.8	59.7
9	38.0	70.8	53.6
8	33.5	61.8	47.1
7	28.8	52.4	40.5
6	24.0	42.9	33.6
5	19.1	33.5	26.7
4	14.3	24.3	19.8
3	9.5	15.6	13.1
2	5.1	8.0	7.1
1	1.7	2.4	2.3
0	0.0	0.0	0.0

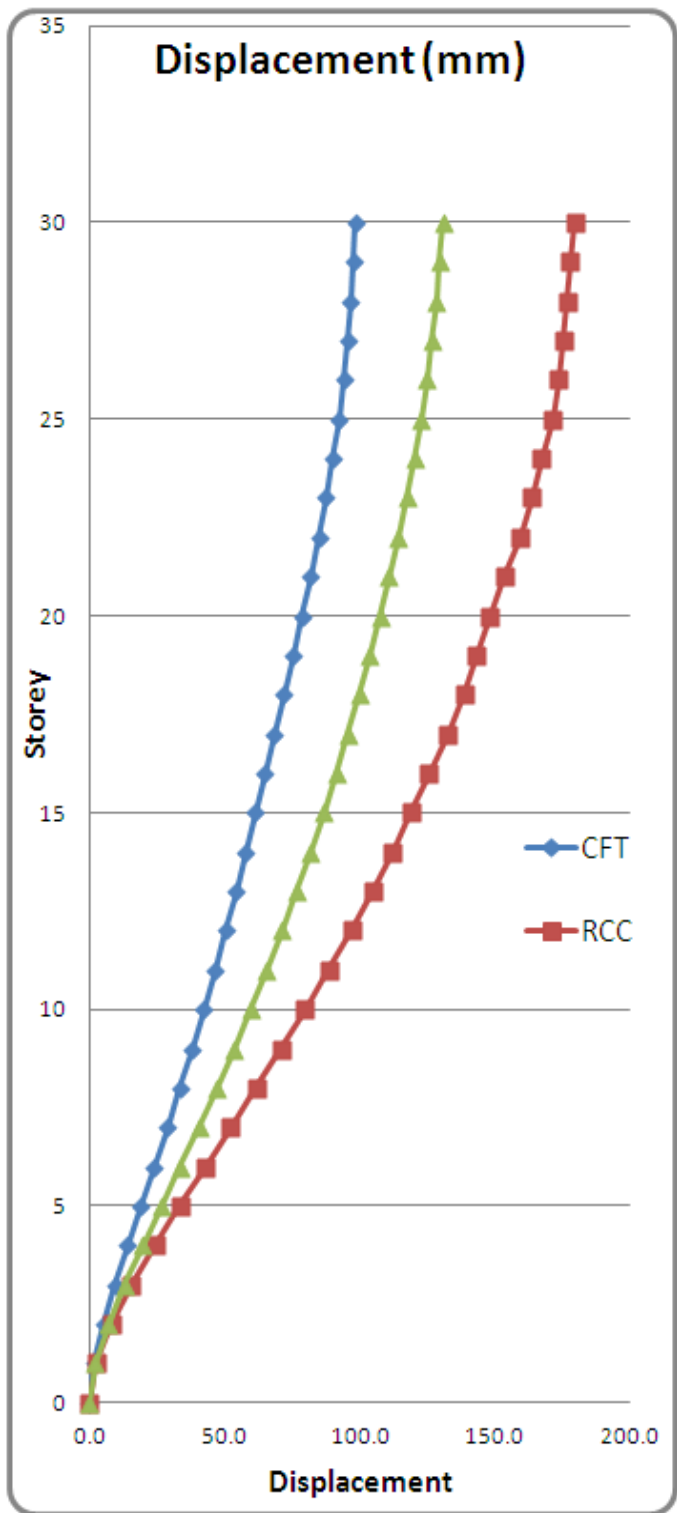


Figure 5.18: Comparison of 30 Storey Displacement

5.8 Cost Comparison

The total quantity of material required for 30 storey CFT, RCC and Steel building calculation is below and cost wise analysis is presented in Table.5.18.

CFT Building Quantity

Column dia D = 1000mm and t = 11mm

$$\text{Concrete Qty} = \pi \div 4 * (0.978)^2 * 90 * 42 = 2838.175m^3$$

$$\text{Structural Qty} = \pi \div 4 * [(1.00)^2 - (0.978)^2] * 90 * 42 * 7850 \div 1000 = 1013.63 \text{ tonnes}$$

RCC Building Quantity

Column dia D (Gf to 10 floor) = 1100mm

Column dia D (11 floor to 20 floor) = 900mm

Column dia D (21 floor to 30 floor) = 700mm

$$\text{Concrete Qty} = \pi \div 4 * [(1.100)^2 + (0.900)^2 + (0.700)^2] * 30 * 42 = 2482.64m^3$$

Average Pt = 2.86% as per STRAP results

$$\text{Reinforce Steel Qty} = 2.86 \div 100 * \pi \div 4 * [(1.100)^2 + (0.900)^2 + (0.700)^2] * 30 * 42 * 7850 \div 1000 = 557.377 \text{ tonnes}$$

$$\text{Shuttering Qty} = [\pi * 1.100 + \pi * 0.900 + \pi * 0.700] * 30 * 42 = 10682.28m^2$$

Steel Building Quantity

Column dia D = 1000mm and t = 20mm

$$\text{Structural Qty} = \pi \div 4 * [(1.00)^2 - (0.960)^2] * 90 * 42 * 7850 \div 1000 = 1826.195 \text{ tonnes}$$

- **30 Storey Building Rate Analysis:**

Table 5.18: 30 Storey Column Rate Analysis

Sr No	Description	Quantity	units	Rate	Amount (Rs)
CFT Building					
1	Str. Steel	1013.63	tonnes	60140	60959708
2	Concrete (M30)	2838.18	cu.m	7669	21765964
Total					82725672
Column cost per meter					21885
RCC Building					
1	Rein. Steel	557.377	tonnes	57375	31979505
2	Concrete (M30)	2482.64	cu.m	7669	19039366
3	Shuttering	10682.28	sq.m	808	8631282
Total					59650153
Column cost per meter					15780
Steel Building					
1	Str. Steel	1826.195	tonnes	60140	109827367
Total					109827367
Column cost per meter					29055

Cost analysis data shows that 30 storey CFT building is 27.9% costly compared to RCC building and 24.7% cheaper compared to Steel building.

- **10, 20 and 30 Storey Column Cost Comparison (Rs/m):**

Table.5.19 shows the 10, 20 and 30 storey CFT, RCC and Steel building, column cost comparison per meter span and Graphical representation of 10, 20 and 30 storey column cost shown in Fig.5.19. in Fig.5.7

Table 5.19: Column Cost Comparison (Rs/m)

Number of Storey	CFT	RCC	STEEL
10 Storey	6581	5941	9550
20 Storey	14235	11596	17453
30 Storey	21885	15780	29055

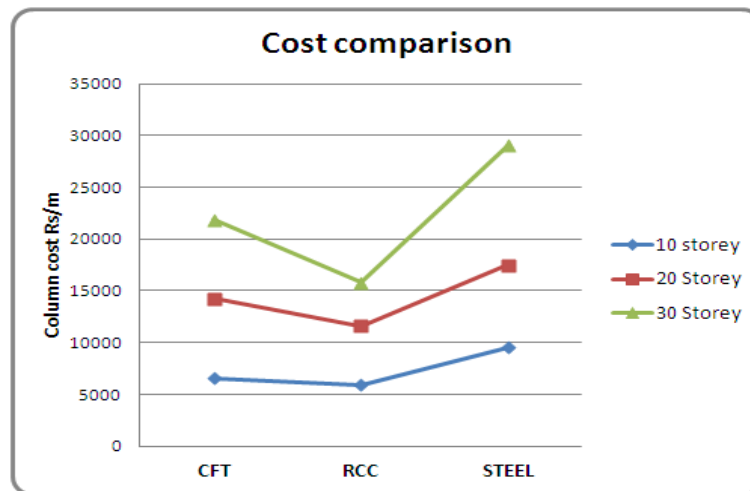


Figure 5.19: Comparison of Column Cost

Observed from Fig.5.19 it can be said that Beyond 30 storey cost comparison, 20 to 30 storey CFT building increase cost 35% and Steel building increase cost 40%. So further 10 storey increase percentage reduction in CFT building cost is 12.5% compared to Steel building.

5.9 Detailing of CFT Member

Fig.5.20 shown cross section view of beam and column member. Also Fig.5.21 shows the design result and all design parameter like moment, Deflection, Combine stress and axial force criteria is within permissible limit.

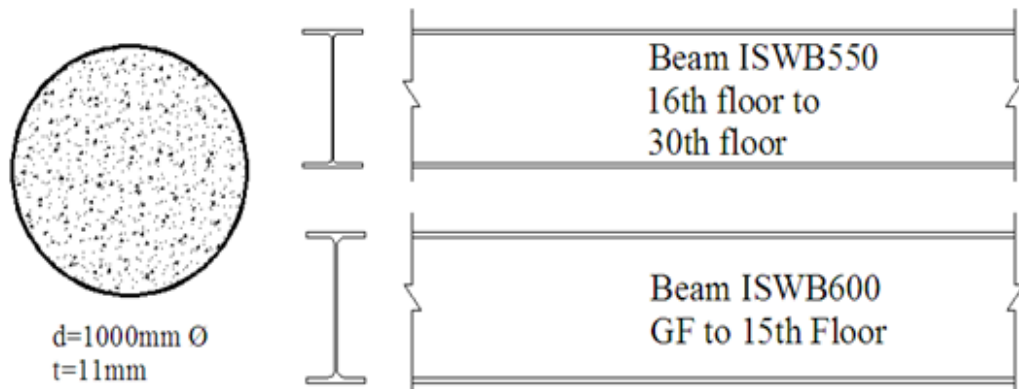


Figure 5.20: 30 Storey CFT Building Column and Beam

DESIGN	EQUATION	FACTORS	VALUES	RESULT
M3 Moment (8.2) Notes:	$\frac{M}{M_d} < 1.00$ LOW Shear Load Used for Moment Design	$Z_{eff} = 8358.44$ $Z_{el} = 8358.44$	$M = 12.20$ $M_d = 2583.52$	0.00
V3 Shear (8.4)	$V/V_d < 1.00$	$A_v = 217.59$	$V = 203.06$ $V_d = 3882.57$	0.05
M2 Moment (8.2) Notes:	$\frac{M}{M_d} < 1.00$ LOW Shear Load Used for Moment Design	$Z_{eff} = 8358.44$ $Z_{el} = 8358.44$	$M = 886.56$ $M_d = 2583.52$	0.34
Deflection	$\frac{defl.}{L / 400} < 1.00$		$defl. = 0.00050$	0.07
Combined Stresses [Local] (9.3)	$\frac{N}{N_d} + \frac{M_x}{M_{dx}} + \frac{M_y}{M_{dy}} < 1.00$	$M_{dx} = 2583.52$ $M_{dy} = 2583.52$ $M_x = 12.20$ $M_y = 886.56$	$N = 12132.9$ $A_g = 288.34$	0.91
Axial Force (7.1) Note:	$\frac{P}{P_d} < 1.00$ buckling curve used is : a	$\frac{[kL/r]_x}{[kL/r]_y} = 11$ $X_{fy} = 823$	$P = 12132.9$ $A_g = 341.77$ $P_d = 21587.9$ $A_{eff} = 288.34$	0.56

Figure 5.21: Design Result For 30 Storey CFT Building

5.10 Summary

In this chapter comparison of 20 and 30 storey building for Load intensity, Time period, Base shear, Maximum load carrying capacity and Top storey displacement of CFT, RCC and Steel building was done.

Result shows that the CFT building is effective in performance wise compared to RCC building in terms of 20 story building reduced the time period by 25.5%, Top storey displacement by 39.5% and increase load carrying capacity 19.1%. Cost wise CFT building is 18.5% costly. Also where compared with Steel building, the CFT building is effective in performance and cost wise in terms of 20 story building with reduction in time period by 17.8%, Top storey displacement by 33.5% and increase load carrying capacity 27.3%. Cost wise CFT building is 18.4% cheaper.

Result shows that the CFT building is effective in performance wise compared to RCC building in terms of 30 story building as there is reduction in the time period by 26.2%, Top storey displacement by 45.1% and increase load carrying capacity 22.8%. Cost wise CFT building is 27.9% costly. For 30 storey building permissible displacement limit is 180mm while 30 story RCC building top story displacement is 179.6mm this is nearer to permissible limit of 180mm so beyond 30 story RCC is not useful with this geometric frame structure.

Result shows that the CFT building is effective in performance and cost wise compared to Steel building in terms of 30 story building while reduction in time period by 3.5%, Top storey displacement by 24.6% and increase load carrying capacity 11.8%. Cost wise CFT building is 24.7% cheaper.

Also 20 to 30 storey CFT building increase cost 35% and Steel building increase cost 40%. So further 10 storey increase, percentage reduction in CFT building cost is

12.5% compared to Steel building. Over all CFT building is effective with increase number of higher story.

Chapter 6

Summary, Conclusion and Future Scope

6.1 Summary

The main objective of this work was to make an attempt to understand the complex behavior of concrete filled steel tube (CFT) which are used in large span buildings, high rise or tall buildings, bridge piers, etc. From point of view of economy, this system reduced large amount of structural steel compared to steel structure and also gives saving in shuttering and material cost compared to RCC structure. In this work type of composite structures, history of concrete filled steel tube column system and behavior of CFT structure under lateral load was discussed in detail.

In the chapter of literature review detail discussion on experimental and analytical behavior of CFT tube under lateral loading was discussed. It was found that confinement provided by closed steel section allowed higher strength achievement in concrete. Circular concrete filled tube developed hoop tension which further increased the overall load carrying capacity. Local buckling of steel tube was delayed due to restraining effect which prevented local crushing and spalling of concrete and also creep and

shrinkage effect. For validation of STRAP software, excel sheets were prepared for earthquake loading and wind loading and the results were compared and very minor difference between the two was found.

The resistance of composite columns can be calculated by two methods given by Eurocode 4. General method and Simplified method, of which Simplified method was used in this work. Therefore, a simply linear version of M-N interaction diagram for cross-sectional resistance to combinations of axial compression and uniaxial bending moment on a composite section was obtained. This was derived for centrally loaded steel column of thin walled hollow circular tube.

When comparison of design strength for American Institute of Steel Construction (AISC) and Eurocode-4, was done with manual results and STRAP software results, the design strength value was nearly same but EC4 gave a conservative result from literature survey and was therefore used in thesis work.

Comparative study of 10, 20, 30 storey CFT, RCC and Steel building was done in this work and therefore loading i.e. Live load, Floor load and Slab load was kept same. This resulted in same loading intensity per meter square but column property was changed. Frame structure was used for modeling.

6.2 Conclusion

Based on the study carried out during major project following conclusions can be drawn:

10 Storey

- Percentage reduction in time period of CFT building was 44.1% and 17.4% with

compared to RCC and Steel building respectively.

- Load carrying capacity of CFT building was found to be higher than RCC by 15.2%, while for steel by 6.8%.
- Percentage reduction in top storey displacement of CFT building was 65.1% and 39.1% with compared to RCC and Steel building respectively.
- Cost analysis data shown, 10 storey CFT building was 9.7% costly compared to RCC building but 31.1% cheaper compared to Steel building.

20 Storey

- Percentage reduction in time period of CFT building was 25.5% compared to RCC and 17.8% compared to Steel building.
- Load caring capacity of CFT building was found to be higher than RCC by 19.1% and Steel by 27.3%.
- Top storey displacement reduction in CFT building was 39.5% and 33.5% with compared to RCC and Steel building respectively.
- Cost wise comparison, CFT building was costly by 18.5% compared to RCC but cheaper by 18.4% compared to Steel.

30 Storey

- Percentage reduction in time period of CFT building was 26.2% and 3.5% with compared to RCC and Steel building respectively.
- Load caring capacity of CFT building was higher 22.8% and 11.8% compared RCC and Steel building respectively.
- Percentage reduction in top storey displacement of CFT building was 45.1% and 24.6% with compared to RCC and Steel building respectively.

- For 30 storey building permissible displacement limit was 180mm as per deflection criteria and RCC building top story displacement was 179.6mm very near to permissible limit. Therefore it can be said that beyond 30 storey RCC will not be useful with this geometric frame structure.
- 30 storey CFT building was 27.9% costly compared to RCC building but 24.7% cheaper compared to Steel building.
- Beyond 30 storey cost comparison, 20 to 30 storey CFT building increase cost 35% and Steel building increase cost 40%. So further 10 storey increase percentage reduction in CFT building cost was 12.5% compared to Steel building. Over all CFT building is effective with increase in number of storey.

6.3 Future Scope of Work

The study in this report is limited up to 30-storey CFT, RCC and Steel building for frame structure. The present study extended to include following aspects:

- Similar study can be carried out by changing various grade of concrete and Structural steel.
- Experimental work can be carried out for Concrete filled steel tube column, Reinforce column and steel column.
- Experimental work can be carried out for Concrete filled steel tube column with axial load and moment.
- Similar study can be carried out by taking concrete filled steel tube column and concrete filled steel tube beam with different number of storey.
- Beyond 30 storey concrete filled steel tube building comparison with other structural system.

Appendix A

Wind Load Calculation

A.1 Manual Wind Load Calculation For 20 Storey

Following are the steps of wind load calculation by using IS 875(III)-1987[4].

Manual Wind Load Calculation

Basic Wind speed V_b = 39 m/s

Terrain category = II

Class = C

k_1 (Probability factor) = 1

k_3 (Topography factor) = 1

Design wind speed $V_z = V_b \times k_1 \times k_2 \times k_3$

Table A.1: Wind Load Parameter

HEIGHT	K1	K2	K3	Vb	Vz	Pz
10	1	0.98	1	39	38.22	876.46
15	1	1.02	1	39	39.78	949.47
20	1	1.05	1	39	40.95	1006.14
30	1	1.1	1	39	42.9	1104.25
50	1	1.15	1	39	44.85	1206.91
100	1	1.22	1	39	47.58	1358.31

Table A.2: Building Parameter

DIMENSION	WIND AT 0	WIND AT 90
a/b	1.20	0.83
h/b	1.88	1.56
Cf	1.25	1.3

Table A.3: Wind Load in X-Direction

Wind at 0 Degree					
STOREY	CF	Ae		PZ	FORCE(kN)
		Width(m)	Length(m)	N/mm ²	
1	1.25	32	3	876.5	105.18
2	1.25	32	3	876.5	105.18
3	1.25	32	2.5	876.5	87.65
	1.25	32	0.5	949.5	18.99
4	1.25	32	3	949.5	113.94
5	1.25	32	1.5	949.5	56.97
	1.25	32	1.5	1006.1	60.37
6	1.25	32	3	1006.1	120.74
7	1.25	32	0.5	1006.1	20.12
	1.25	32	2.5	1104.2	110.42
8	1.25	32	3	1104.2	132.51
9	1.25	32	3	1104.2	132.51
10	1.25	32	1.5	1104.2	66.25
	1.25	32	1.5	1206.9	72.41
11	1.25	32	3	1206.9	144.83
12	1.25	32	3	1206.9	144.83
13	1.25	32	3	1206.9	144.83
14	1.25	32	3	1206.9	144.83
15	1.25	32	3	1206.9	144.83
16	1.25	32	3	1206.9	144.83
17	1.25	32	0.5	1206.9	24.14
	1.2	32	2.5	1358.3	130.40
18	1.25	32	3	1358.3	163.00
19	1.25	32	3	1358.3	163.00
20	1.25	32	1.5	1358.3	81.50
Total base shear due to wind load					2634.24

Table A.4: Wind Load in Y-Direction

Wind at 90 Degree					
STOREY	CF	Ae		PZ	FORCE(kN)
		Width(m)	Length(m)	N/mm ²	
1	1.3	38.4	3	876.5	131.26
2	1.3	38.4	3	876.5	131.26
3	1.3	38.4	2.5	876.5	109.38
	1.3	38.4	0.5	949.5	23.70
4	1.3	38.4	3	949.5	142.19
5	1.3	38.4	1.5	949.5	71.10
	1.3	38.4	1.5	1006.1	75.34
6	1.3	38.4	3	1006.1	150.68
7	1.3	38.4	0.5	1006.1	25.11
	1.3	38.4	2.5	1104.2	137.81
8	1.3	38.4	3	1104.2	165.37
9	1.3	38.4	3	1104.2	165.37
10	1.3	38.4	1.5	1104.2	82.69
	1.3	38.4	1.5	1206.9	90.37
11	1.3	38.4	3	1206.9	180.75
12	1.3	38.4	3	1206.9	180.75
13	1.3	38.4	3	1206.9	180.75
14	1.3	38.4	3	1206.9	180.75
15	1.3	38.4	3	1206.9	180.75
16	1.3	38.4	3	1206.9	180.75
17	1.3	38.4	0.5	1206.9	30.12
	1.3	38.4	2.5	1358.3	169.52
18	1.3	38.4	3	1358.3	203.42
19	1.3	38.4	3	1358.3	203.42
20	1.25	38.4	1.5	1358.3	97.80
Total base shear due to wind load					3290.40

A.2 Manual Wind Load Calculation For 30 Storey

Following are the steps of wind load calculation by using IS 875(III)-1987[4].

Manual Wind Load Calculation

Basic Wind speed V_b = 39 m/s

Terrain category = II

Class = C

k_1 (Probability factor) = 1

k_3 (Topography factor) = 1

Design wind speed $V_z = V_b \times k_1 \times k_2 \times k_3$

Table A.5: Wind Load Parameter

HEIGHT(m)	K1	K2	K3	Vb	Vz	Pz
10	1	0.98	1	39	38.22	876.46
15	1	1.02	1	39	39.78	949.47
20	1	1.05	1	39	40.95	1006.14
30	1	1.1	1	39	42.9	1104.25
50	1	1.15	1	39	44.85	1206.91
100	1	1.22	1	39	47.58	1358.31

Table A.6: Building Parameter

DIMENSION	WIND AT 0	WIND AT 90
a/b	1.20	0.83
h/b	2.81	2.34
Cf	1.3	1.35

Table A.7: Wind Load in X-Direction

Wind at 0 Degree					
STOREY	CF	Ae		PZ	FORCE(kN)
		Width(m)	Length(m)	N/mm ²	
1	1.3	32	3	876.5	109.38
2	1.3	32	3	876.5	109.38
3	1.3	32	2.5	876.5	91.15
	1.3	32	0.5	949.5	19.75
4	1.3	32	3	949.5	118.49
5	1.3	32	1.5	949.5	59.25
	1.3	32	1.5	1006.1	62.78
6	1.3	32	3	1006.1	125.57
7	1.3	32	0.5	1006.1	20.93
	1.3	32	2.5	1104.2	114.84
8	1.3	32	3	1104.2	137.81
9	1.3	32	3	1104.2	137.81
10	1.3	32	1.5	1104.2	68.90
	1.3	32	1.5	1206.9	75.31
11	1.3	32	3	1206.9	150.62
12	1.3	32	3	1206.9	150.62
13	1.3	32	3	1206.9	150.62
14	1.3	32	3	1206.9	150.62
15	1.3	32	3	1206.9	150.62
16	1.3	32	3	1206.9	150.62
17	1.3	32	0.5	1206.9	25.10
	1.35	32	2.5	1358.3	146.70
18	1.3	32	3	1358.3	169.52
19	1.3	32	3	1358.3	169.52
20	1.3	32	3	1358.3	169.52
21	1.3	32	3	1358.3	169.52
22	1.3	32	3	1358.3	169.52
23	1.3	32	3	1358.3	169.52
24	1.3	32	3	1358.3	169.52
25	1.3	32	3	1358.3	169.52
26	1.3	32	3	1358.3	169.52
27	1.3	32	3	1358.3	169.52
28	1.3	32	3	1358.3	169.52
29	1.3	32	3	1358.3	169.52
30	1.3	32	1.5	1358.3	84.76
Total base shear due to wind load					4445.87

Table A.8: Wind Load in Y-Direction

Wind at 90 Degree					
STOREY	CF	Ae		PZ	FORCE(kN)
		Width(m)	Length(m)	N/mm ²	
1	1.35	38.4	3	876.5	136.31
2	1.35	38.4	3	876.5	136.31
3	1.35	38.4	2.5	876.5	113.59
	1.35	38.4	0.5	949.5	24.61
4	1.35	38.4	3	949.5	147.66
5	1.35	38.4	1.5	949.5	73.83
	1.35	38.4	1.5	1006.1	78.24
6	1.35	38.4	3	1006.1	156.48
7	1.35	38.4	0.5	1006.1	26.08
	1.35	38.4	2.5	1104.2	143.11
8	1.35	38.4	3	1104.2	171.73
9	1.35	38.4	3	1104.2	171.73
10	1.35	38.4	1.5	1104.2	85.87
	1.35	38.4	1.5	1206.9	93.85
11	1.35	38.4	3	1206.9	187.70
12	1.35	38.4	3	1206.9	187.70
13	1.35	38.4	3	1206.9	187.70
14	1.35	38.4	3	1206.9	187.70
15	1.35	38.4	3	1206.9	187.70
16	1.35	38.4	3	1206.9	187.70
17	1.35	38.4	0.5	1206.9	31.28
	1.35	38.4	2.5	1358.3	176.04
18	1.35	38.4	3	1358.3	211.24
19	1.35	38.4	3	1358.3	211.24
20	1.35	38.4	3	1358.3	211.24
21	1.35	38.4	3	1358.3	211.24
22	1.35	38.4	3	1358.3	211.24
23	1.35	38.4	3	1358.3	211.24
24	1.35	38.4	3	1358.3	211.24
25	1.35	38.4	3	1358.3	211.24
26	1.35	38.4	3	1358.3	211.24
27	1.35	38.4	3	1358.3	211.24
28	1.35	38.4	3	1358.3	211.24
29	1.35	38.4	3	1358.3	211.24
30	1.35	38.4	3	1358.3	211.24
Total base shear due to wind load					5639.09

Appendix B

Earthquake Load Calculation

B.1 Manual Earthquake Load Calculation For 20 Storey

Manual Earthquake Load Calculation

Time period as per “STRAP”:

$$T_y = 2.089 \text{ sec}$$

$$T_x = 2.056 \text{ sec}$$

$$\text{Zone factor} = 0.16$$

$$\text{Importance factor} = 1$$

$$\text{Response reduction factor} = 5$$

$$\text{Soil Strata} = \text{Medium}$$

$$(S_a/g) = 1.36/T$$

$$A_{hy} = (Z/2) * (I/R) * (S_a/g) = 0.01041$$

$$A_{hx} = (Z/2) * (I/R) * (S_a/g) = 0.01058$$

Base Shear

$$Vb_y = A_h * W = 1832 \text{ kN}$$

$$Vb_x = A_h * W = 1861 \text{ kN}$$

B.2 Manual Earthquake Load Calculation For 30 Storey

Manual Earthquake Load Calculation

Time period as per “STRAP”:

$$T_y = 3.297 \text{ sec}$$

$$T_x = 3.238 \text{ sec}$$

$$\text{Zone factor} = 0.16$$

$$\text{Importance factor} = 1$$

$$\text{Response reduction factor} = 5$$

$$\text{Soil Strata} = \text{Medium}$$

$$(S_a/g) = 1.36/T$$

$$A_{hy} = (Z/2) * (I/R) * (S_a/g) = 0.00659$$

$$A_{hx} = (Z/2) * (I/R) * (S_a/g) = 0.00672$$

Base Shear

$$Vb_y = A_h * W = 1923 \text{ kN}$$

$$Vb_x = A_h * W = 1958 \text{ kN}$$

References

- [1] *IS: 1893-2002, Criteria for earthquake resistant design of structures.* Bureau of Indian Standard, New Delhi.
- [2] *IS 456-2000, Plain and Reinforced Concrete Code of Practice.* Bureau of Indian Standard, New Delhi.
- [3] *IS 800-2007, Code of practice for general construction in steel.* Bureau of Indian Standard, New Delhi.
- [4] *IS: 875(part 3)-1987, Code of practice for design loads (other than earthquake)for buildings and structures, wind loads.* Bureau of Indian Standard, New Delhi.
- [5] Sami Rizkalla Amir Fam, Frank S. Qie. Concrete-filled steel tubes subjected to axial compression and lateral cyclic loads. *Journal of Structural Engineering, Vol. 130, No. 4,* April 2004.
- [6] K. K. Choi and Y. Xiao. Analytical studies of concrete-filled circular steel tubes under axial compression. *Journal of Structural Engineering, Vol. 130, No. 5,* May 2010.
- [7] Code and Commentary on Eurocode 4. *Design of composite steel and concrete structures, Part 1.1: General rules and rules for buildings.* January 2004.
- [8] E. Cosenza and R. Zandonini. "*Composite Construction*" *Structural Engineering Handbook Chapter 6.6.* CRC Press LLC, January 1999.
- [9] Shosuke Morino and Keigo Tsuda. Design and construction of concrete-filled steel tube column system in japan. *Earthquake Engineering and Engineering Seismology,, Vol. 4, No. 1.*
- [10] N.E. Shanmugam and B. Lakshmi. State of the art report on steel-concrete composite columns, journal of constructional steel research. Technical report, 57, (2001) 1041-1080.
- [11] B. Uy. Strength of short concrete filled high strength steel box columns. *Journal of Constructional Steel Research 57,* 113-134 2001.

- [12] B. Uy. Stability and ductility of high performance steel sections with concrete infill. *Journal of Constructional Steel Research* 64, 748-754 2008.
- [13] Ana Lcia H. de Cresce El Debs Mounir Khalil El Debs Walter Luiz Andrade de Oliveira, Silvana De Nardin. Influence of concrete strength and length/diameter on the axial capacity of cft columns. *Journal of Constructional Steel Research* 65, 2103-2110 2009.
- [14] P.E. Kai H. Hsieh MarvinW. Halling S.E. F.ASCE Zhijing Ou, Baochun Chen and M.ASCE Paul J. Barr. Experimental and analytical investigation of concrete filled steel tubular columns. *Journal of Structural Engineering*, Vol. 137, No. 6, June 2011.